NASA Contractor Report 3174

Influence of Precursor Heating on Viscous Flow Around a Jovian Entry Body

S. N. Tiwari and K. Y. Szema

CONTRACT NAS1-14193-27
OCTOBER 1979

NASA

NASA Contractor Report 3174

Influence of Precursor Heating on Viscous Flow Around a Jovian Entry Body

S. N. Tiwari and K. Y. Szema
Old Dominion University Research Foundation
Norfolk, Virginia

Prepared for
Langley Research Center
under Contract NAS1-14193-27

NASA
National Aeronautics
and Space Administration

**Scientific and Technical
Information Branch**

1979

TABLE OF CONTENTS

LIST OF TABLES

LIST OF FIGURES

LIST OF FIGURES (continued)

LIST OF FIGURES (continued)

SUMMARY

The influence of changes in precursor region flow properties (resulting from the absorption of radiation from the shock layer) on the entire shock-layer flow phenomena is investigated. The axially symmetric case is considered for both the preheating zone (precursor region) and shock layer. The flow in the shock layer is considered to be viscous with chemical equilibrium but radiative nonequilibrium. Realistic thermophysical and spectral models are employed, and results are obtained by implicit finite difference and iterative procedures. The results indicate that precursor heating increases the radiative heating of the body by a maximum of 7.5 percent for 116-km entry conditions.

LIST OF SYMBOLS

C_i	mass fraction of species i in the shock layer, ρ_i/ρ
C_α	mass fraction of species α in the precursor zone
C_p	equilibrium specific heat of mixture, $\Sigma\ C_i\ C_{p,i}$
$C_{p,i}$	specific heat of species i, $C^*_{p,i}/C^*_{p,\infty}$
D_{ij}	binary diffusion coefficient
h	specific enthalpy, h^*/V^{*2}_∞, (also Planck constant)
H_T	total enthalpy, $h = (u^2 + v^2)/2$
J_i	mass diffusion flux of species i, $J^*_i\ R_N/\mu^*_{ref}$
k	thermal conductivity of mixture, $k^*/\mu^*_{ref}\ C^*_{p,\infty}$, (also Boltzmann constant)
K^*_α	net rate of production of species α
Le	Lewis number, $\rho^*\ D^*_{ij}\ C^*_p/k^*$
M^*	molecular weight of mixture
n	coordinate normal to the bow shock, n^*/R^*_N
p	pressure, $p^*/(\rho^*_\infty\ V^{*2}_\infty)$
Pr	Prandtl number, $\mu^*\ C^*_p/k^*$
q_R	net radiant heat flux, $q^*_R/(\rho^*_\infty\ V^{*3}_\infty)$
r	radius measured from axis of symmetry to a point on the body surface, r^*/R^*_N
r_s	radius measured from axis of symmetry to a point on the bow shock, r^*_s/R^*_N
R^*	universal gas constant
R^*_b	radius of the body

R_N^* body nose radius (same as R_n^*)

R_s^* radius of the bow shock

s coordinate along the bow shock, s^*/R_N^*

T temperature, t^*/T_{ref}^*

T_o^* reference temperature, 27315 °K

T_{ref}^* reference temperature, $V_\infty^*/C_{p,\infty}^*$

u velocity tangent to body surface, u^*/V_∞^*

u' velocity tangent to bow shock, cm/sec

v velocity normal to body surface, u^*/V_∞^*

v' velocity normal to bow shock, cm/sec

x coordinate along the body surface, x^*/R_N^*

y coordinate normal to the body surface, y^*/R_N^*

α shock angle defined in fig. 2.1

ε Reynolds number parameter or surface emittance

θ body angle defined in fig. 2.1

η transformed y coordinate, y/y_s

κ body curvature, κ^*/R_N^*

κ_ν spectral absorption coefficient

μ viscosity of mixture, μ^*/μ_{ref}^*

μ_{ref}^* reference viscosity, $\mu^*(T_{ref}^*)$

ξ coordinate along the body surface, $\xi=x$

ρ density of mixture, ρ^*/ρ_∞^*

σ^* Stefan Boltzmann constant

τ optical coordinate

τ_o optical thickness

Subscript

i ith species

s shock value

w wall value

∞ free-stream condition

ν radiation frequency

1. INTRODUCTION

Radiation plays a very important role in the analyses of flow phenomena around an entry body at high-speed entry conditions. In many instances, the radiative energy transferred to the body exceeds the convective and aerodynamic heat transfers (refs. 1-10). Radiative energy transfer from the shock layer of a blunt body into the free stream reduces the total enthalpy of the shock layer while increasing the enthalpy of the free-stream gases. Because of this increase in enthalpy, the entire flow field ahead of the shock layer and around the body is influenced significantly. The precursor flow region is considered to be the region ahead of a shock wave in which the flow field parameters have been changed from free-stream conditions due to absorption of radiation from the incandescent shock layer. Most of the radiative energy transferred from the shock layer into the cold region ahead of the shock is lost to infinity unless it is equal to or greater than the energy required for dissociation of the cold gas. When the photon energy is greater than the dissociation energy, it is strongly absorbed by the cold gas in the ultraviolet continuum range. The absorbed energy dissociates and ionizes the gas, and this results in a change of flow properties in the precursor region. In particular, the temperature and pressure of the gas is increased while velocity is decreased. The change in flow properties of the precursor region, in turn, influences the flow characteristics within the shock layer itself. The problem, therefore, becomes a coupled one, and iterative methods are required for its solution.

Only a limited number of analyses on radiation-induced precursor flow are available in the literature. Works available until 1968 are discussed, in detail, by Smith (ref. 11). By employing the linearized theory of aerodynamics, Smith investigated the flow in the precursor region of a reentry body in the Earth's atmosphere. The cases of plane, spherical, and cylindrical point sources were considered, and solutions were obtained for a range of altitudes and free-stream conditions. It was found that for velocities exceeding 18 km/s, precursor flow effects are greatest at altitudes between 30 and 46 km. It was further concluded that preheating of air may cause an order of magnitude increase in the static pressure and temperature ahead of the shock wave for velocities exceeding 15 km/s. In a preliminary study, Tiwari and Szema (ref. 12) investigated the change in flow properties ahead of the bow shock of a Jovian entry body resulting from the absorption of radiation from the shock layer. The analysis was done by employing the small perturbation technique of classical aerodynamics as well as the thin layer approximation for the precursor region. By employing appropriate thermodynamic and spectral data for the hydrogen/helium atmosphere, variations in precursor region flow quantities (velocity, pressure, density, temperature, and enthalpy) were calculated by the two entirely different methods. For Jovian entry conditions, one-dimensional results obtained by the two methods were found to be in good agreement for the range of parameters considered. It was found that preheating of the gas significantly increases the static pressure and temperature ahead of the shock for entry velocities exceeding 35 km/s. It was concluded that for certain combinations of entry speeds and altitudes of entry, the precursor effects cannot be ignored while analyzing flows around Jovian entry bodies. Specifically, it was seen that at an altitude of 95 km, the precursor effects are important for entry velocities greater than 35 km/s.

In the analyses of most shock-layer flow phenomena, the contribution of radiation-induced precursor effects usually is neglected. However, a limited number of analyses which include this effect are available in the literature. Lasher and Wilson (refs. 13, 14) investigated the level of precursor absorption and its resultant effect on surface radiation heating for the Earth's entry conditions. They concluded that, for velocities less than 18 km/s, precursor heating effects are relatively unimportant in determining the radiative flux reaching the surface. At velocities greater than 18 km/s, the amount of energy loss from the shock layer and resultant precursor-heating correction was found to be significantly large. Liu (refs. 15, 16) also investigated the influence of upstream absorption by cold air on the stagnation region, shock layer radiation. The thin layer approximation was applied to both the shock layer and the preheating zone (the precursor region). The problem was formulated for the inviscid flow over smooth blunt bodies, but the detailed calculations were carried out only for the stagnation region. The general results were compared with results of two approximate formulations. The first approximate formulation neglects the upstream influence, and the second one essentially uses the iterative procedure described by Lasher and Wilson (refs. 13, 14). The results are compared for different values of a radiation/convection parameter. A few other works, related to the effects of upstream absorption by air on the shock-layer radiation, are discussed by Liu (refs. 15, 16). Some works on precursor ionization for air as well as hydrogen/helium atmosphere are presented in references 17 through 21.

The first purpose of this study is to investigate the flow properties in the entire precursor region ahead of a Jovian entry body. To accomplish this, the precursor region is assumed to be thin, and the flow in this region is considered to be inviscid. In this respect, therefore, the proposed study may appear as an extension of the analysis presented in reference 12. Next, it is proposed to investigate the influence of changes in the precursor region flow properties on the entire shock-layer flow phenomena. The flow in the shock layer is considered to be viscous and in chemical equilibrium. The solutions of the governing viscous shock-layer equations are obtained by employing the numerical procedures outlined in reference 9 and 22. It should be emphasized again that the flow phenomena in the shock and precursor regions are coupled, and iterative procedures are needed for finding solutions. In this respect the proposed investigation differs from the analysis presented in reference 12.

The basic formulation of the problem is presented in section 2. Radiation absorption models and radiative flux equations are given in section 3. The data required for finding the solutions of the governing equations are given in section 4, and the solution methods are presented in section 5. The results are obtained for the Jupiter's entry conditions and for an entry body which is a 45° hyperboloid. Precursor as well as shock-layer results are discussed in section 6.

2. BASIC FORMULATION

The physical model and coordinate system for a Jovian entry body are shown in figure 2.1. The entire flow field ahead of the body can be divided essentially into three regions: the free stream, the precursor region, and the shock layer. The flow properties are considered to be uniform at large distances from the body. In this section, basic governing equations and the boundary conditions are presented for the precursor as well as shock-layer regions.

2.1. Precursor Region

In this region, the flow is considered to be steady and inviscid. With reference to the coordinate system shown in figure 2.1, the governing equations for an axisymmetric flow can be written as (refs. 12, 23)

Mass continuity:

$$(\partial/\partial s)(\rho u r) + (\partial/\partial n)(\rho v X r) = 0 \tag{2.1}$$

Momentum:

$$\rho[u(\partial u/\partial s) + Xv(\partial u/\partial n) - Kuv] + (\partial p/\partial s) = 0 \tag{2.2}$$

$$\rho[u(\partial v/\partial s) + v(\partial v/\partial n) + Ku^2] + X(\partial p/\partial n) = 0 \tag{2.3}$$

Energy:

$$\rho[(u/X)(\partial H/\partial s) + v(\partial H/\partial n)] + (Xr)^{-1}[(\partial/\partial n)(Xrq_R)] = 0 \quad (2.4)$$

Species continuity:

$$\rho[(u/X)(\partial C_\alpha/\partial s) + v(\partial C_\alpha/\partial n)] - K_\alpha = 0 \quad (2.5)$$

where $K = K(s) = 1/R_s$, $X = 1 + Kn$. It should be noted that, according to the notations used in figure 2.1, all quantities appearing in the above equations should have a prime superscript (i.e., u', v', ρ', H', etc.), and all physical coordinates should have a superscript * (i.e., s^*, n^*, r^*, etc.). However, for the sake of clarity, these notations have been omitted from the equations.

If the precursor region is assumed to be thin, then one can make the approximation that $(n/R_s) \ll 1$, $(\partial/\partial s)$, $(\partial/\partial n)$, and R_s is not a function of n. In this case, $X = 1$, and equations (2.1) through (2.5) reduce to

$$(\partial/\partial n)\ (\rho v) = 0 \quad (2.6)$$

$$\rho v(\partial u/\partial n) = 0 \quad (2.7)$$

$$\rho v(\partial v/\partial n) + (\partial p/\partial n) = 0 \quad (2.8)$$

$$\rho v(\partial H/\partial n) + (\partial q_R/\partial n) = 0 \quad (2.9)$$

$$\rho v(\partial c_\alpha/\partial n) - K_\alpha = 0 \quad (2.10)$$

The boundary conditions for this region are the free-stream conditions and the conditions at the outer edge of the shock. For the coupled precursor/shock-layer flow phenomena, the boundary conditions at the outer edge of the shock are obtained through iterative procedures.

2.2. Shock-Layer Region

In this region, the conditions for which the present analysis is carried out are that the flow is axisymmetric, steady, laminar, and compressible. It is further assumed that the gas is in the local thermodynamic and chemical equilibrium, and that the tangent slab approximation is valid for radiative transport. For this region, the viscous shock-layer equations presented in references 9 and 22 are a set of equations that are valid uniformly throughout the shock layer. The methods of obtaining these equations are discussed in detail in the those references. First the conservation equations are written for both the inviscid and the boundary-layer regions in the body-oriented coordinate system. Then these equations are nondimensionalized in each of the two flow regions with variables which are of order one. Terms in the resulting sets of equations are retained up to second order in the inverse square root of Reynolds number. Upon combining these two sets of equations so that terms up to second order in both regions are retained, a set of equations uniformly valid to second order in the entire shock layer is obtained. The nondimensional form of the viscous shock-layer equations that are applicable in the present case can be written as

Continuity:

$$(\partial/\partial x)\Big[(r + y\cos\theta)\rho u + (\partial/\partial y)(1 + y\kappa)(r + y \times \cos\theta)\rho v\Big] = 0 \tag{2.11}$$

x-momentum:

$$\rho\left(\frac{u}{1 + y\kappa}\frac{\partial u}{\partial x} + v\frac{\partial u}{\partial y} + \frac{uv\kappa}{1 + y\kappa}\right) + \frac{1}{1 + y\kappa}\frac{\partial p}{\partial x} = \varepsilon^2\left\{\frac{\partial}{\partial y}\left[\mu\left(\frac{\partial u}{\partial y} - \frac{u\kappa}{1 + y\kappa}\right)\right] + \mu\left(\frac{2\kappa}{1 + y\kappa} + \frac{\cos\theta}{r + y\cos\theta}\right) \cdot\left(\frac{\partial u}{\partial y} - \frac{u\kappa}{1 + y\kappa}\right)\right\} \tag{2.12}$$

y-momentum:

$$\rho\left(\frac{u}{1 + y\kappa}\frac{\partial v}{\partial x} + v\frac{\partial v}{\partial y} - \frac{u^2\kappa}{1 + y\kappa}\right) + \frac{\partial p}{\partial y} = 0 \qquad (2.13)$$

Energy:

$$\rho\left(\frac{u}{1 + y\kappa}\frac{\partial H}{\partial x} + v\frac{\partial H}{\partial y}\right) - v\frac{\partial p}{\partial y} + \frac{p\kappa u^2 v}{1 + y\kappa}$$

$$= \varepsilon^2\left\{\frac{\partial}{\partial y}\left[\frac{\mu}{Pr}\frac{\partial H}{\partial y} - \frac{\mu}{Pr}\sum_{i=1}^{N_s} h_i\frac{\partial C_i}{\partial y} - \sum_{i=1}^{N_s} h_i J_i + \frac{\mu}{Pr}(Pr - 1)u\frac{\partial u}{\partial y}\right.\right.$$

$$\left. - \frac{\mu\kappa u^2}{1 + y\kappa}\right] + \left(\frac{\kappa}{1 + y\kappa} + \frac{\cos\theta}{r + y\cos\theta}\right)\left[\frac{u}{Pr}\frac{\partial H}{\partial y} - \frac{\mu}{Pr}\sum_{i=1}^{N_s} h_i\frac{\partial C_i}{\partial y}\right.$$

$$\left.\left. - \sum_{i=1}^{N_s} h_i J_i + \frac{\mu}{Pr}(Pr - 1)u\frac{\partial u}{\partial y} - \frac{\mu\kappa u^2}{1 + y\kappa}\right]\right\} - \left[\frac{\partial q_R}{\partial y}\right.$$

$$\left. + q_R\left(\frac{\kappa}{1 + y\kappa} + \frac{\cos\theta}{r}\right)\right] \qquad (2.14)$$

where $H = h + u^2/2$.

The terms used to nondimensionalize the above equations are defined as

$$x = x^*/R_n^* \qquad v = v^*/V_\infty^*$$

$$y = y^*/R_n^* \qquad \rho = \rho^*/\rho_\infty^*$$

$$r = r^*/R_n^* \qquad \mu = \mu^*/\mu_{ref}^*$$

$$K = K^*/(\mu_{ref}C_{p\infty}^*) \qquad C_p = C_p^*/C_{p\infty}^*$$

$$q_R = q_R^*/(\rho_\infty^* V_\infty^{*3}) \qquad \mu_{ref} = \bar{\mu}^*(V_\infty^{*2}/C_{p\infty}^*)$$

$$h = h^*/V_\infty^{*2} \qquad \kappa = \kappa^*/R_n^*$$

$$J_i = J_i^* R_n^*/\mu_{ref}^* \qquad \varepsilon = \left[\mu_{ref}^*/(\rho_\infty^* V_\infty^* R_n^*)\right]^{1/2} \qquad (2.15)$$

(cont'd.)

$$p = p^*/(\rho_\infty^* V_\infty^{*2}) \qquad Pr = C_p^* \mu^*/K^*$$

$$T = T^* C_{p\infty}/V_\infty^{*2} \qquad Le_{ij} = \rho^* C_p^* D_{ij}^*/K^*$$

$$u = u^*/V_\infty^* \qquad L_{ij} = \rho^* C_p^* D_{ij}^*/K^* \tag{2.15}$$

(concl'd.)

In equation (2.14), J_i represents the mass flux relative to the mass average velocity and is given by the expression (refs. 24, 25)

$$J_i = -(\mu/Pr)\left[\sum_{k=1}^{NI} \bar{b}_{iK}(\partial C_K/\partial y) + (L_i^T/T)(\partial T/\partial y)\right] \tag{2.16a}$$

where

$$\bar{b}_{iK} = \begin{Bmatrix} Le_i, & i = K \\ \Delta\bar{b}_{iK}, & i \neq K \end{Bmatrix}$$

$$Le_i = \sum_{\substack{j=1 \\ j\neq i}}^{NI} \left(\frac{C_j}{M_j}\right) \Bigg/ \sum_{\substack{j=1 \\ j\neq i}}^{NI} (C_j/M_j L_{ij})$$

$$\Delta\bar{b}_{iK} = Le_i - \left\{(M_i/M)Le_{iK} + [1-(M_i/M_K)]\sum_{j=1}^{NI} Le_{ij}C_j\right\}$$

The last term in equation (16a) represents the contribution of thermal diffusion. The quantity Le_{ij} represents the multicomponent Lewis number, and L_{ij} represents the binary Lewis Semenov numbers; both are defined in equation (2.15). If thermal diffusion can be neglected and L_{ij} can be taken as constant for all species, then equation (2.16a) reduces to

$$J_i = -(\mu/Pr)L_{ij}(\partial C_i/\partial y) \quad (2.16b)$$

In the present study, use is made of equation (2.16b), and the value for L_{ij} is taken to be 1.1 (ref. 26).

The expression for the equation of state for a hydrogen/helium mixture is given by Zobi et al. (ref. 27) as

$$T^* = C_T[(p^*/1013250)^{\ell}/(\rho^*/0.001292)^{K}] \quad (2.17a)$$

$$H^* = C_H[(p^*/1013250)^{m}/(\rho^*/0.001292)^{n}](RT_o/M) \quad (2.17b)$$

where

$$K = 0.65206 - 0.04407\ \ell n(X_{H_2})$$

$$\ell = 0.67389 - 0.04637\ \ell n(X_{H_2})$$

$$m = 0.95252 - 0.1447\ \ell n(X_{H_2})$$

$$n = 0.97556 - 0.16149\ \ell n(X_{H_2})$$

$$U_t = V_\infty \sin\theta[1 + 0.7476(1-X_{H_2})]$$

$$CTU = -545.37 + 61.608\ U_t - 22459\ U_t^2 + 0.039922\ U_t^3 - 0.00035148\ U_t^4 + 0.0000012361\ U_t^5$$

$$CHU = 5.6611 - 0.52661\ U_t + 0.020376\ U_t^2 - 0.00037861\ U_t^3 + 0.0000034265\ U_t^4 - 0.000000012206\ U_t^5$$

$$C_T = CTU + 61.2(1 - X_{H_2})$$

$$C_H = CHU - 0.3167(1 - X_{H_2})$$

and X_{H_2} represents the mole fraction of H_2.

The set of governing equations presented above has a hyperbolic/parabolic nature. The hyperbolic nature enters through the normal momentum equation. If the shock layer is assumed to be thin, then the normal momentum equation can be expressed as

$$\rho u^2 \kappa/(1 + y\kappa) = (\partial p/\partial y) \tag{2.18}$$

If equation (2.13) is replaced with equation (2.18), then the resulting set of equations is parabolic. These equations can, therefore, be solved by using numerical procedures similar to those used in solving boundary-layer problems (refs. 9, 22).

In order to solve the above set of governing equations, it is essential to specify appropriate boundary conditions at the body surface and at the shock. At the body surface, the no-slip boundary conditions are used in this study. Thus, the following conditions are imposed at the body surface:

$$u = v = 0 \tag{2.19}$$

$$T = T_b = \text{constant} \tag{2.20}$$

The conditions in front of the shock are obtained from the solution of the precursor region flow field. The conditions immediately behind the shock are obtained by using the Rankin-Hugoniot relations. The nondimensional form of the shock relations are expressed as

Mass continuity:

$$\rho_{s^-} v'_{s^-} = -\sin\alpha \tag{2.21}$$

Momentum:

$$u'_{s^-} = \cos \alpha \tag{2.22}$$

$$p_{s^-} = p_{s^+} + \sin^2 \alpha [1 - (1/\rho_{s^-})] \tag{2.23}$$

Energy:

$$h_{s^-} = h_{s^+} + [\sin^2 (\alpha/2)][1 - (1/\rho_{s^-}^2)] \tag{2.24}$$

Note that in the above equations u'_s and v'_s represent the velocity components in the shock-oriented coordinate system. The relations for u_s and v_s in the body-oriented coordinate system can be obtained from

$$u_s = u'_s \sin(\alpha + \beta) + v'_s \cos(\alpha + \beta) \tag{2.25}$$

$$v_s = - u'_s \cos(\alpha + \beta) + v'_s \sin(\alpha + \beta) \tag{2.26}$$

The governing equations and the boundary conditions presented in the above two subsections essentially describe the flow field in the precursor/shock-layer regions. In the next two sections appropriate relations for the radiative flux, thermodynamic and transport properties, and equilibrium composition of the gas will be presented.

3. RADIATION MODELS

An appropriate expression for the radiative flux q_R is needed for the solution of the energy equation presented in the previous section. This requires a suitable transport model and a meaningful spectral model for variation of the absorption coefficient of the gas. In this section, appropriate expressions for the spectral and total radiative flux are given and information on the spectral absorption by the hydrogen/helium gas is presented.

3.1. Radiative Flux Equations

The equations for radiative transport, in general, are integral equations which involve integration over both frequency spectrum and physical coordinates. In many physically realistic problems, the complexity of the three-dimensional radiative transfer can be reduced by introduction of the "tangent slab approximation." This approximation treats the gas layer as a one-dimensional slab in calculation of the radiative transport. Radiation in directions other than normal to either the body or shock is neglected in comparison. Discussions on the validity of this approximation for planetary entry conditions are given in references 28 to 32.

As mentioned earlier, the tangent slab approximation for radiative transfer is used in this study. It should be pointed out here that the tangent slab approximation is used only for the radiative transport and not for other flow variables. For a nonscattering medium and diffuse nonreflecting bounding surfaces, a one-dimensional expression for the spectral radiative flux is given by (refs. 33, 34):

$$q_{R\nu}(\tau_\nu) = 2\pi\Bigg\{\varepsilon_\nu[B_\nu(0)E_3(\tau_\nu) - B_\nu(\tau_{o\nu})E_3(\tau_{o\nu} - \tau_\nu)] + \int_o^{\tau_\nu} B_\nu(t)E_2(\tau_\nu - t)dt - \int_{\tau_\nu}^{\tau_{o\nu}} B_\nu(t)E_2(t - \tau_\nu)dt\Bigg\} \quad (3.1)$$

where

$$\tau_\nu \int_o^y \alpha_\nu(y')dy'$$

$$E_n(t) = \int_o^1 \exp(-\ t/\mu)\mu^{n-2}\ d\mu$$

$$B_\nu = (h\nu^3/c^2)[\exp(h\nu/KT) - 1]$$

The quantities $B_\nu(0)$ and $B_\nu(\tau_{o\nu})$ represent the radiosities of the body surface and shock respectively.

The expression of total radiative flux is given by

$$q_R = \int_0^\infty q_{R\nu}(\tau_\nu) d_\nu \tag{3.2}$$

To obtain specific relations for the total radiative flux for the precursor and shock-layer regions, it is essential to know the spectral absorption characteristics of the absorbing-emitting species in these regions.

In the precursor region, the radiative contribution from the free stream usually is neglected. For a diffuse, nonreflecting shock front, the expression for one-dimensional radiative flux for this region is obtained from equations (3.1) and (3.2) as

$$q_R(n) = 2\int_0^\infty \{q_\nu(0) E_3(\kappa_\nu n)$$

$$+ \pi\kappa_\nu \int_0^\infty B_\nu(T) E_2[\kappa_\nu(n - n')]dn'\}d\nu \tag{3.3}$$

where $q_\nu(0) = \varepsilon_\nu \pi B_\nu(T_s)$. In obtaining the above equation it was assumed that the absorption coefficient κ_ν is independent of position.

The information on the spectral absorption model for hydrogen/helium species in the precursor region is given in reference 12 and is briefly discussed in subsection 3.2. The model essentially consists of approximating the actual absorption of active species by three different step models. For this model, equation (3.3) can be expressed as (ref. 12):

$$q_R(n) = 2\pi \sum_{i=1}^{N} \left\{ (15/\pi^5) q(0) E_3(\kappa_i n) \int_{v_{1i}}^{v_{2i}} [v^3/(e^v - 1)] dv \right.$$

$$\left. + \kappa_i \int_0^n E_2[\kappa_i (n - n')] \int_{\nu_{1i}}^{\nu_{2i}} B_\nu(T) d_\nu dn' \right\} \tag{3.4}$$

where $v = h\nu/KT_s$ and $q(0) = \varepsilon\sigma T_s^4$. In writing the above equation it has been assumed that the shock front radiates in the precursor zone as a gray body.

In the shock layer, the radiative energy from the bow shock usually is neglected in comparison to the energy absorbed and emitted by the gas layer. This implies that the transparent shock front does not absorb but emits radiation. The expression for the net radiative flux in the shock layer, therefore, is given by

$$q_R = 2\int_0^\infty \left[q_\nu(0) E_3(\tau_\nu) + \int_0^{\tau_\nu} B_\nu(t) E_2(\tau_\nu - t) dt \right.$$

$$\left. - \int_{\tau_\nu}^{\tau_{o\nu}} B_\nu(t) E_2(t - \tau_\nu) dt \right] d\nu \tag{3.5a}$$

In this equation, the first two terms on the right represent the radiative energy transfer towards the bow shock while the third term represents the energy transfer towards the body. Upon denoting these contributions by q_R^+ and q_R^-, equation (3.5a) can be written as

$$q_R = q_R^+ - q_R^- \tag{3.5b}$$

A few spectral models for absorption by the hydrogen/helium species in the shock layer have been proposed in the literature (refs. 35 to 37). For Jovian entry conditions, the absorption by helium usually is neglected. The spectral absorption of hydrogen species was represented by a 58-step model by Sutton (ref. 36) and was approximated by a 30-step model by Tiwari and Subramanian (ref. 37). The results of these step models are compared with the detailed model of Nicolet (ref. 35) in reference 37. The 58-step model proposed by Sutton is employed in this study. The details of radiative absorption and computational procedure are given in references 36 and 37. The information on spectral absorption by this model is summarized in subsection 3.2. In essence, the step model replaces the frequency integration in equation (3.5) by a summation over 58 different frequency intervals. In each interval, the absorption coefficient is taken to be independent of frequency. For this model, equation (3.5) can be expressed as

$$q_R = 2\pi \sum_{j=1}^{N} \left\{ \varepsilon_\nu B_\nu(T_w) E_3\left[\int_0^y \alpha_\nu(y')\,d_y'\right] + \int_0^y \alpha_\nu(\xi) B_\nu(\xi) E_2\left[\int_\xi^y \alpha_\nu(y')\,dy'\right] d\xi - \int_y^{y_s} \alpha_\nu(\xi) B_\nu(\xi) E_2\left[\int_y^\xi \alpha_\nu(y')\,dy'\right] d\xi \right\} \tag{3.6}$$

where y_s denotes the shock location and N represents the number of spectral intervals. In each of the jth intervals, the absorption coefficient is assumed constant while the Planck function is not. In accordance with equation (3.5b), equation (3.6) can be expressed in terms of q_R^+ and q_R^-, and for a gray body one finds

$$q_R^+(y) = (4\pi h/c^2) \sum_{j=1}^{N} \left\{ \varepsilon F(\nu_j, T_w) E_3\left[\int_0^y \alpha_{\nu j}(y')\,dy'\right] + \int_0^y (KT/h)^4\, F(\nu_j, T)\, \alpha_{\nu j}(\xi) E_2\left[\int_\xi^y \alpha_{\nu j}(y')\,dy'\right] d\xi \right\} \tag{3.7a}$$

$$q_R^-(y) = -(4\pi h/c^2)\sum_{j=1}^{N}\left\{\int_y^{y_s}(KT/h)^4\, F(v_j,T)\alpha_{\nu j}E_2\left[\int_y^{\xi}\alpha_{\nu j}(y')\right.\right.$$

$$\left.\left.\times\, dy'\right]d\xi\right\} \tag{3.7b}$$

where

$$F(\nu_j,T_w) = \int_{\nu_{j1}}^{\nu_{j2}}\{\nu^3/[\exp(h\nu/KT_w) - 1]\}d\nu$$

$$F(v_j,T) = \int_{v_{j1}}^{v_{j2}}\{\nu^3/[\exp(v) - 1]\}dv,\ v = h\nu/KT$$

From the knowledge of the temperature distribution normal to the body, equations (3.7) can be solved by numerical integration over frequency and space. The final temperature profile is obtained through an iterative procedure. Use of equations (3.7) is made in obtaining the radiative flux towards the body and shock as well as the net radiative flux.

For evaluation of the radiative flux, usually it is essential to express the exponential integrals $E_n(t)$ in simpler approximate forms. Quite often, these integrals are approximated by appropriate exponential functions (refs. 33, 34). In this study it was established that better results are obtained if the exponential integrals are expressed in series form for small and large arguments. The series expansion of the exponential integral of first order is given as

For $t < 1$:

$$E_1(t) = -0.5772 - \ln t + t - \frac{t^2}{2(2)!} + \frac{t^3}{3(3)!} + \ldots \tag{3.8a}$$

For $t > 1$:

$$E_1(t) = \exp(-t)\left[\frac{a_0 + a_1t + a_2t^2 + a_3t^3 + t^4}{t(b_0 + b_1t + b_2t^2 + b_3t^3 + t^4)}\right] \tag{3.8b}$$

where

$a_0 = 0.26777343$ $\qquad b_0 = 3.958469228$

$a_1 = 8.63476089$ $\qquad b_1 = 21.09965309$

$a_2 = 18.059016973$ $\qquad b_2 = 25.63295614$

$a_3 = 8.57322874$ $\qquad b_3 = 9.5733223454$

Relations for exponential integrals of higher order are obtained by employing the recursion relations given in reference (34).

3.2. Radiation Absorption Model

Appropriate spectral models for gaseous absorption are needed for solutions of the radiative flux equations. Information on spectral absorption by the precursor and shock-layer species is presented in this subsection.

3.2.1. Spectral absorption model for precursor region: - In the precursor region, the photoionization absorption coefficient is a continuous nonzero function of photon energy (because of bound-free transition) for all values of photon energy that exceed the ionization potential of the atom. Similar remarks apply to the photodissociation and radiative recombination. A critical review of ultraviolet photoabsorption cross sections for molecules of astrophysical and aeronomic interest, available in the literature up to 1971, is given by Hudson (ref. 38). Specific information on photoionization and absorption coefficient of molecular hydrogen is available in references 38 to 44.

Photoionization and absorption cross sections of H_2, as obtained from references 38 to 44, are plotted in figure 3.1. From this figure it is evident that the ionization continuum starts at about 804 Å and continues towards lower wavelengths. Between the wavelengths of 600 Å and 804 Å, the absorption cross section for the ionization continuum is included in the total absorption (i.e., absorption due to ionization as well as dissociation). For wavelengths below 600 Å, however, the ionization continuum absorption is equal to the total absorption. The total absorption cross section for the continuum range below 804 Å can be closely approximated by the two rectangles (I and II) shown in the figure with broken lines. The ratio of the ionization cross section to the total absorption cross-section (i.e., the value of Y_I) is taken to be unity for rectangle I and 0.875 for rectangle II. For wavelengths greater than 804 Å (where $h\nu$ is below ionization energy), the value Y_I is taken to be zero. Little information is available in the literature on the absorption cross section for dissociation of H_2 molecules. There is strong evidence, however, that photodissociation starts at about 2600 Å and continues towards lower wavelengths to about 750 Å (refs. 39 to 41). There are also a few diffuse bands in this spectral range (refs. 39, 41). Thus, it becomes difficult to evaluate the absorption cross section in this spectral range. For this study, the absorption cross section in the spectral range between 804 Å and 2600 Å was approximated by rectangle III. The specific values of $\sigma(\nu)$ for the three rectangles are found to be $\sigma_I(\nu)$ = 4.1 E-18, $\sigma_{II}(\nu)$ = 8.2 E-18, and $\sigma_{III}(\nu)$ = 2.1 E-18. The value of Y_D is taken to be zero for rectangle I and 0.125 for rectangle II. The numerical procedure for employing this model in the radiative flux equations is discussed in detail in reference 12 and is summarized in section 5.

<u>3.2.2. Spectral absorption model for shock layer</u>: - As mentioned earlier, the 58-step model proposed by Sutton (ref. 36) for spectral absorption by the hydrogen species in the shock layer is employed in this study. For atomic hydrogen, all three transitions (bound-bound, bound-free, and free-free) are considered. The total absorption of the jth step is a summation of the average absorption for the ith transitions in the jth step, i.e.,

$$\bar{\kappa}_j = \sum_i \kappa_{ij} \tag{3.9a}$$

$$\kappa_{ij} = (1/\Delta\nu_j) \int_{\nu_j}^{\nu_j+\Delta\nu_j} \kappa_i d\nu \tag{3.9b}$$

$$\kappa_i = f(T, N_i, \nu) \tag{3.9c}$$

where N_i represents the number density in cm^{-3}.

For the free-free transition, the absorption coefficient is calculated by

$$\kappa_{ff}^{H} = (2.61E - 35) N_e N_{H^+} / (\nu^3 T^{1/2}) \tag{3.10}$$

The absorption coefficient for bound-free transitions is calculated by employing two separate relations as

$$\kappa_{bf}^{H} = (1.99E - 14)(N_H/\nu^3) \sum_{n_\ell=1}^{4} (1/n_\ell^3) \exp(C_1), \quad 1 \leq n_\ell \leq 4 \tag{3.11a}$$

$$\kappa_{bf}^{H} = (6.31E - 20)(TN_H/\nu^3) \exp(C_2) \exp(C_3), \quad 5 \leq n_\ell \leq n_{\ell,max} \tag{3.11b}$$

where

$$C_1 = (-157780/T)[1 - (1/n_\ell^2)]$$

$$C_2 = (-157780/T)(1 - \delta/13.6)$$

$$C_3 = [(157780/T)(1/25 - \delta/13.6)] - 1$$

$$\delta = (1.79E - 5)(N_e^{2/7})/(T^{1/7})$$

In the above equations, n_ℓ represents the principal quantum numbers, δ is the reduction in ionization potential in eV, and the values 157780 and 13.6 are the ionization potential in °K and eV respectively.

The bound-bound transitions are included for principle quantum numbers up to five. The absorption coefficient is calculated by using the relation

$$\kappa_{bb}^{H} = SL(\nu) \tag{3.12}$$

where S is the line strength and $L(\nu)$ is the line shape factor. The line strength is given by the relation

$$S = (1.10E - 16) f n_{\ell}^{2} N_{H} \exp[(-157780/T)(1 - 1/n_{\ell}^{2})] \tag{3.13}$$

The line shape factor is given by the relation

$$L(\nu) = \gamma / \left\{\pi[\gamma^{2} + (\nu - \nu_{o})^{2}]\right\} \tag{3.14}$$

where ν_o is the frequency at the line center and α is the line half-width, and these are given by

$$\nu_{o} = 13.6[(1/n_{\ell}^{2}) - (1/n_{u}^{2})] \tag{3.15}$$

$$\gamma = a[1.05E\ 15(n_{u}^{2} - n_{\ell}^{2})N_{e}^{2/3}] \tag{3.16}$$

The constant a in the above equation is taken to be 0.642 for the first line and unity for the remaining lines.

The absorption coefficients for the free-free and bound-free transitions of the negative hydrogen are

$$\kappa_{ff}^{H^-} = (6.02E - 39)N_{H}N_{e}/\nu^{3} \tag{3.17}$$

$$\kappa_{bf}^{H^-} = (2.89E - 17)(\beta^{4} - 4\beta^{3} + 3.64\beta^{2} + 0.73\beta)N_{H^-} \tag{3.18}$$

where $\beta = 1.502/\nu$. The threshold for the bound-free transition of H^- is 0.757 eV.

The absorption coefficient for molecular hydrogen in the jth step is obtained in accordance with equation (3.9) and is expressed as

$$\bar{\kappa}_j^{H_2} = f_j(T) N_{H_2} \tag{3.19}$$

where $f_j(T)$ is dependent on the particular step. The molecular bands cover the steps from 7 to 17 eV.

Further details on constructing the step-function model and utilizing it in the radiative flux equations are given in references 36 and 37.

4. PHYSICAL CONDITIONS AND DATA SOURCE

For this study, the entry body is considered to be a 45° hyperboloid blunt body which enters the Jovian atmosphere at a zero degree angle of attack. The body nose radius, R_N^*, is taken to be 23 cm. The body surface is assumed to be gray having a surface emittance of 0.8, and the surface temperature is taken to be uniform at 4,000 °K.

4.1. Free-Stream Conditions

Information on Jupiter's atmospheric conditions are available in reference 45, and some of these are illustrated in figure 4.1. For different altitudes of entry, the free-stream conditions used in this study are given in reference 12 and are summarized in table 4.1. The free-stream atmospheric composition is assumed to be 85 percent hydrogen and 15 percent helium by mole fraction. The temperature of the atmosphere is taken to be constant at 145 °K, and the free-stream enthalpy is given by the relation $H_\infty = 1.527 \; RT_\infty$. The number density of hydrogen can be calculated by the relation

$$N_{H_2} = (7.2431172 \times 10^{22})(p_\infty/T_\infty) X_{H_2} \tag{4.1}$$

where X_{H_2} is the mole fraction of H_2 and p_∞ has units of N/m^2.

Table 4.1. Altitudes of entry and free-stream conditions for Jovian entry.

Z km	$\bar{V}_\infty$ cm/sec	ρ_∞ g/cm^3	T_∞ K	p_∞ dync/cm^2	$\rho_\infty \bar{V}_\infty^3$	ε
116	3.909E6	4.65E-7	145	2.44E3	2.777E13	0.006645
143	4.517E6	1.27E-7	145	6.66E2	1.17E13	0.01272
190	4.736E6	1.33E-8	145	69	1.412E12	0.03930
225	4.756E6	2.50E-9	145	13	2.69E11	0.09064
261	4.758E6	4.53E-10	145	2.38	4.879E10	0.2129

4.2. Gaseous Composition of Precursor and Shock-Layer Regions

Initially the gas composition ahead of the shock is, of course, the free-stream composition. Absorption of high intensity radiation from the shock, however, produces H, H_2^+, and electrons in the precursor region as a result of photodissociation and photoionization. Any other species which may be produced usually are neglected. Thus, the precursor gas is considered to be a mixture of H_2, He, H, H_2^+, and e^-. Further information on production of these species in the precursor region is available in reference 12.

The shock-layer gas is assumed to be in chemical equilibrium and is taken to be a mixture of eight chemical species, H_2, H, H^+, H^-, He, H_e^+, He^{++}, and e^-. The number density of these species are obtained by considering five chemical reactions as

1. $H_2 \rightleftarrows 2H$

2. $H \rightleftarrows H^+ + e^-$

3. $He \rightleftarrows He^+ + e^-$

4. $He^+ \rightleftarrows He^{++} + e^-$

5. $H^- \rightleftarrows H + e^-$ (4.2a)

In general, these reactions can be expressed by

$$\sum a_i A_i \rightleftarrows \sum b_i B_i \tag{4.2b}$$

The number densities (particle/m^3) are related to the equilibrium constant for the jth reaction by

$$K_j = [\Pi N^{b_i}(B_i)]/[\Pi N^{a_i}(A_i)] \tag{4.3}$$

The equilibrium constants are calculated from the species partition function, and for the five chemical reactions they are found to be (ref. 36)

$$\ell n\ K_1 = 52.2042 + 0.5\ \ell n\ T$$
$$+ \ell n[1 - \exp(-6331/T)] - 51964/T$$

$$\ell n\ K_2 = 35.4189 + 1.6\ \ell n\ T - 157810/T$$

$$\ell n\ K_3 = 36.8052 + 1.5\ \ell n\ T - 285287/T$$

$$\ell n\ K_4 = 35.4189 + 1.5\ \ell n\ T - 631310/T$$

$$\ell n\ K\ \ = 36.8052 + 1.5\ \ell n\ T - 8750/T \tag{4.4}$$

The conservation equations for the hydrogen and helium nuclei and charge are

$$N_H + 2N_{H_2} + N_{H^+} + N_{H^-} = N_H^O \tag{4.5}$$

$$N_{He} + N_{He^+} + N_{He^{++}} + N^o_{He} \quad (4.6)$$

$$N_{H^+} + N_{He^+} + 2N_{He^{++}} - N_{H^-} = N_{e^-} \quad (4.7)$$

The number densities of the hydrogen and helium nuclei are calculated by

$$N^o_H = 2x_{H_2}(A_o\rho/M_o) \quad (4.8)$$

$$N^o_{He} = x_{He}(A_o\rho/M_o) \quad (4.9)$$

where

$$M_o = 2.016x_{H_2} + 4.003x_{He}$$

In the above equations, A_o represents the Avogadro's constant, ρ is the mixture density in g/cm^3, x_{H^2} is the mole fraction of molecular hydrogen, and x_{He} is the mole fraction of helium.

The solution procedure for obtaining the eight unknown number densities is discussed in reference 36. The closed-form solutions are obtained by solving equation (4.3) for each reaction independently. This is accomplished by setting the appropriate values in equations (4.5) to (4.7) to zero if the species are not present in the reaction. The closed-form solutions for the number densities (in particles/cm^3) of each species are given by

$$H_2: \quad N_{H_2} = (N^o_H/2) + (K_1/8)[(1 + 8N^o_H/K_1)^{1/2} - 1] \quad (4.10)$$

$$H^+: \quad N_{H^+} = (K/2)[(1 + 4N^o_H/K_2)^{1/2} - 1] \quad (4.11)$$

$$H: \quad N_H = N^o_H - 2N_{H_2} - N_{H^+} \quad (4.12)$$

$$H_e^{+}: \quad N_{He}^{+} = (D_1/2)[(1 + 4K_3N_{He}^{o}/D_1^2)^{1/2} - 1], \quad D_1 = K_3 + N_{H^+} \tag{4.13}$$

$$He^{++}: \quad N_{He}^{++} = (D_2/2)[(1 + 4K_4N_{He}^{o}/D_2^2)^{1/2} - 1], \quad D_2 = K_4 + N_H + N_{He}^{o} \tag{4.14}$$

$$He: \quad N_{He} = N_{He}^{o} - N_{He} + N_{He}^{++} \tag{4.15}$$

$$e^{-}: \quad N_{e^-} = N_{H^+} + N_{He}^{+} + 2N_{He}^{++} \tag{4.16}$$

$$H^{-}: \quad N_{H^-} = N_H N_{e^-}/K_5 \tag{4.17}$$

4.3 Thermodynamic and Transport Properties

Thermodynamic properties for specific heat, enthalpy, and free energy, and transport properties for viscosity and thermal conductivity are required for each species considered in different flow regimes. For the precursor zone as well as shock layer, the general expression for total enthalpy, specific enthalpy, and specific heat at constant pressure are given respectively by

$$H_T = h + (u^2 + v^2)/2 \tag{4.18}$$

$$h = \sum x_i h_i = \sum (C_\alpha/M_\alpha) h_\alpha \tag{4.19}$$

$$C_p = \sum x_i C_{pi} \tag{4.20}$$

However, specific relations for h and C_p for the two regions are quite different.

For the precursor region, the relation for the specific enthalpy is obtained by following the procedure described by Smith (ref. 1) as

$$h = 1.4575RT + (0.75RT + D)C_H + (1.25RT + I/2)C_{H_2^+} \qquad (4.21)$$

where D and I represent the dissociation and ionization energy respectively, and their values are available in reference 40.

The derivation of equation (4.21) essentially follows from the consideration of equation (4.19). If it is assumed that the internal energy of each particle can be described only by translational and rotational modes, then the relation for specific enthalpy of each species can be expressed as

$$h_{He} = \frac{3}{2} RT + p/\rho = \frac{5}{2} RT$$

$$h_{H_2} = \frac{3}{2} RT + \frac{2}{2} RT + p/\rho + I = \frac{7}{2} RT$$

$$h_{H_2^+} = \frac{3}{2} RT + \frac{2}{2} RT + p/\rho + I = \frac{7}{2} RT + I$$

$$h_H = \frac{3}{2} RT + p/\rho + D = \frac{5}{2} RT + D$$

$$h_e = \frac{5}{2} RT$$

Also, from the conservation of charged particles one can write

$$C_e/M_e = C_{H_2^+}/M_{H_2^+}$$

Now , for 85 percent H_2 and 15 percent He on volume basis (or 76 percent H_2 and 24 percent He on mass basis), equation (4.19) is written as

$$\sum(C_\alpha/M_\alpha)h_\alpha = (0.26/4)(5RT/2) + [(0.74 - C_{H_2^+} - C_H)/2](7RT/2)$$

$$+ [(5RT/2 + D)]C_H + (7RT/2 + I)(C_{H_2^+}/2)$$

$$+ (5RT/2)(C_{H_2^+}/2)$$

A simplification of the above equation results in equation (4.21).

In the shock region, equations (4.19) and (4.20) are used to calculate h and C_p. With x_i representing the mole fraction of the ith species, the expressions for h_i and C_{pi} are found from references 46 and 47 as

$$h_i = RT[a_1 + (a_2/2)T + (a_3/3)T^2 + (a_4/4)T^3$$

$$+ (a_5/5)T^4 + a_6/T] \tag{4.22}$$

$$C_{pi} = R(a_1 + a_2T + a_3T^2 + a_4T^3 + a_5T^4 \tag{4.23}$$

where R is the universal gas constant (= 1.98726 cal/mole - K) and T is the local fluid temperature in K. For different species, values of the constants a_1, a_2, ... a_6 are given in reference 47, and for species under present investigation they are listed in table 4.2. It should be pointed out here that in this study, instead of employing equation (2.17b), equations (4.18), (4.19), and (4.22) are used to calculate the enthalpy variation in the shock layer. This is because slightly better results are obtained by using the above set of equations.

For the shock-layer gas, the mixture viscosity and thermal conductivity are obtained by using the semi-empirical formulas of Wilke (ref. 48) as

Table 4.2. Coefficient for evaluation of the specific heat at constant pressure and enthalpy for various hydrogen/helium species.

Species	Coefficients						Temp. Range
	a_1	a_2	a_3	a_4	a_5	a_6	K
	2.5	0	0	0	0	2.547162E+4	> 300
H	2.5	0	0	0	0	2.547162E+4	> 1,000
	2.475164	7.366387E-5	-2.537593E-8	2.386674E-12	4.551431E-17	2.523626E+4	> 6,000
	3.057445	2.676520E-3	-5.809916E-6	5.521039E-9	-1.812273E-12	-9.889047E+2	> 300
H_2	3.10019	5.111946E-4	5.264421E-8	-3.490997E-11	3.694534E-15	-8.773804E+2	> 1,000
	3.363	4.656000E-4	-5.127000E-8	2.802000E-12	4.905000E-17	-1.018000E+3	> 6,000
	2.5	0	0	0	0	1.840334E+5	> 300
H^+	2.5	0	0	0	0	1.840334E+5	> 1,000
	2.5	0	0	0	0	1.840334E+5	> 6,000
	2.5	0	0	0	0	-7.453749E+2	> 300
He	2.5	0	0	0	0	-7.453749E+2	> 1,000
	2.5	0	0	0	0	-7.453749E+2	> 6,000
	2.5	0	0	0	0	2.853426E+5	> 300
He^+	2.5	0	0	0	0	2.853426E+5	> 1,000
	2.5	0	0	0	0	2.853426E+5	> 6,000
	2.5	0	0	0	0	-7.453749E+2	> 300
e^-	2.5	0	0	0	0	-7.453749E+2	> 1,000
	2.508	-6.332000E-6	1.364000E-9	-1.094000E-13	2.934000E-18	-7.450000E+2	> 6,000

$$\mu = \sum_{i=1}^{N} [x_i \mu_i / (\sum_{j=1}^{N} x_j \phi_{ij})] \tag{4.24}$$

$$K = \sum_{i=1}^{N} [x_i K_i / (\sum_{j=1}^{N} x_j \phi_{ij})] \tag{4.25}$$

where

$$\phi_{ij} = [1 + (\mu_i/\mu_j)^{1/2} (M_j/M_i)^{1/4}]^2 / \{\sqrt{8}[1 + (M_i/M_j)]\}^{1/2}$$

and M_i is the molecular weight of species i. For hydrogen/helium species, specific relations for viscosity and thermal conductivity are given in references 49 and 50. The viscosity of H_2 and He, as a function of temperature, can be obtained from reference 49 as

$$\mu_{H_2} = (0.66 \times 10^{-6})(T)^{3/2}/(T + 70.5) \tag{4.26}$$

$$\mu_{He} = (1.55 \times 10^{-6})(T)^{3/2}/(T + 97.8) \tag{4.27}$$

The thermal conductivity of H_2 and H are obtained from reference 50 as

$$K_{H_2} = 3.212 \times 10^{-5} + (5.344 \times 10^{-8})T \tag{4.28}$$

$$K_H = 2.496 \times 10^{-5} + (5.129 \times 10^{-8})T \tag{4.29}$$

The viscosity of H and thermal conductivity of He are obtained from the relation between viscosity and thermal conductivity of monatomic gases as given in reference 48 by

$$K = (15/4)(R/M)\mu \tag{4.30}$$

Very little information is available on transport properties of other species such as H_2^+, H^+, e^-, etc. Fortunately, transport properties are important only in the boundary-layer region where the temperature is not high enough to produce these species.

It should be noted that all relations presented in this section are expressed in dimensional form.

5. SOLUTION PROCEDURES

An iterative procedure has been used to couple the precursor and shock-layer solutions. In this method, the shock-layer solutions are obtained first with no consideration of precursor effect. From this solution, the radiative flux at the shock front (which influences the precursor region flow) is determined. By employing this value of the radiative flux, different precursor region variables are calculated through use of equations (2.6) through (2.10). Values of these flow variables are obtained just ahead of the bow shock, and then the Rankine-Hugoniot relations are used to determine the conditions behind the shock. These conditions are used to obtain new shock-layer solutions from which a new value of the radiative flux at the shock is calculated. The procedure is continued until the radiative flux at the shock becomes invariant.

The solution procedures for the precursor and shock-layer regions are described in some detail in the following subsections.

5.1. Precursor Region Solutions

A direct integration of equations (2.6) through (2.10) results in the following governing equations for the precursor region

$$\rho v = \rho_\infty v_\infty \tag{5.1}$$

$$\rho_\infty v_\infty (u - u_\infty) = 0 \tag{5.2}$$

$$\rho_\infty v_\infty (v - v_\infty) + (p - p_\infty) = 0 \tag{5.3}$$

$$\rho_\infty\ v_\infty(H - H_\infty) + q_R = 0 \tag{5.4}$$

$$\rho_\infty\ v_\infty(\partial C_\alpha/\partial n) - K_\alpha = 0 \tag{5.5}$$

In equation (5.4), H represents the total enthalpy and is given by a combination of equations (4.18) and (4.21). The expression for the radiative flux, q_R, is given by equation (3.4). For the present application, equation (5.5) will be written for atomic hydrogen and hydrogen ions. By following the procedure outlined in reference 12 and 19 the expressions for species concentration are found to be

$$C_H = -2\beta_4 \sum_{i=1}^{N} Y_{D_i} E_3(\tau_i)(kT_s)^{-1} I(v_i^2) \tag{5.6}$$

$$C_{H_2^+} = -2\beta_4 \sum_{i=1}^{N} Y_{I_i} E_3(\tau_i)(kT_s)^{-1} I(v_i^2) \tag{5.7}$$

where

$$\beta_4 = (15/\pi^4)[q(0)m_1/(\rho_\infty V_\infty)]$$

$$I(v_i^2) = \int_{v_{1i}}^{v_{2i}} \{v^2/[\exp(v) - 1]\}dv$$

and m_1 represents the weight of the H_2 molecule in grams per molecule.

Note that there are nine algebraic equations to evaluate the nine unknowns ρ, v, u, p, h, H, C_H, $C_{H_2^+}$. The solutions of this set of algebraic equations are obtained by using the Gauss-Seidel method (ref. 51). The properties at the infinity are used as the first initial guess in the Gauss-Seidel method. The iteration is continued until all the quantities in this region become invariant. The flow chart of the computational procedure is illustrated in figures 5.1 and 5.2.

5.2. Shock-Layer Solutions

A numerical procedure for solving the viscous shock-layer equations for stagnation and downstream regions is given by Davis (ref. 22). Moss applied this method of solution to reacting multicomponent mixtures in references 9 and 10. A modified form of this procedure is used in this study to obtain solutions of the viscous shock-layer equations. In this method, a transformation is applied to the viscous shock-layer equations in order to simplify the numerical computations. In this transformation most of the variables are normalized with their local shock values. The transformed variables are (ref. 9):

$$\eta = y/y_s \qquad \bar{p} = p/p_s \qquad \bar{\mu} = \mu/\mu_s$$

$$\xi = x \qquad \bar{\rho} = \rho/\rho_s \qquad \bar{K} = K/K_s$$

$$\bar{u} = u/u_s \qquad \bar{T} = T/T_s \qquad \bar{C}_p = C_p/C_{ps}$$

$$\bar{v} = v/v_s \qquad \bar{H} = H/H_s \tag{5.8}$$

The transformations relating the differential quantities are

$$\frac{\partial}{\partial x}\;(\;) = \frac{\partial}{\partial \xi}\;\frac{1}{y_s}\;(dy_s/d\xi)\,\eta\frac{\partial}{\partial \eta}\;(\;) \tag{5.9a}$$

where

$$\frac{\partial}{\partial y}\;(\;) = \frac{1}{y_s}\,\frac{\partial}{\partial \eta}\;(\;),\quad \frac{\partial^2}{\partial y^2}\;(\;) = \frac{1}{y_s^2}\,\frac{\partial^2}{\partial \eta^2}\;(\;) \tag{5.9b}$$

The transformed equations can be expressed in a general form as

$$\partial^2 W/\partial\eta^2 + a_1\partial W/\partial\eta + a_2 W + a_3 + a_4\partial W/\partial\xi = 0 \tag{5.10}$$

The quantity W represents $\bar{u}$ in the x-momentum equation, $\bar{T}$ in the temperature energy equation, $\bar{H}$ in the enthalpy energy equation, and C_i in the species continuity equations. In most cases, the coefficients a_1 to a_4 to be used in this study are exactly the same as given in reference 9. However, there is one exception. Since radiation is included in the present study, the coefficients of the energy equation are different from those used in reference 9. For example, in the enthalpy energy equation, coefficients a_1, a_2, and a_4 are the same as given in reference 9, but a_3 is different, and this is given by

$$a_3 = \frac{P_{r,s}\bar{P}_r y_s^2}{\mu_s \bar{\mu} H_s}\left[\frac{1}{y_s}\frac{\partial \Psi}{\partial \eta} + \left(\frac{\kappa}{1 + y_s \eta \kappa} + \frac{\cos\theta}{r + y_s \eta \cos\theta}\right)\Psi\right]$$

$$+ \frac{y_s P_r p_s v_s \bar{v}}{\varepsilon^2 \mu_s \bar{\mu} H_s}\frac{\partial p}{\partial \eta} - \frac{y_s^2 \bar{P}_r P_{r,s}}{\varepsilon^2 \mu_s H_s \bar{\mu}}\left[\frac{1}{y_s}\frac{\partial q_R}{\partial \eta}\right.$$

$$\left. + q_R\left(\frac{\kappa}{1 + y_s \eta \kappa} + \frac{\cos\theta}{r + y_s \eta \cos\theta}\right)\right] \tag{5.11}$$

where

$$\psi = \frac{\mu s}{y_s Pr,s}\left[\frac{0.1\bar{\mu}}{Pr}\sum_{i=1}^{N} h_i \frac{\partial C_i}{\partial \eta} + \frac{u_s^2 \bar{\mu}\bar{u}}{\bar{P}r}(Pr,_s\bar{P}_r - 1)\frac{\partial \bar{\mu}}{\partial \eta}\right]$$

$$- \frac{\mu_s \mu_s^2 \kappa \bar{\mu} u^2}{1 + y_s \eta \kappa}$$

Other transformed equations are the same as given in reference 9.

The surface boundary conditions in terms of transformed variables are

$$\bar{\mu} = 0,\ \bar{v} = 0,\ \bar{T} = \bar{T}_w \tag{5.12}$$

The transformed shock conditions are found to be

$$\bar{u} = \bar{v} = \bar{T} = \bar{H} = \bar{\rho} = \bar{p} = 1 \tag{5.13}$$

at $\eta = 1$.

The second order partial differential equations as expressed by equation (5.10), along with the surface boundary and shock conditions, are solved by employing an implicit finite-difference method. In order to obtain numerical solutions for the downstream region, it is necessary to have an accurate stagnation streamline solution. Since the shock shape is affected by the downstream flow, a truncated series of shock standoff distance is used to develop the stagnation streamline equations. As such, the shock standoff distance is expressed by

$$y_s = y_{1s} + y_{2s}\,\xi^2 + \cdots \tag{5.14}$$

Since ξ is small and the curvature κ is approximately one in the stagnation region, it is logical to say that (see fig. 2.1)

$$\beta \simeq \xi \tag{5.15}$$

Since $\theta = (\pi/2) - \beta$, there is obtained

$$\begin{aligned} \alpha &= \theta + \tan^{-1}[(\partial n_s/\partial\xi)/(1 + \kappa y_s)] \\ &= (\pi/2) + \xi\left\{[2y_{2s}/(1 + y_{1s})] - 1\right\} \end{aligned} \tag{5.16}$$

By using equations (5.14) to (5.16), the shock relations [eqs. (2.21) - (2.26)] can be expressed in terms of expanded variables as

$$v^*_{s^-} = 1/\rho_{s^-},\ v_{s^-} = 1/\rho_{s^-} \tag{5.17}$$

$$u^*_{s^-} = -\xi[2y_{2s}/(1 + y_{1s}) - 1] \tag{5.18}$$

$$u_{s^-} = \xi\left\{1 - [2y_{2s}/(1 + y_{1s})](1 + 1/\rho_{s^-})\right\} \tag{5.19}$$

$$\begin{aligned} p_{s^-} = p_{s^+} + (1 - 1/\rho_{s^-}) + \xi^2\Big\{&(1 - 1/\rho_{s^-}) \\ &\cdot [1 - 2y_{2s}/(1 + y_{1s})]^2\Big\} \end{aligned} \tag{5.20}$$

$$h_{s^-} = h_{s^+} + (1 - 1/\rho_{s^-})/2 \tag{5.21}$$

In equations (5.17) through (5.21), only p_s and u_s involve y_{2s} in the first terms of their expansions. Thus, a series expansion for the flow variables is assumed about the axis of symmetry with respect to nondimensional distance ξ near the stagnation streamline as

$$p(\xi,\eta) = p_1(\eta) + p_2(\eta)\xi^2 + --- \tag{5.22a}$$

$$u(\xi,\eta) = u_1(\eta)\xi + --- \tag{5.22b}$$

$$v(\xi,\eta) = v(\eta) + --- \tag{5.22c}$$

$$\rho(\xi,\eta) = \rho_1(\eta) + --- \tag{5.22d}$$

$$T(\xi,\eta) = T_1(\eta) + --- \tag{5.22e}$$

$$\mu(\xi,\eta) = \mu_1(\eta) + --- \tag{5.22f}$$

$$K(\xi,\eta) = K_1(\eta) + --- \tag{5.22g}$$

$$C_p(\xi,\eta) = C_{p_1}(\eta) + --- \tag{5.22h}$$

$$C_i(\xi,\eta) = C_{i_1}(\eta) + --- \tag{5.22i}$$

Since y_{2s} is a function of downstream flow, it cannot be determined by the stagnation solutions. Thus, a value of $y_{2s} = 0$ is assumed initially. This assumption is removed by iterating on the solution by using the previous shock standoff distances to define y_{2s}.

The new form of x-momentum and energy equations in the ξ,η plane can be written as

$$\frac{\partial^2 W}{\partial \eta^2} + a_1 \frac{\partial W}{\partial \eta} + a_2 W + a_3 = 0 \tag{5.23}$$

For x-momentum, $W = \bar{u}$ and coefficients a_1, a_2, and a_3 are exactly the same as given in reference 9. For the enthalpy equation, $W = \bar{H}$ and again a_1 and a_2 are the same as defined in reference 9, but a_3 is given by

$$a_3 = (Pr,_{1s} y_{1s}^2/\mu_{1s} H_{1s})(Pr,_1/\bar{\mu}_1)[(1/y_{1s})(\partial\Psi/\partial\eta)$$

$$+ 2\Psi/(1 + \eta y_{1s})] + (y_{1s} \bar{P}_r p_s v_s \bar{v}_1/\varepsilon^2 \mu_s \bar{\mu} H_s)(\partial\bar{p}_1/\partial\eta) \quad (5.24)$$

Other stagnation streamline equations are the same as given in reference 9. It should be noted that at the body surface $\bar{p}_1 = 1$ and $\bar{p}_2 = 0$.

As mentioned earlier, the governing second-order partial differential equations are solved by employing an implicit finite-difference method. For this purpose, the shock layer is considered as a network of nodal points with a variable grid space in the η-direction. The scheme is shown in figure 5.3, where m is a station measured along the body surface and n denotes the station normal to the body surface. The derivatives are converted to finite-difference form by using Taylor's series expansions. Thus, unequal space central difference equations in the η-direction at point m, n can be written as

$$\left.\frac{\partial W}{\partial\eta}\right)_n = \frac{\Delta\eta_{n-1}}{\Delta\eta_n(\Delta\eta_{n-1} + \Delta\eta_n)} W_{m,n+1} - \frac{\Delta\eta_n}{\Delta\eta_{n-1}(\Delta\eta_{n-1} + \Delta\eta_n)} W_{m,n-1}$$

$$+ \frac{\Delta\eta_n - \Delta\eta_{n-1}}{\Delta\eta_n \Delta\eta_{n-1}} W_{m,n} \quad (5.25a)$$

$$\left.\frac{\partial^2 W}{\partial\eta^2}\right)_n = \frac{2}{\Delta\eta_n(\Delta\eta_n + \Delta\eta_{n-1})} W_{m,n+1} - \frac{2}{\Delta\eta_n \Delta\eta_{n-1}} W_{m,n}$$

$$+ \frac{2}{\Delta\eta_{n-1}(\Delta\eta_n + \Delta\eta_{n-1})} W_{m,n-1} \quad (5.25b)$$

$$\frac{\partial W}{\partial \xi}\Big)_m = \frac{W_{m,n} - W_{m-1,n}}{\Delta\xi} \tag{5.25c}$$

A typical difference equation is obtained by substituting the above equations in equation (5.10) or (5.23) as

$$W_{m,n} = -(D_n/B_n) - (A_n/B_n)W_{m,n+1} - (C_n/B_n)W_{m,n-1} \tag{5.26}$$

where

$$A_n = (2 + a_1\Delta\eta_{n-1})/[\Delta\eta_n(\Delta\eta_n + \Delta\eta_{n-1})]$$

$$B_n = -[2 - a_1(\Delta\eta_n - \Delta\eta_{n-1})]/(\Delta\eta_n\Delta\eta_{n-1}) - a_2 - a_4/\Delta\xi_{m-1}$$

$$C_n = (2 - a_1\Delta\eta_n)/[\Delta\eta_{n-1}(\Delta\eta_n + \Delta\eta_{n-1})]$$

$$D_n = a_3 - a_4 W_{m-1,n}/\Delta\xi_{m-1}$$

Now, if it is assumed that

$$W_{m,n} = E_n W_{m,n+1} + F_n \tag{5.27}$$

or

$$W_{m,n-1} = E_{n-1}W_{m,n} + F_{n-1} \tag{5.28}$$

then by substituting equation (5.28) into equation (5.26), there is obtained

$$W_{m,n} = [-A_n/(B_n + C_nE_{n-1})]W_{m,n+1} + (-D_n - C_nF_{n-1})/(B_n + C_nE_{n-1}) \tag{5.29}$$

By comparing equations (5.27) and (5.29), one finds

$$E_n = - A_n/(B_n + C_n E_{n-1}) \tag{5.30}$$

$$F_n = (- D_n - C_n F_{n-1})/(B_n + C_n E_{n-1}) \tag{5.31}$$

Now, since E_1 and F_1 are known from the boundary conditions, E_n and F_n can be calculated from equations (5.30) and (5.31). The quantities $W_{m,n}$ at point m, n can now be calculated from equation (5.27).

The overall solution procedure starts with evaluation of the flow properties immediately behind the shock by using the Rankine-Hogoniot relations. With known shock and body surface conditions, each of the second-order partial differential equations are integrated numerically by using the tridiagonal formalism of equation (5.10) and following the procedure described by equations (5.26) to (5.31). As mentioned before, the solutions are obtained first for the stagnation streamline. With this solution providing the initial conditions, the solution is marched downstream to the desired body location. The first solution pass provides only an approximate flow-field solution. This is because in the first solution pass the thin shock-layer form of momentum equation is used, the stagnation streamline solution is assumed to be independent of downstream influence, the term $dy_s/d\xi$ is equated to zero at each body station, and the shock angle α is assumed to be the same as the body angle θ. All these assumptions are removed by making additional solution passes.

In the first solution pass, the viscous shock-layer equations are solved at any location m after obtaining the shock conditions (to establish the outer boundary conditions) from the precursor region solutions. The converged solutions at station m-1 are used as the initial guess for the solutions at station m. The solution is then iterated locally until convergence is achieved.

For the stagnation streamline, guess values for dependent variables are used to start the solution. In the first local iteration, both $(\partial y_s/\partial \xi)$ and $(\partial W/\partial \xi)$ are assumed to be zero. The energy equation then is integrated numerically to obtain a new temperature. By using this temperature, new values of thermodynamic and transport properties are calculated. Next, the x-momentum equation is integrated to find the $\bar{u}$ component of velocity. The continuity equation is used to obtain both the shock standoff distance and the $\bar{v}$ component of velocity. The pressure $\bar{p}$ is determined by integrating the normal momentum equation. The equation of state is used to determine the density. For example, the integration of the stagnation streamline continuity equation from 0 to η results in

$$[(1 + y_{1s}\eta)^2 \rho_{1s} v_{1s} \rho_1] v_1 = (-2y_{1s}\rho_{1s}u_{1s})A \tag{5.32}$$

where

$$A = \int_0^\eta (1 + y_{1s}\eta)\bar{\rho}_1\bar{u}_1 d\eta \tag{5.32}$$

This equation gives the v-velocity component along the stagnation streamline. However, integration of the continuity equation from $\eta = 0$ to $\eta = 1$ results in

$$(1 + y_{1s})^2 \rho_{1s} v_{1s} = - 2\rho_{1s}u_{1s}y_{1s}(B + C) \tag{5.33}$$

where

$$B = \int_0^1 \bar{\rho}_1\bar{u}d\eta, \quad C = y_{1s}\int_0^1 \bar{\rho}_1\bar{u}_1\eta d\eta$$

The shock standoff distance can be obtained from the solution of equation (5.33) as

$$y_{1s} = \frac{-(2v_{1s} + 2Bu_{1s}) + [(2v_{1s} + 2Bu_{1s})^2 - 4(v_{1s} + 2Cu_{1s})v_{1s}]^{1/2}}{2(v_{1s} + 2Cu_{1s})} \qquad (5.34)$$

Similarly, other quantities at the stagnation streamline are obtained.

With known stagnation streamline solution and body surface and shock conditions, the above procedure is used to find solutions for any body location m. The downstream shock standoff distance and the v-velocity component are obtained by integrating the continuity equation in the η-direction from 0 to 1, and 0 to η respectively. Integration of the continuity equation from $\eta = 0$ to $\eta = 1$ results in

$$\frac{\partial}{\partial \xi}[y_s^2 \cos\theta\ \rho_s u_s \int_0^1 \bar{\rho}\bar{u}\eta d\eta + y_s r \rho_s u_s \int_0^1 \bar{\rho}\bar{u} d\eta$$

$$= (r + y_s \cos\theta)[y_s^1 \rho_s u_s - (1 + y_s\kappa)\rho_s v_s] \qquad (5.35)$$

By defining, for station m

$$C_1 = \cos\theta\ \rho_s u_s \int_0^1 \bar{\rho}\bar{u}\eta d\eta, \quad C_2 = r\rho_s u_s \int_0^1 \bar{\rho}\bar{u} d\eta$$

and denoting the same relations by C_3 and C_4 for station m-1, equation (5.35) can be expressed in terms of a difference equation as

$$[(C_1 y_s^2 + C_2 y_s)_m - (C_3 y_s^2 + C_4 y_s)_{m-1}]/\Delta\xi$$

$$= r\rho_s u_s y'_{sm} + \cos\theta\ \rho_s u_s y'_{sm} y_{sm} - r\rho_s v_s$$

$$- r\rho_s v_s \kappa y_{sm} - \cos\theta\ \rho_s v_s y_{sm} - \cos\theta\ \rho_s v_s \kappa y_{sm}^2 \qquad (5.36)$$

This can be expressed in a quadratic form as

$$(AA)y_{sm}^2 + (BB)y_{sm} + (CC) = 0 \tag{5.37}$$

where

$$AA = C_1 + \cos\,\theta\kappa\rho_s v_s\Delta\xi$$

$$BB = C_2 + r\rho_s v_s\kappa\Delta\xi - \cos\,\theta\;\rho_s u_s y_s'\Delta\xi + \cos\,\theta\;\rho_s v_s\Delta\xi$$

$$CC = -\;[C_3(y_s)_{m-1}^2 + C_4(y_s)_{m-1} + r\rho_s u_s y_s'\Delta\xi - r\rho_s v_s\Delta\xi]$$

The shock standoff distance at station m is obtained from equation (5.37) as

$$y_{sm} = \{-(BB) + [(BB)^2 - 4(AA)(CC)]^{1/2}\}/2(AA) \tag{5.38}$$

The v-velocity component can be obtained in a similar manner. Integration of the continuity equation from 0 to y gives

$$\frac{\partial}{\partial\xi}\left[\int_0^{\eta} y_{sm}(r + y_{sm}\eta\,\cos\,\theta)\rho_s u_s\bar{\rho}\bar{u}d\eta\right]$$

$$+\;(r + y_{sm}\eta\,\cos\,\theta)[(1 + \eta y_{sm}\kappa)(\rho_s v_s\bar{\rho}\bar{v})$$

$$-\;y_{sm}'\eta\rho_s u_s\bar{\rho}\bar{u}] = 0 \tag{5.39}$$

As before, this can be expressed in terms of a difference equation as

$$\left\{\left[(KK)_m - (KK)_{m-1}\right]/\Delta\xi\right\} + (II)_m\bar{v} + (JJ)_m = 0 \tag{5.40}$$

where

$$(II)_m = (r + y_{sm}\eta \cos\theta)(1 + y_{sm}\eta\kappa)\rho_s v_s \bar{\rho}$$

$$(JJ)_m = -(r + y_{sm}\eta \cos\theta) y'_{sm}\eta\rho_s u_s \bar{\rho}\bar{u}$$

$$(KK)_m = \int_0^{\eta} y_{sm}(r + y_{sm}\eta \cos\theta)\rho_s u_s \bar{\rho}\bar{u}\, d\eta$$

Thus, the v-velocity component at each point on the station m can be obtained from equation (5.40). Other quantities at station m are obtained by a similar manner. As mentioned before, the first pass is only an approximate solution because of several inherent assumptions. These assumptions are removed by iteration in the next pass. For the subsequent solution passes, the shock angle and y_{2s} are given by

$$\alpha = \theta + \tan^{-1}[y'_{sm}/(1 + \kappa y_{sm})] \tag{5.41}$$

$$y_{s_2} = (y_{s_3} - y_{s_1})/4(\Delta\xi)^2 \tag{5.42}$$

The flow diagrams for computation procedure are shown in figures 5.1, figures 5.4 to 5.8.

6. RESULTS AND DISCUSSION

The governing equations of both the precursor and shock-layer regions were solved for physically realistic Jovian entry conditions. Results of the complete parametric study are presented in this section. First, the results are presented for quantities just behind the shock wave, and then a few results of flow variables within the shock layer are presented. Next, results are presented for the entire shock-precursor region. Finally, a few results are presented to demonstrate the influence of precursor heating (i.e., preheating of the gas in front of the shock) on different heat fluxes.

The radiative flux from the shock layer towards the precursor region is found to be highest at the stagnation line shock location.

Results of the radiative flux from the shock front are shown in figure 6.1 for different altitudes of entry. As would be expected, precursor heating results in a higher radiative flux at the shock front. It is seen that the radiative flux reaches a maximum value for an altitude of about 116 km, and the largest precursor effect (PE) of about 8 percent is found to be for this altitude. This is a direct consequence of the free stream and entry conditions at this altitude. For other entry conditions (altitudes), precursor effects are seen to be relatively lower.

Figure 6.2 shows the shock standoff variation with distance along the body surface for different entry altitudes. The shock standoff distance, in general, is seen to decrease with increasing altitudes. This is because higher entry velocities are associated with higher altitudes. The precursor heating results in a slight increase in the shock standoff distance (a maximum of about 2 percent for z = 116 km) because the density of the shock layer is slightly reduced.

The conditions just behind the shock are illustrated in figures 6.3 to 6.8 as a function of distance along the body for different entry altitudes. For z = 116 km, figure 6.3 shows that precursor heating increases the enthalpy by a maximum of about 2 percent at the stagnation streamline. The change in shock temperature is shown in figure 6.4 for different altitudes. As would be expected, precursor heating results in a relatively higher temperature. The effect of precursor heating on the pressure just behind the shock is shown in figure 6.5, and it is seen to be very small. Since the pressure essentially remains unchanged, precursor heating results in a decrease in the density, (see fig. 6.6) mainly because of an increase in the temperature. Figure 6.7 shows that precursor heating has no significant influence on the u-velocity component, but the v-velocity is slightly increased (see fig. 6.8) as a result of decrease in the shock density.

Variations in temperature, pressure, density, velocity, chemical species, and transport properties across the shock layer are shown in figures 6.9 to 6.13 for entry conditions corresponding to an altitude of z = 116 km. Results presented in these figures are normalized by their shock values, and they show that precursor effects are felt throughout the shock layer. Results presented in figures 6.9 to 6.11 for two body locations ($\xi = 0$ and 1) indicate the relative change in temperature, pressure, density, and velocity as compared with their shock values. For $\xi = 0$, figure 6.12 shows that precursor heating slightly decreases the concentration (mole fraction) of atomic hydrogen and increases the concentration of ions and electrons throughout the shock layer. For the stagnation streamline, results presented in figure 6.13 indicate that the transport properties (μ and K) are changed only slightly in the vicinity of the bow shock.

Variations of temperature, pressure, density, and velocity along the stagnation streamline in the entire shock-layer/precursor zone are illustrated in figures 6.14 to 6.17 for different altitudes. Since higher entry velocities are associated with higher altitudes, precursor effects, in general, are found to be larger for higher altitudes. The results for the precursor region show a dramatic increase in the pressure and temperature but only a slight change in the density and velocity. The changes are largest near the shock front because a major portion of radiation from the shock layer gets absorbed in the immediate vicinity of the shock front. A complete discussion on changes in flow variables in the precursor region is given by Tiwari and Szema in reference 12. Figures 6.14 and 6.15 show that, in spite of a large increase in the temperature and pressure in the precursor region, precursor heating does not change the temperature and pressure distribution in the shock layer dramatically. The change in temperature, however, is significant, the maximum change occurring, as would be expected, just behind the shock. There is a slight change in the pressure near the body, but virtually no change closer to the shock. Figure 6.16 shows that the change in density in the shock layer is higher for higher altitudes and towards the shock.

As discussed before, precursor heating results in a slight decrease in the shock-layer density. Virtually no change in the u-component of the shock-layer velocity was found, but, as shown in figure 6.17, the v-component is slightly increased.

The effects of precursor heating on different heat fluxes in the shock layer are illustrated in figures 6.18 to 6.24. These results clearly demonstrate that precursor heating has a significant influence on increasing the heat transfer to the entry body. This increase essentially is a direct consequence of higher shock-layer temperatures resulting from the upstream absorption of radiation. Figures 6.18 to 6.20 show the variations in radiative and convective heat fluxes with distance along the body surface for three different altitudes. For $z = 116$ km, results illustrated in figure 6.19 reveal that the precursor heating results in a 7.5 percent increase in the radiative flux and about a 3 percent increase in the convective flux to the body at the stagnation point. The increase in heat transfer at other body locations and for other entry conditions (altitudes) is relatively lower. A similar conclusion can be drawn from the results presented in figures 6.21 to 6.23 for the radiative flux towards the shock and the body for two body locations ($\xi = 0$ and 1) and for three different entry conditions. Results of radiative and convective heat flux at the body (for $\xi = 0$) are illustrated in figure 6.24 for different altitudes of entry. The radiative flux results are seen to follow the trend exhibited in figure 6.1 for radiation at the shock front. The convective heat flux, however, is seen to increase slowly with the altitude up to $z = 131$ km, and thereafter to decrease with increasing altitudes. The precursor effect is found to increase the radiative heating by a maximum of about 7.5 percent at $z = 116$ km and the convective heating by 4.5 percent at $z = 131$ km.

It should be emphasized here that the results presented in this study were obtained for carefully selected entry conditions. For other conditions, precursor heating may have an entirely different influence on flow variables in the shock layer. For example, if entry velocities higher than 38 km/s are considered for altitudes lower than 116 km, then one would expect precursor heating to have a considerably greater influence on the shock layer flow phenomena. This, in turn, would result in higher radiative and convective heating of the entry body.

7. CONCLUSIONS

The main objective of this study was to investigate the influence of precursor heating on the entire shock-layer flow phenomena. For Jovian entry conditions, results were obtained for the precursor zone as well as the shock layer. For the precursor region, results indicate that the temperature and pressure are increased significantly because of absorption of radiation from the shock layer, but only a slight change is noticed in other flow variables. In the shock layer, results of flow variables were obtained along the body and the bow shock and across the shock layer for different altitudes of entry. The influence of precursor heating was found to be larger at higher altitudes. Specific results indicate that, in most cases, precursor heating has a maximum influence on flow variables (except the pressure) at the stagnation line shock location. It was found that while pressure essentially remains unchanged in the shock layer, the precursor heating results in an increase in the enthalpy, temperature, and v-component of velocity, and a decrease in the shock layer density. For the entry conditions considered in this study, results clearly demonstrate that precursor heating has a significant influence on increasing the heat transfer to the entry body. It was found that the radiative heating is increased by 7.5 percent at $z = 116$ km and the convective heating by 4.5 percent at $z \approx 131$ km.

For further study, it is suggested that the precursor region flow phenomena be investigated without making the thin layer approximation. Also, it would be advisable to use different free-stream temperatures for different entry altitudes. In the shock layer, the case of chemically nonequilibrium flow should be included, and then the influence of precursor heating on different flow variables should be investigated.

REFERENCES

1. Anderson, J.D.: An Engineering Survey of Radiating Shock Layers. AIAA , vol. 7, no. 9, Sept. 1969, pp. 1665-1675.

2. Olstad, W.B.: Nongray Radiating Flow About Smooth Symmetric Bodies. AIAA, vol. 9, no. 1, Jan. 1971, pp. 122-130.

3. Callis, L.B.: Coupled Nongray Radiating Flow About Long Blunt Bodies. AIAA, vol. 9, no. 4, April 1971, pp. 553-559.

4. Sutton, K.: Characteristic of Coupled Nongray Gas Flows with Ablation Product Effects About Blunt Bodies During Planetary Entries. Ph.D. Dissertation, North Carolina State Univ., 1973.

5. Sutton, K.: Coupled Nongray Radiating Flow About Ablating Planetary Entry Bodies. AIAA, vol. 12, no. 8, Aug. 1974, pp. 1099-1105.

6. Walberg, G.D.; and Sullivan, E.M.: Ablative Heat Shields for Planetary Entries - A Technology Review. Presented at the ASTM/IES/AIAA Space Simulation Conference, Gaithersburg, Md., 1970.

7. Rigdon, W.S.; Dirling, R.B., Jr.; and Thomas, M.: Stagnation Point Heat Transfer During Hypervelocity Atmospheric Entry. NASA CR-1462, Feb. 1970.

8. Page, W.A.: Aerodynamic Heating for Probe Vehicles Entering the Outer Planets. AAS Paper no. AAI-71-144, 1971.

9. Moss, J. N.: Reacting Viscous-Shock-Layer Solutions with Multicomponent Diffusion and Mass Injection. NASA TR R-411, June 1974.

10. Moss, J.N.: Radiative Viscous-Shock-Layer Solutions with Coupled Ablation Injection. AIAA, vol. 14, no. 9, Sept. 1976, pp. 1311-1316.

11. Smith, G.L.: Radiation-Induced Precursor Flow Field Ahead of a Reentering Body. Ph.D. dissertation, Virginia Polytechnic Institute, March 1968. Also, AIAA paper no. 68-667, June 1968.

12. Tiwari, S.N.; and Szema, K.Y.: Radiation-Induced Precursor Flow Field Ahead of a Jovian Entry Body. Technical report NAS1-11707-92, May 1977, School of Engineering, Old Dominion Univ., Norfolk, Va. Also, AIAA paper no. 77-768, June 1977.

13. Lasher, L.E.; and Wilson, K.H.: Effect of Shock Precursor Absorption on Superorbital Entry Heating. AIAA, vol. 6, no. 12, Dec. 1968, pp. 2419-2420.

14. Lasher, L.E.; and Wilson, K.H.: Effect of Shock Precursor Heating on Radiative Flux to Blunt Bodies. NASA CR-1265, Feb. 1969.

15. Liu, J.T.C.: Synoptic: Influence of Upstream Absorption on the Stagnation Region Shock Layer Radiation. AIAA, vol. 8, no. 10, Oct. 1970, pp. 1729-1730.

16. Liu, J.T.C.: Influence of Upstream Absorption on the Stagnation Region Shock Layer Radiation. AIAA, vol. 8, no. 10, Oct. 1970, pp. 1730-1737.

17. Murty, S.S.R.: Effect of Line Radiation on Precursor Ionization. J. Quantitative Spectroscopy & Radiative Transfer, vol. 8, no. 1, Jan. 1968, pp. 531-554.

18. Nelson, H.F.; and Goulard, R.: Structure of Shock Waves with Nonequilibrium Radiation and Ionization. The Physics of Fluids, vol. 12, no. 8, Aug. 1969, pp. 1605-1617.

19. Perri, A.N.; and Clarke, J.H.: Radiative Ionization Patterns in Cold Precursor of Axisymmetric Detached Shock. AIAA, vol. 8, no. 9, Sept. 1970, pp. 1574-1581.

20. Leibowitz, L.P.; and Kuo, T.J.: Ionizational Nonequilibrium Heating During Outer Planetary Entries. AIAA, vol. 14, no. 9, Sept. 1976, pp. 1324-1329.

21. Livingston F.R.; and Poon, T.Y.: Relaxation Distance and Equilibrium Electron Density Measurement in Hydrogen-Helium Plasmas. AIAA, vol. 14, no. 9, Sept. 1976, pp. 1335-1337.

22. Davis, R.T.: Numerical Solution of the Hypersonic Viscous Shock-Layer Equations. AIAA, vol. 8, May 1970, pp. 843-851.

23. Hayes, W.D.; and Probstein, R.F.: Hypersonic Flow Theory: vol. I, Inviscid Flows. Academic Press, 1966.

24. Blottner, F.G.: Finite Difference Methods of Solution of the Boundary-Layer Equations. AIAA, vol. 8, no. 2, Feb. 1970, pp. 193-205.

25. Blottner, F.G.: Viscous Shock Layer at the Stagnation Point with Nonequilibrium Air Chemistry. AIAA, vol. 7, no. 12, Dec. 1969, pp. 2281-2287.

26. Grier, N.T.: Calculation of Transport Properties and Heat Transfer Parameters of Dissociating Hydrogen. NASA TN D-1406, 1962.

27. Zoby, E.V.; Gnoffo, P.A.; and Graves, R.A.: Correlations for Determining Thermodynamic Properties of Hydrogen-Helium Gas Mixtures at Temperatures from 7,000 to 35,000 K. NASA TN D-8262, Aug. 1976.

28. Kennet, H.; and Strack, S.L.: Stagnation Point Radiative Heat Transfer: ARS J., vol. 31, no. 3, 1961, pp. 370-372.

29. Hoshizaki, H.; and Lasher, L.E.: Convective and Radiative Heat Transfer to an Ablating Body. AIAA, vol. 6, no. 8, 1968, pp. 1441-1449.

30. Chien, Kuei-Yuan: Application of the S_n Method to Spherically Symmetric Radiative-Transfer Problems. AIAA paper no. 71-466, 1971.

31. Wilson, K.H.: Evaluation of One-Dimensional Approximations for Radiative Transport in Blunt Body Shock Layers. LMSC N-EE-71-3, Lockheed Missiles and Space Co., Sunnyvale, Calif., 1971.

32. Page, W.A.: Aerodynamic Heating for Probe Vehicles Entering the Outer Planets. AAS paper no. AAS-71-144, 1971.

33. Vincenti, W.G.; and Kruger, C.H.: Introduction to Physical Gas Dynamics, John Wiley and Sons, 1965.

34. Sparrow, E.M.; and Cess, R.D.: Radiation Heat Transfer, Brooks/Cole Publishing Co., Belmont, Calif., 1966.

35. Nicolet, W.E.: Users Manual for RAD/EQUIL/1973, A General Purpose Radiation Transport Program. NASA CR-132470, 1973.

36. Sutton, K.: A 58-Step Radiation Model for Absorption by Hydrogen Species (unpublished work). Also, Zoby, E.V.; Sutton, K.; Olstad, W.B.; and Moss, J.N.: An Approximate Inviscid Radiating Flow Field Analysis for Outer Planet Entry Probes. AIAA paper no. 78-189, Jan. 1978.

37. Tiwari, S.N.; and Subramanian, S.V.: Significance of Radiation Models in Investigating the Flow Phenomena Around a Jovian Entry Body. Technical Report NAS1-14193-26, Jan. 1978, School of Engineering, Old Dominion Univ., Norfolk, Va. Also, AIAA paper no. 78-188, Jan. 1978.

38. Hudson, R.D.: Critical Review of Ultraviolet Photoabsorption Cross Section for Molecules of Astrophysical and Aeronomic Interest, Review of Geophysics and Space Physics, vol. 9, no. 2, May 1971, pp. 305-406.

39. Lee, P.; and Weissler, G.L.: Absolute Absorption of the H_2 Continuum. Astrophysical J., vol. 115, 1952, pp. 570-571.

40. Ditchburn, R.W.: Absorption of Ultra-Violet Radiation by the Atmospheric Gases. Proceedings of the Royal Society, Series A, Mathematical and Physical Sciences No. 1205, vol. 236, Aug. 1956, pp. 216-226.

41. Cook, G.R.; and Metzer, P.H.: Photoionization and Absorption Cross Section of H_2 and D_2 in the Vacuum Ultraviolet Region. J. Opt. Soc. America, vol. 54, no. 8, Aug. 1964, pp. 968-972.

42. Samson, J.A.R.; and Cairns, R.B.: Total Absorption Cross Section of H_2, N_2, and O_2 in the Region 550-200 Å. J. Opt. Soc. America, vol. 55, no. 8, Aug. 1965, p. 1035.

43. McCarty, R.D. Hydrogen Technology Survey: Thermophysical Properties. NASA Report SP-3089, 1975.

44. Lee, L.C.; Carson, R.W.; and Judge, D.L.: The Absorption Cross Sections of H_2 and D_2 from 180 to 780°A. J. Quantitative Spectroscopy and Radiation Transfer, vol. 16, no. 10, Oct. 1972, pp. 873-877.

45. Anon., The Planet Jupiter, NASA Report SP-8069, Dec. 1971.

46. Babu, S.G.: Approximate Thermochemical Tables for Some C-H and C-H-O Species. NASA CR-2178, March 1973.

47. McBride, B.J.; Heimel, S.; Ehlers, J.G.; and Gordon, S.: Thermodynamic Properties to 6000°K for 210 Substances Involving the First 18 Elements. NASA Report SP-3001, 1963.

48. Bird, R.B.; Stewart, W.E.; and Lightfoot, E.N.: Transport Phenomena, John Wiley & Sons Inc., 1960.

49. Hall, N.A.: Thermodynamics of Fluid Flow, Prentice Hall, Inc., 1957.

50. Esch, D.D.; Pike, R.W.; Engel, C.D.; Farmer, R.C.; and Balhoff, J.F.: Stagnation Region Heating of a Phenotic-Nylon Ablator During Return from Planetary Mission. NASA CR-112026, Sept. 1971.

51. Gerald, C.F.: Applied Numerical Analysis, Addison Wesley, 1970.

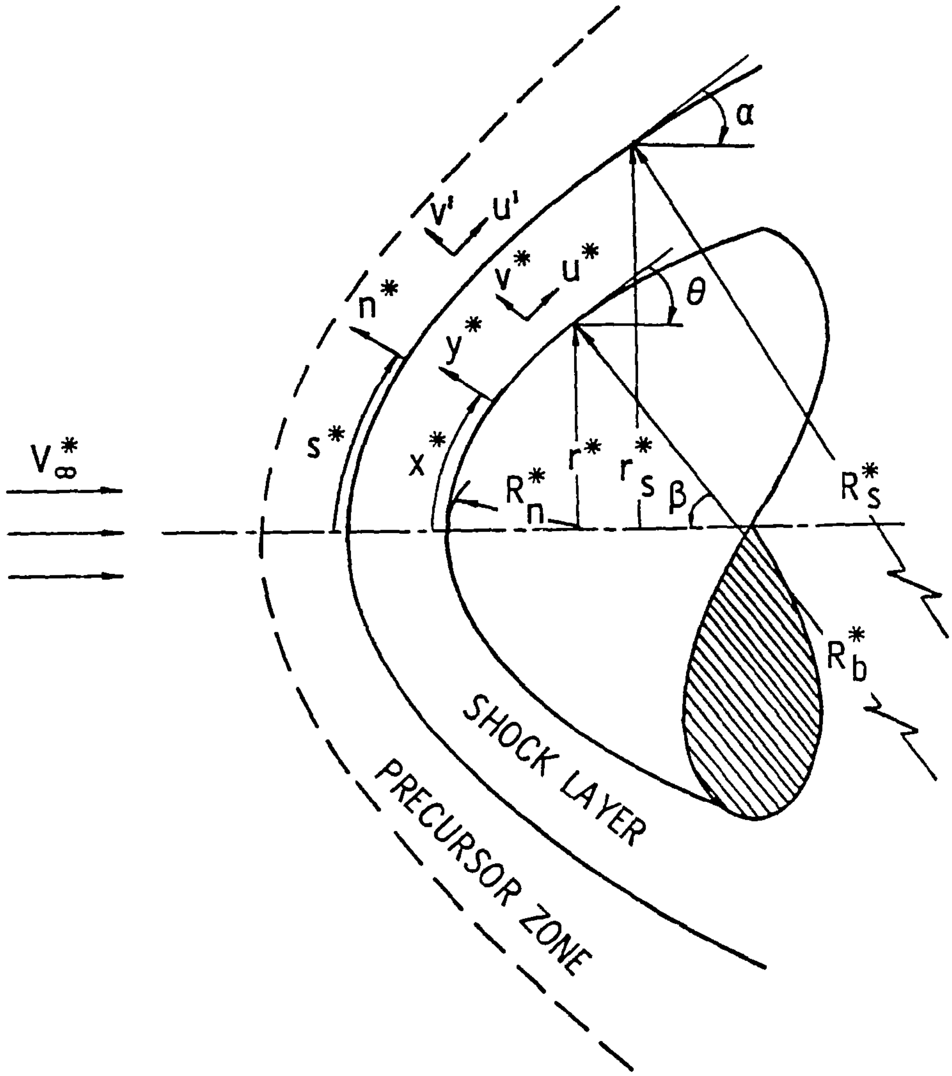

Figure 2.1. Physical model and coordinate system.

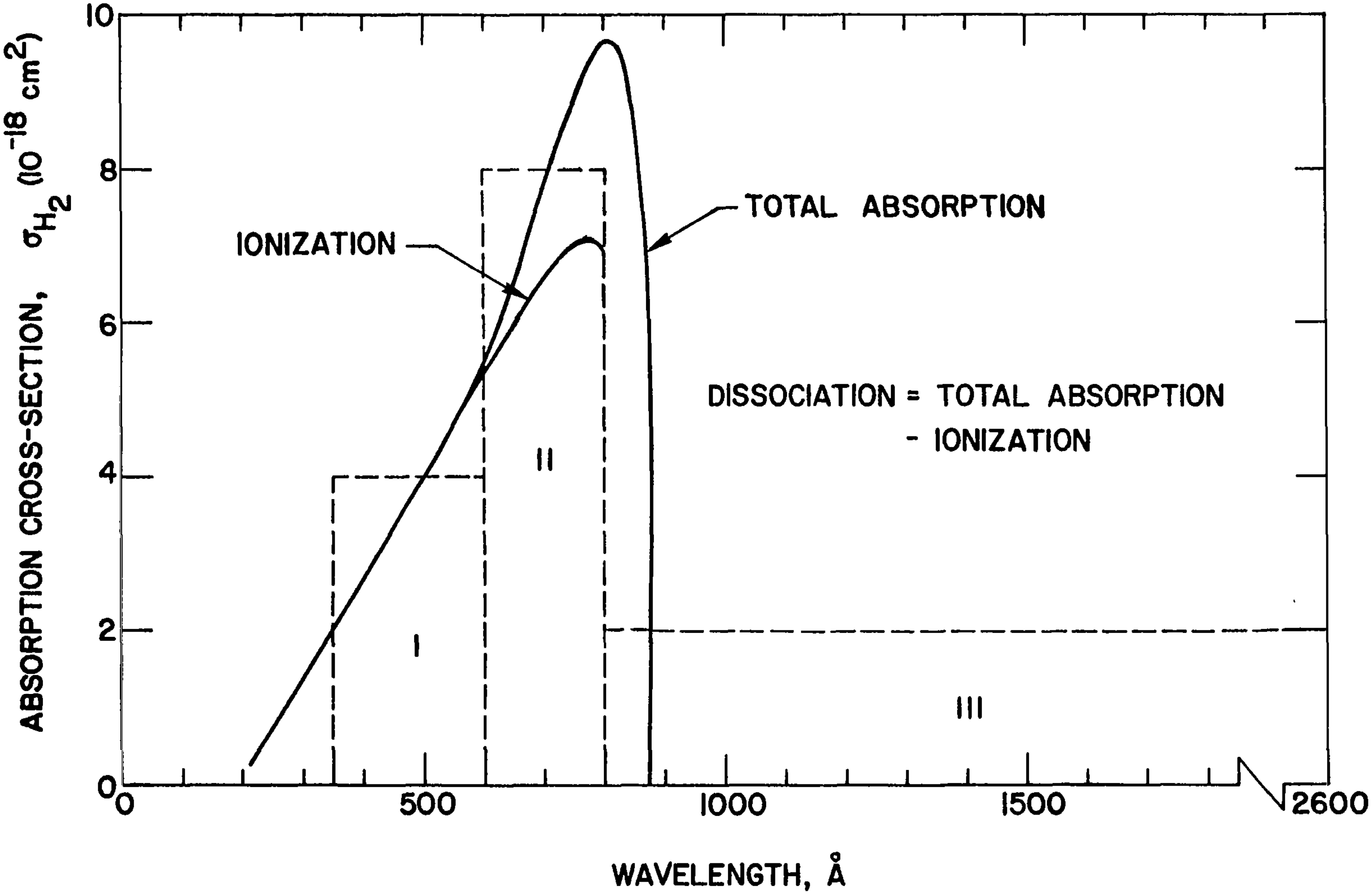

Figure 3.1. Absorption cross section of H_2 in ultraviolet region.

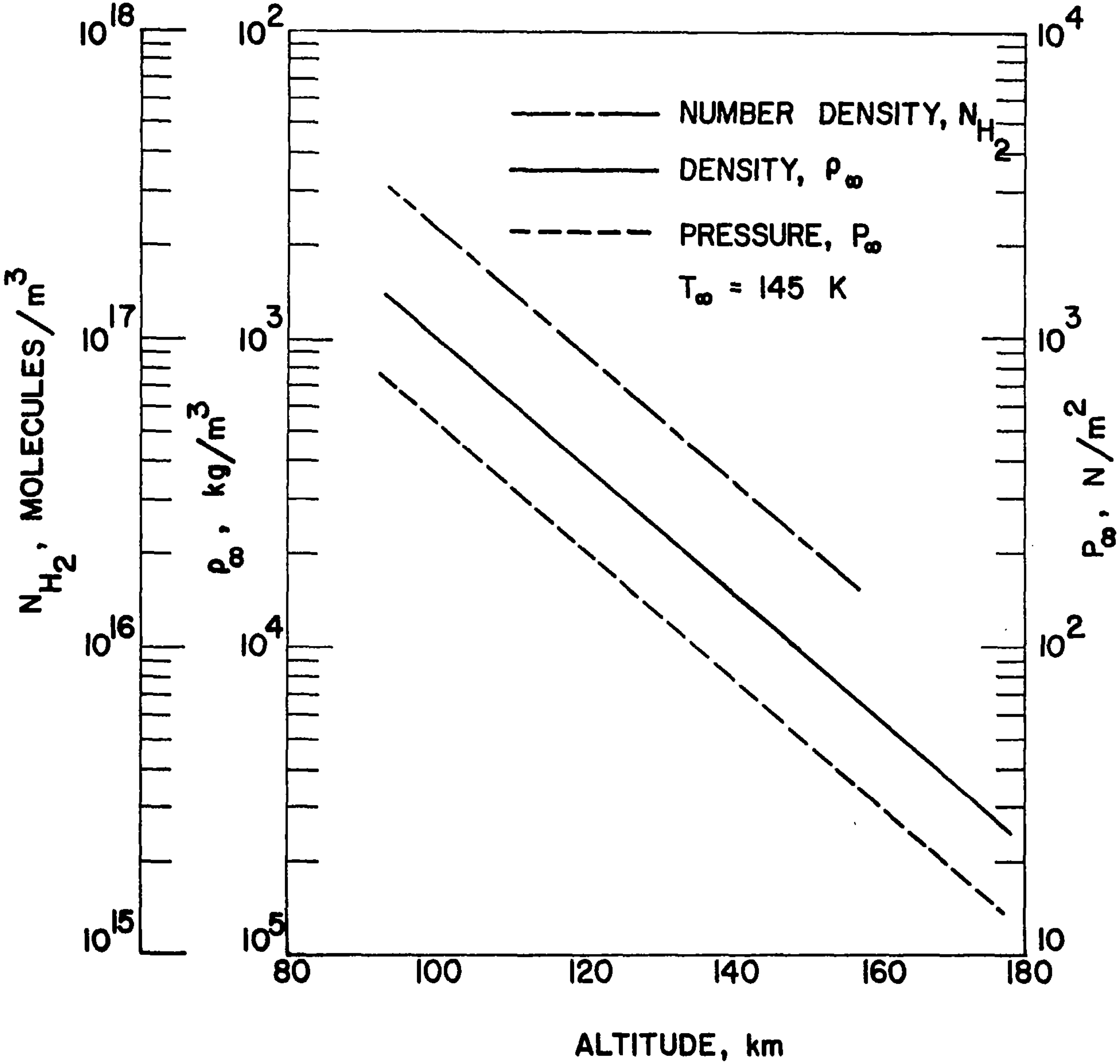

Figure 4.1. Atmospheric conditions for Jupiter's entry.

PRECURSOR SHOCK-LAYER SOLUTION PROCEDURE

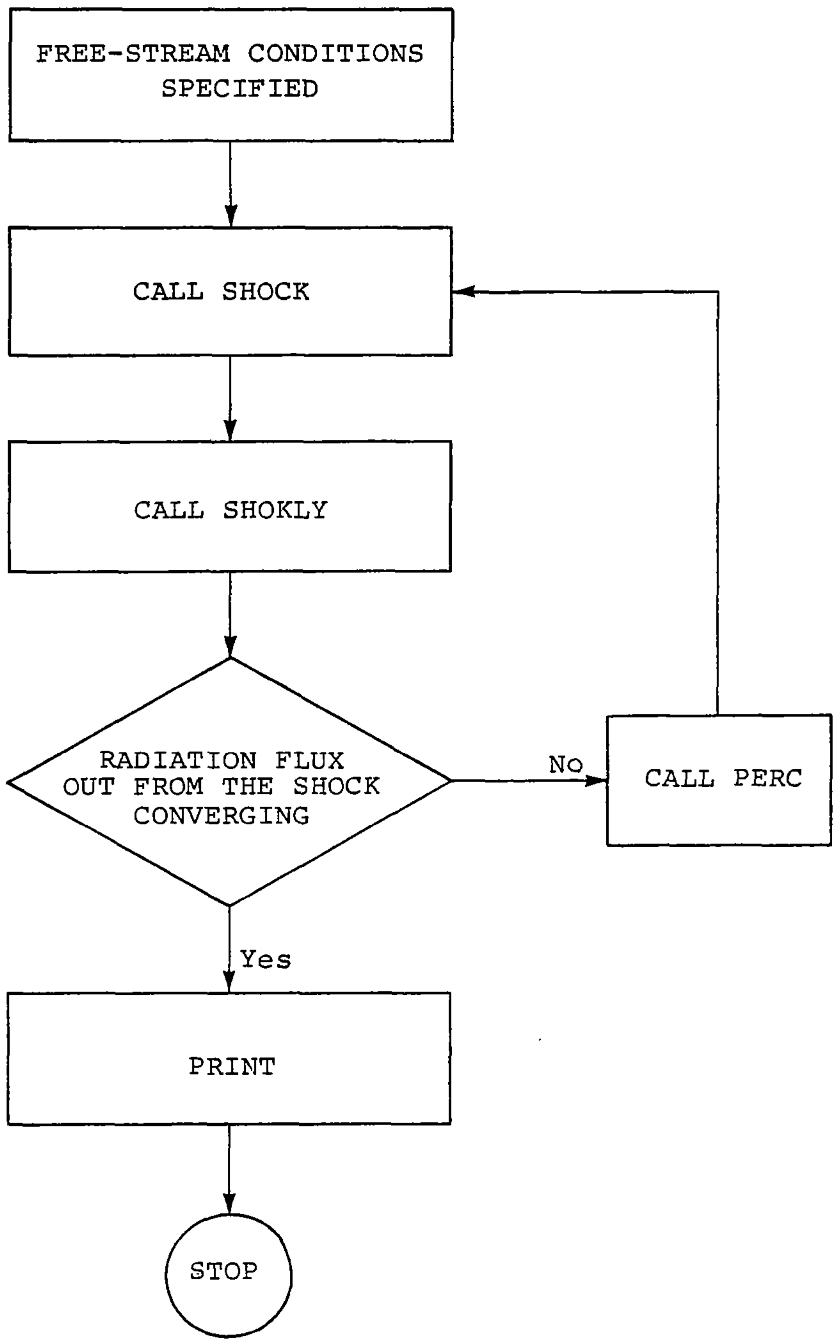

Figure 5.1. Flow chart for combined precursor/ shock-layer solution procedure.

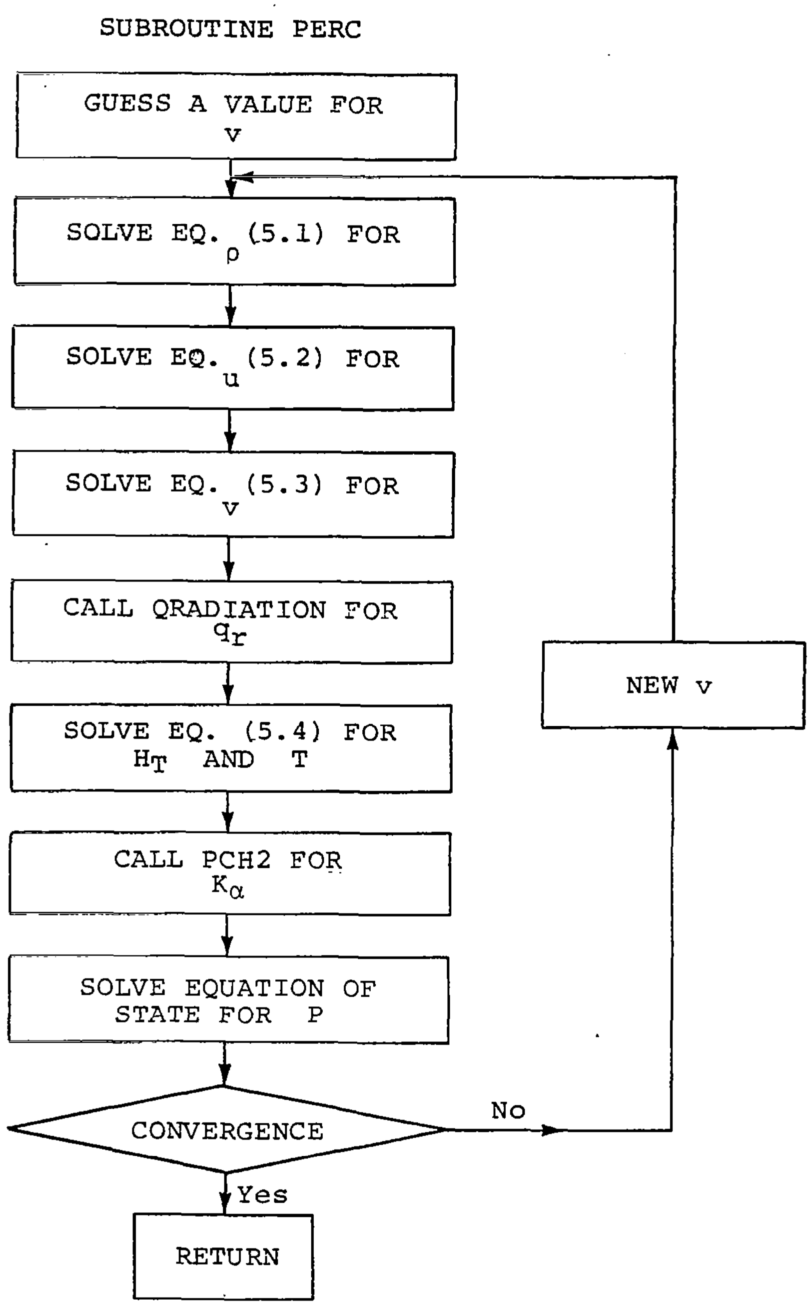

Figure 5.2. Flow chart for subroutine PERC used in the precursor region solution procedure.

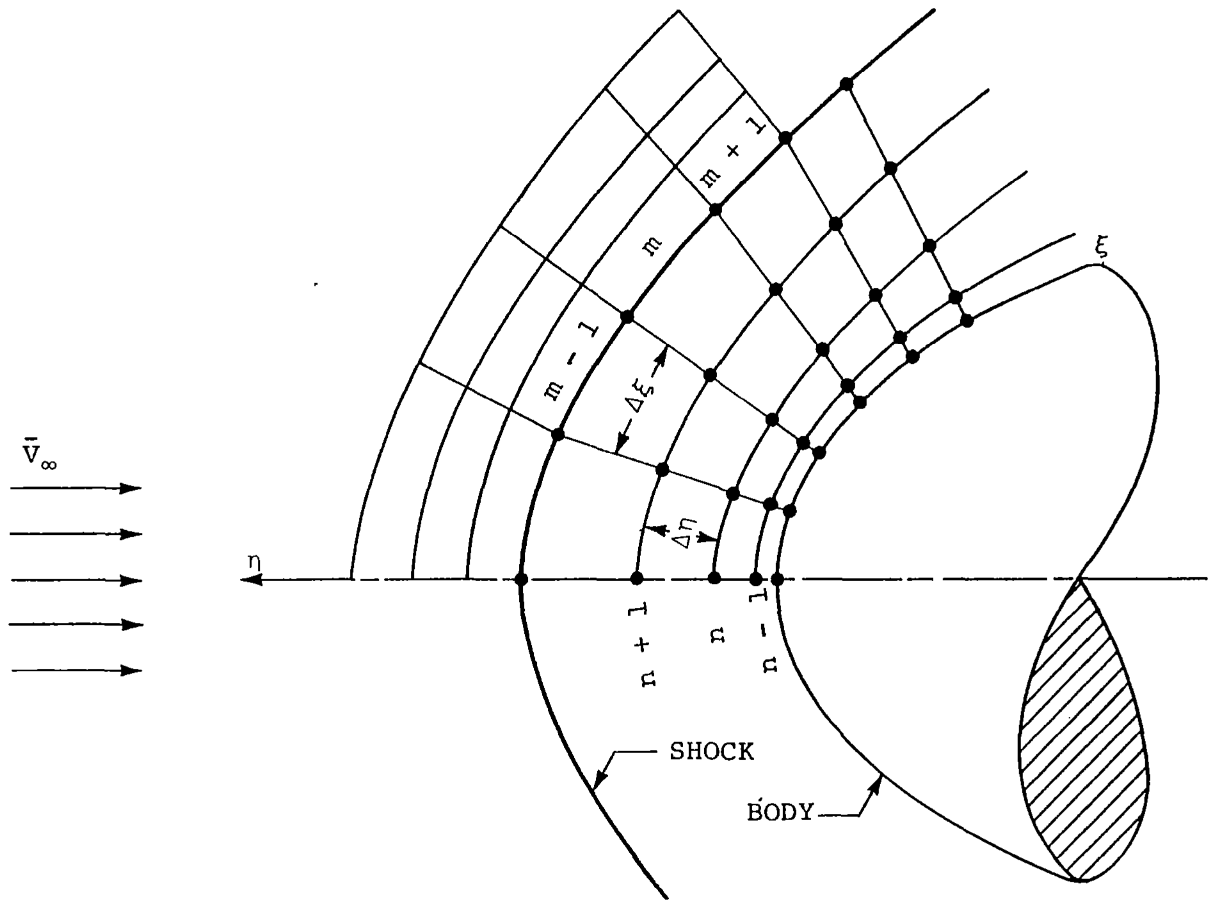

Figure 5.3. Finite difference representation of flow field.

SUBROUTINE SHOCK

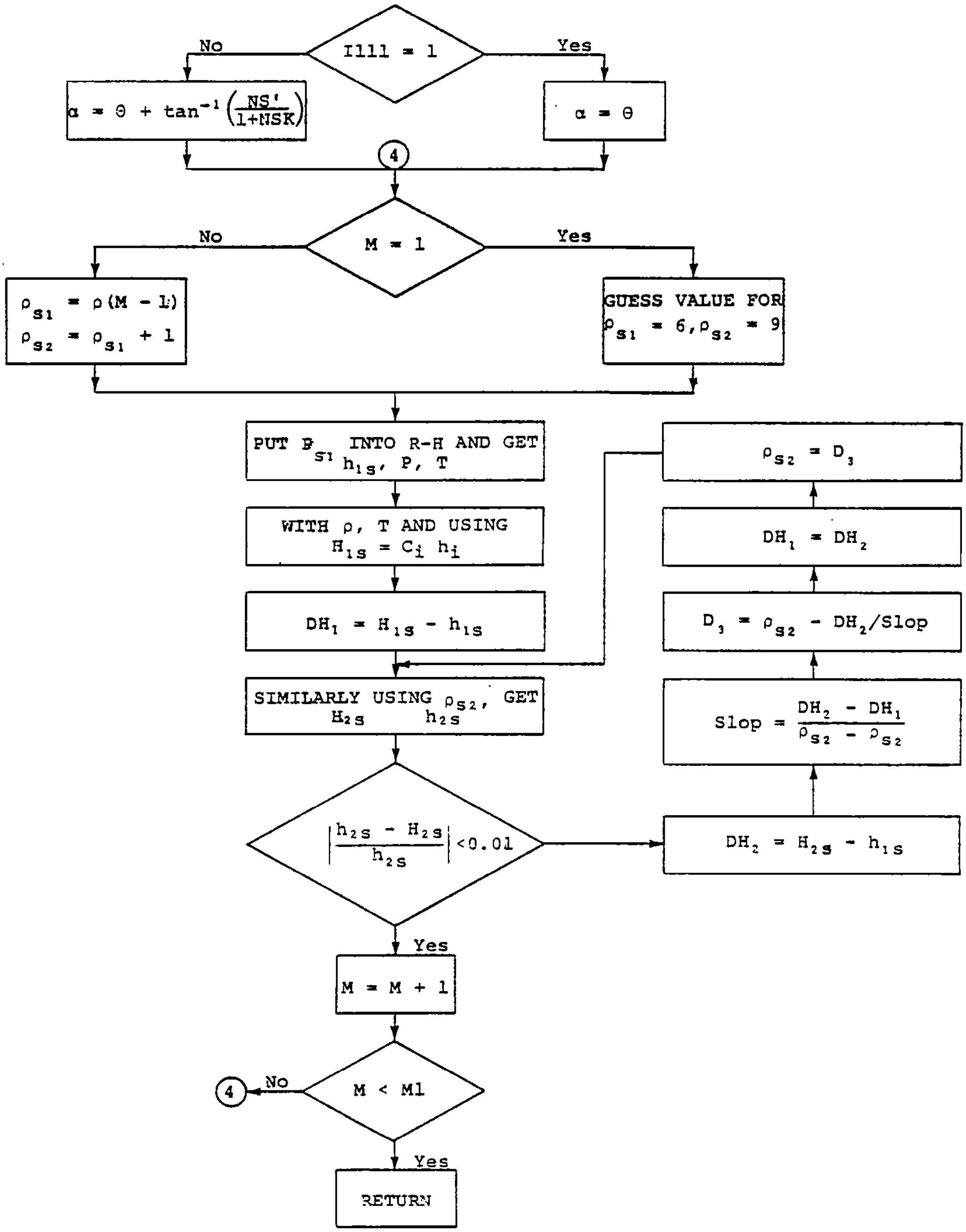

Figure 5.4. Flow chart for subroutine SHOCK for shock-layer solution.

SUBROUTINE SHOKLY

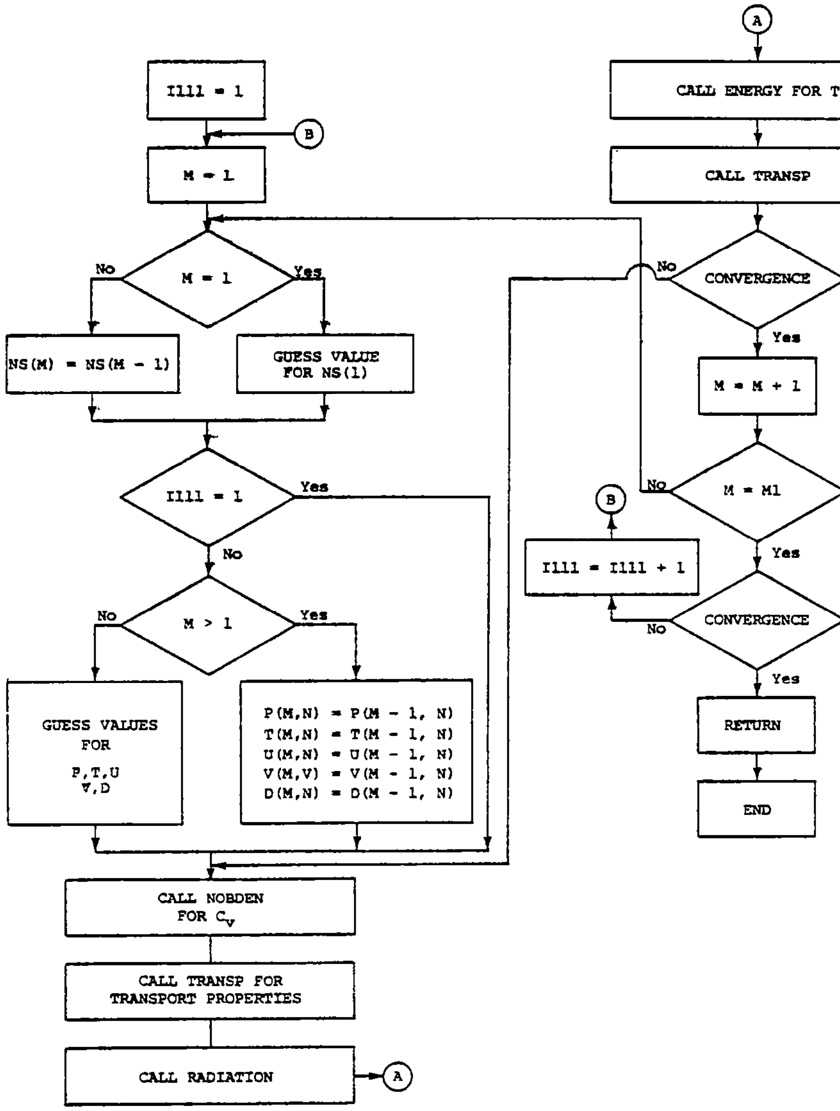

Figure 5.5. Flow chart for subroutine SHOKLY for shock-layer solution.

SUBROUTINE ENERGY

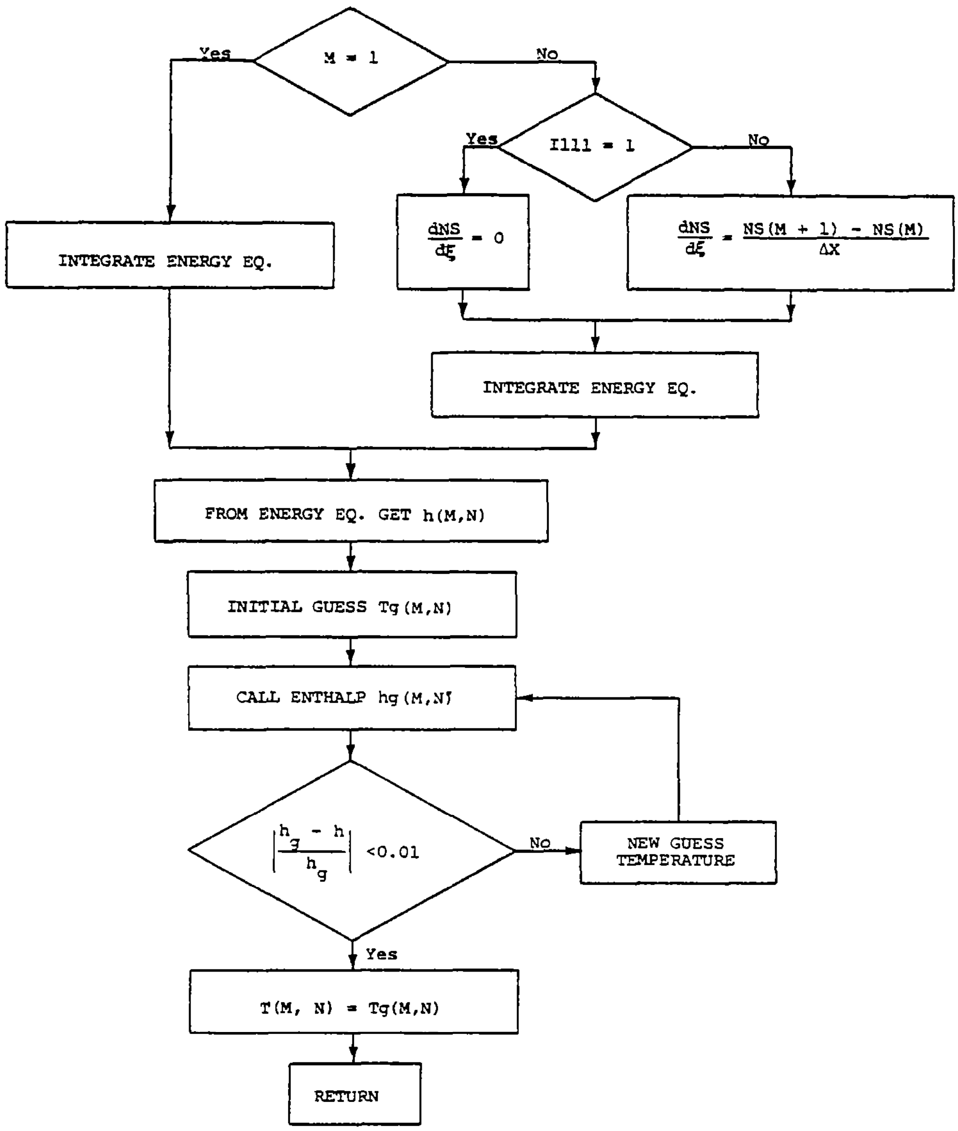

Figure 5.6. Flow chart for subroutine ENERGY for shock-layer solution.

SUBROUTINE MOMENTM

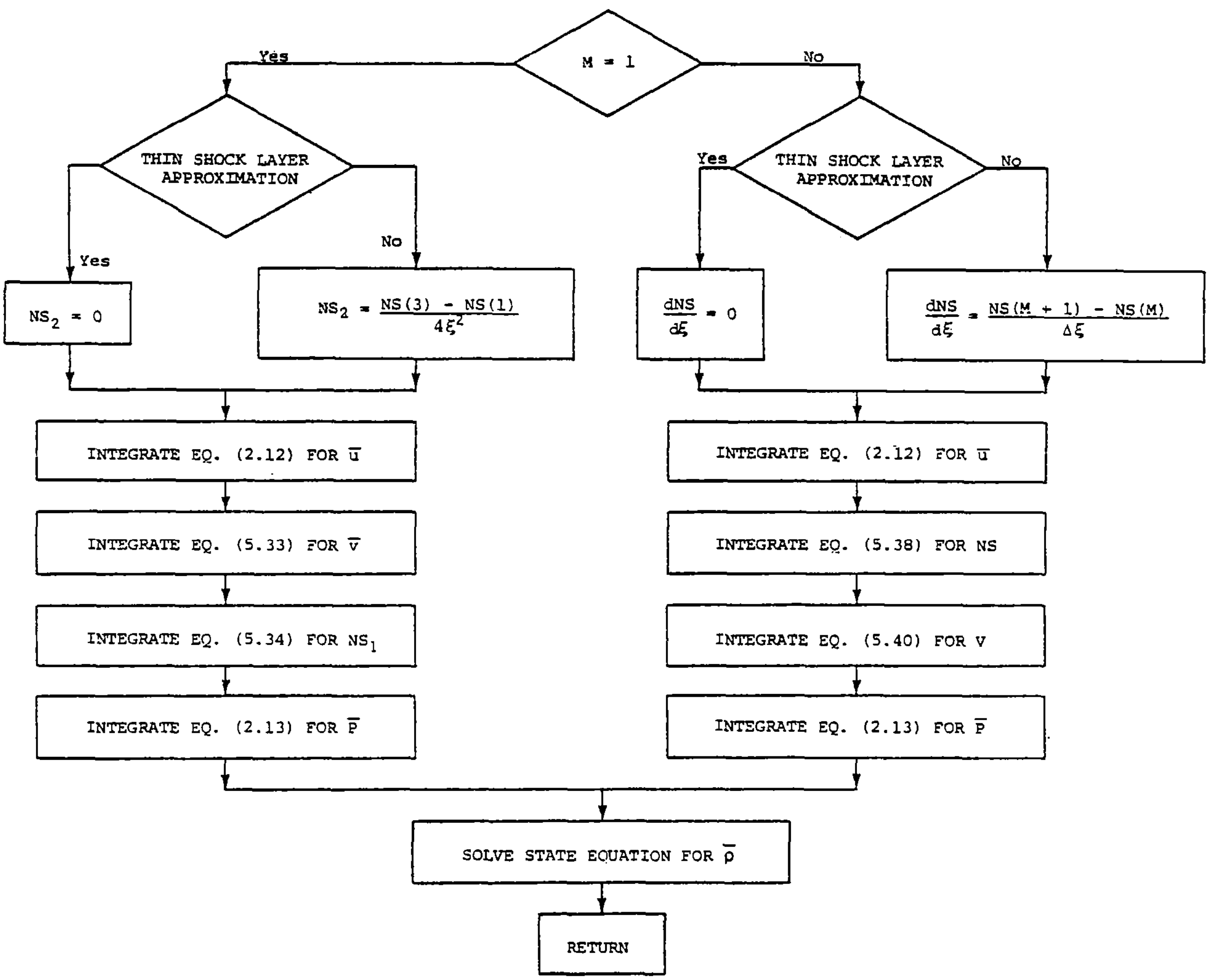

Figure 5.7. Flow chart for subroutine MOMENTM for shock-layer solution.

SUBROUTINE RADIATION

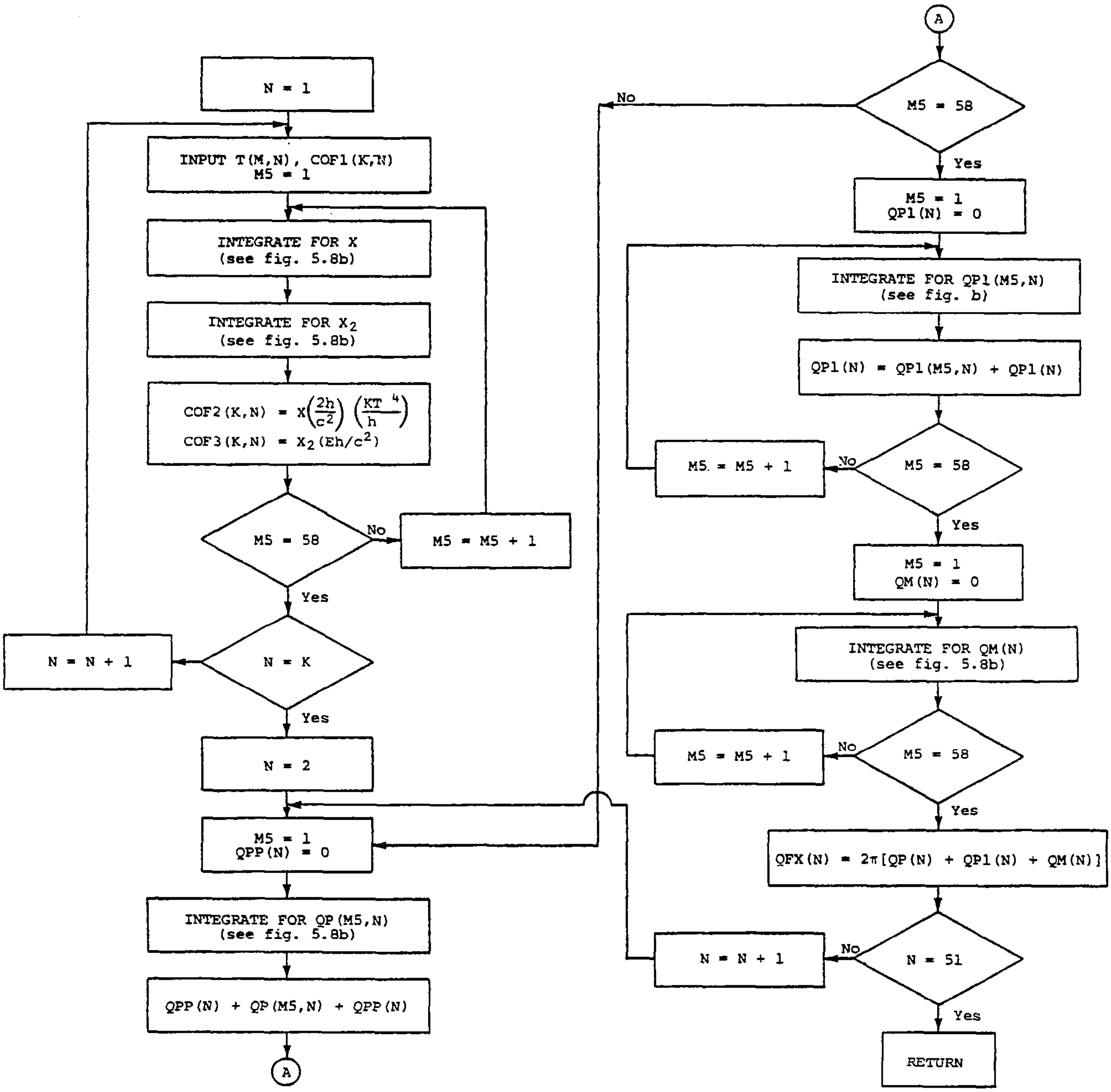

Figure 5.8a. Flow chart for subroutine RADIATION for shock-layer solution.

INTEGRALS FOR SUBROUTINE RADIATION

$$X = \int_{\nu_{K1}}^{\nu_{K2}} \left\{ v^3 / \left[\exp(v) - 1 \right] \right\} dv$$

$$X_2 = \int_{\nu_{K2}}^{\nu_{K1}} \left\{ \nu^3 / \left[\exp(\kappa\nu) - 1 \right] \right\} d\nu$$

$$QP(M5,N) = \int_{0}^{N} COF2(M5,N)\ COF1(M5,N)\ E_2 \left[\int_{0}^{N} \alpha_j(N')dN' \right] d\xi$$

$$QP1(M5,N) = \int_{0}^{N} COF3(M5,N)\ E_3 \left[\int_{0}^{N} \alpha_j(N')dN' \right] d\xi$$

$$QM(N) = \int_{0}^{N} COF2(K,N)\ COF3(K,N)\ E_2 \left[\int_{N}^{\xi} \alpha_j(N')dN' \right] d\xi$$

Figure 5.8b. Definition of integrals used in subroutine RADIATION.

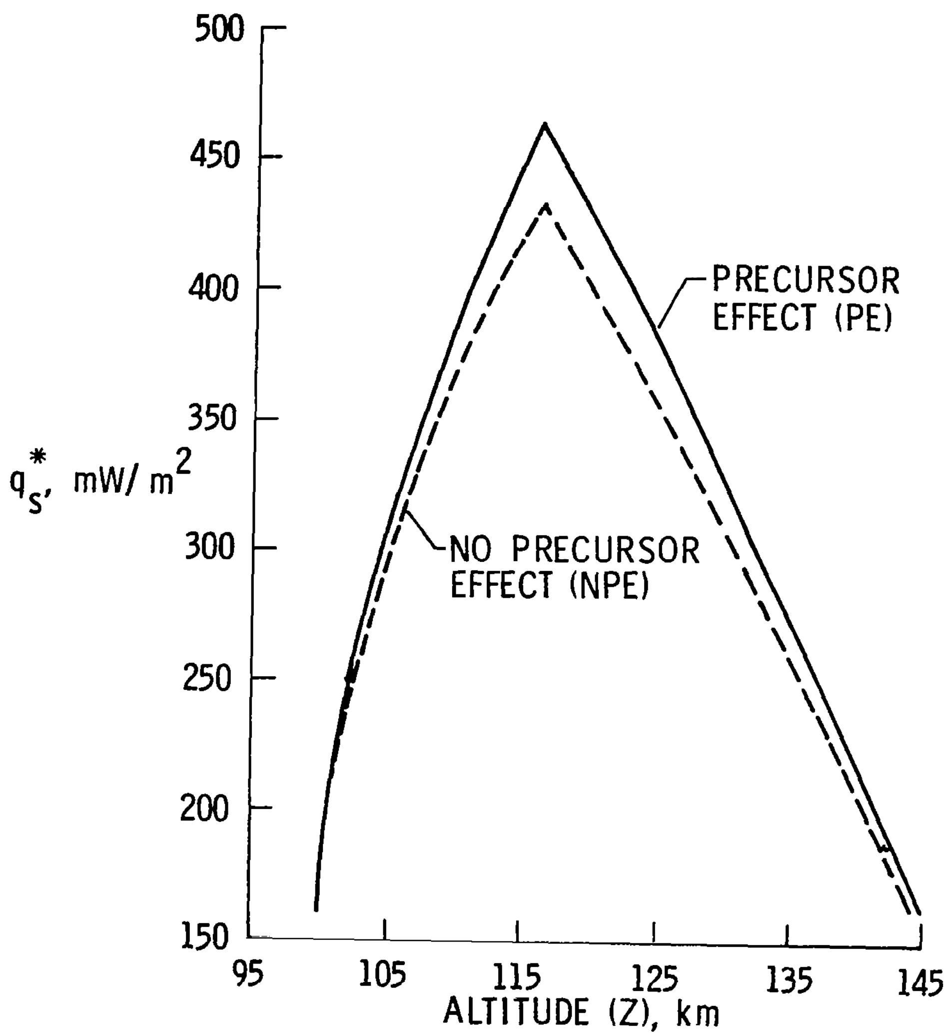

Figure 6.1. Radiation flux towards the precursor region at the stagnation line shock location.

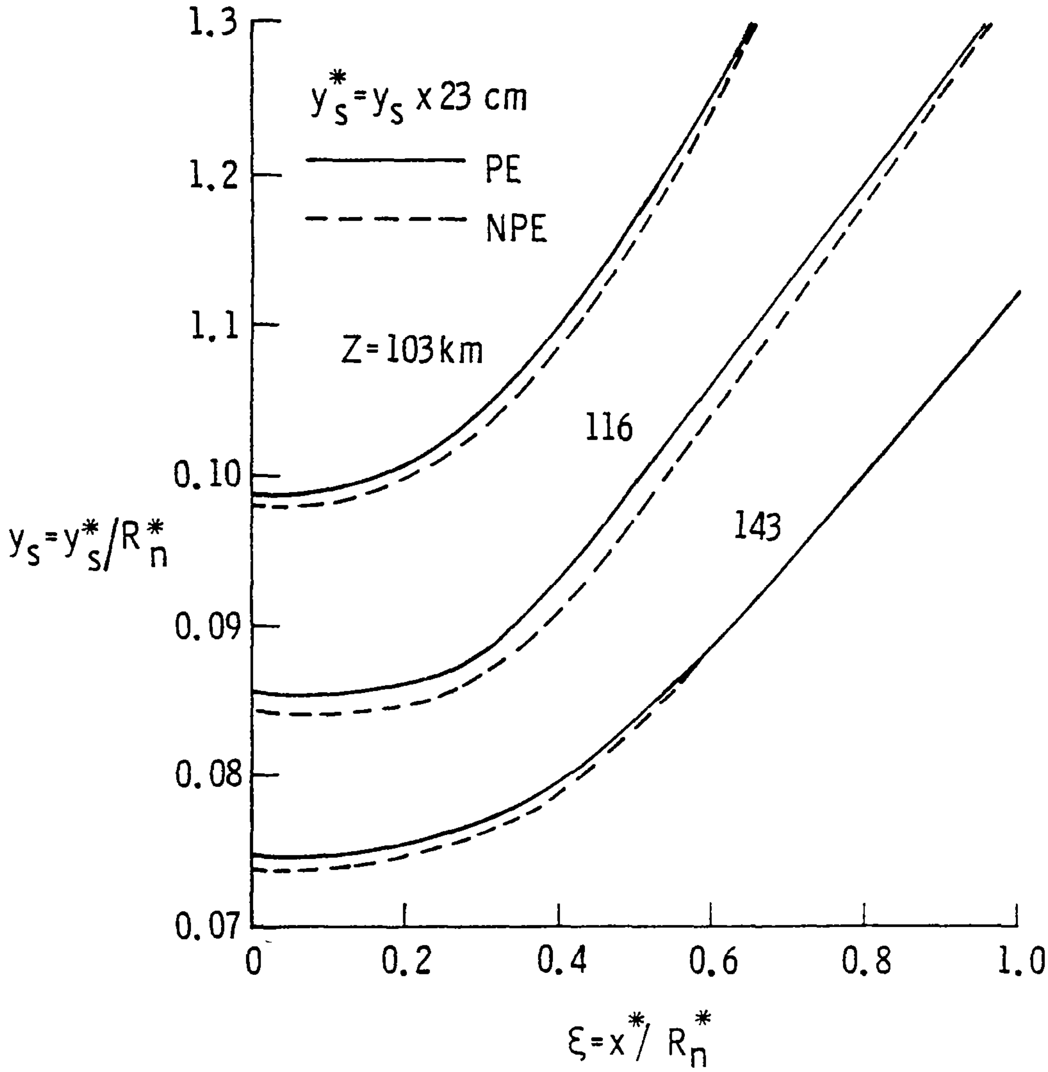

Figure 6.2. Shock standoff distance variation with distance along body surface.

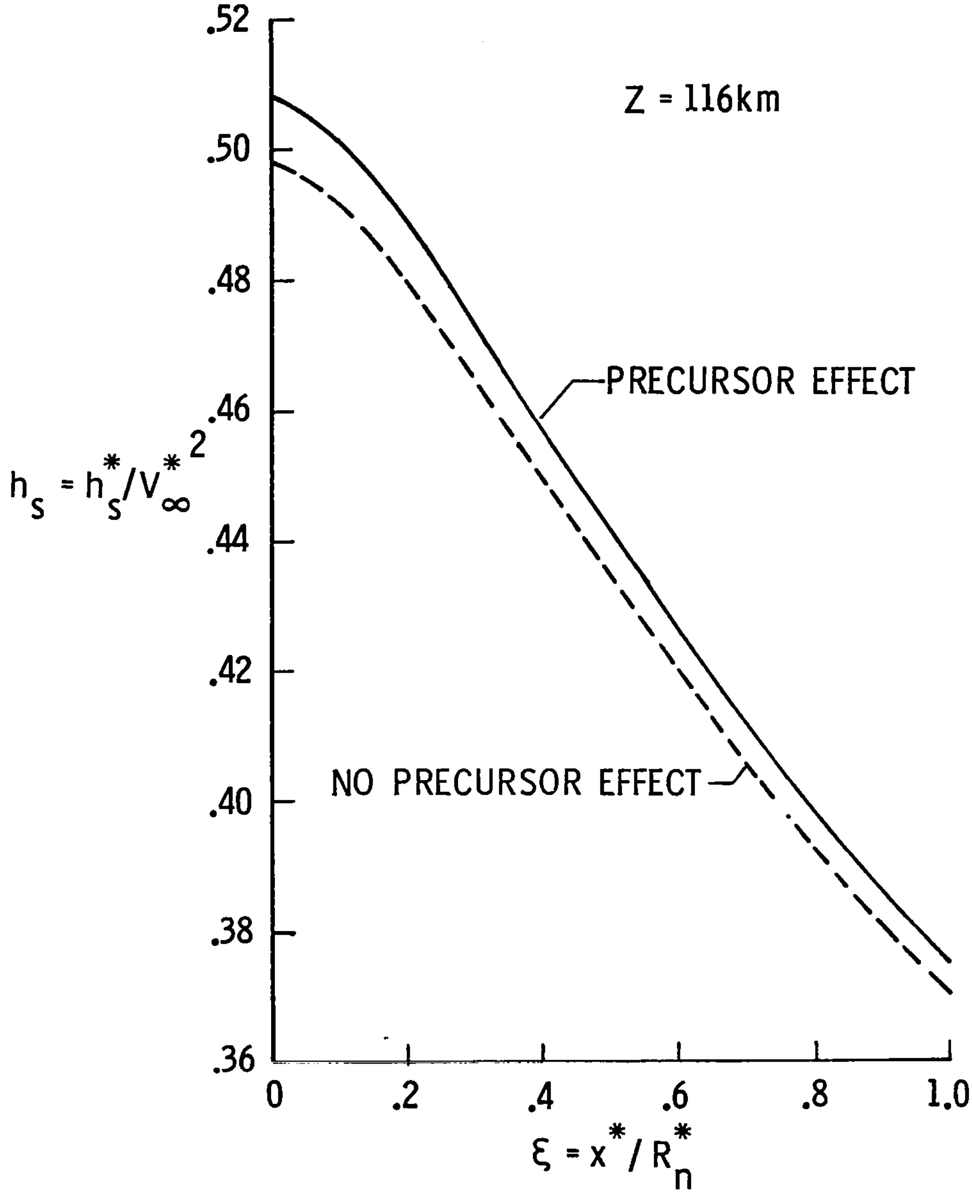

Figure 6.3. Enthalpy variation just behind the shock with distance along the body surface.

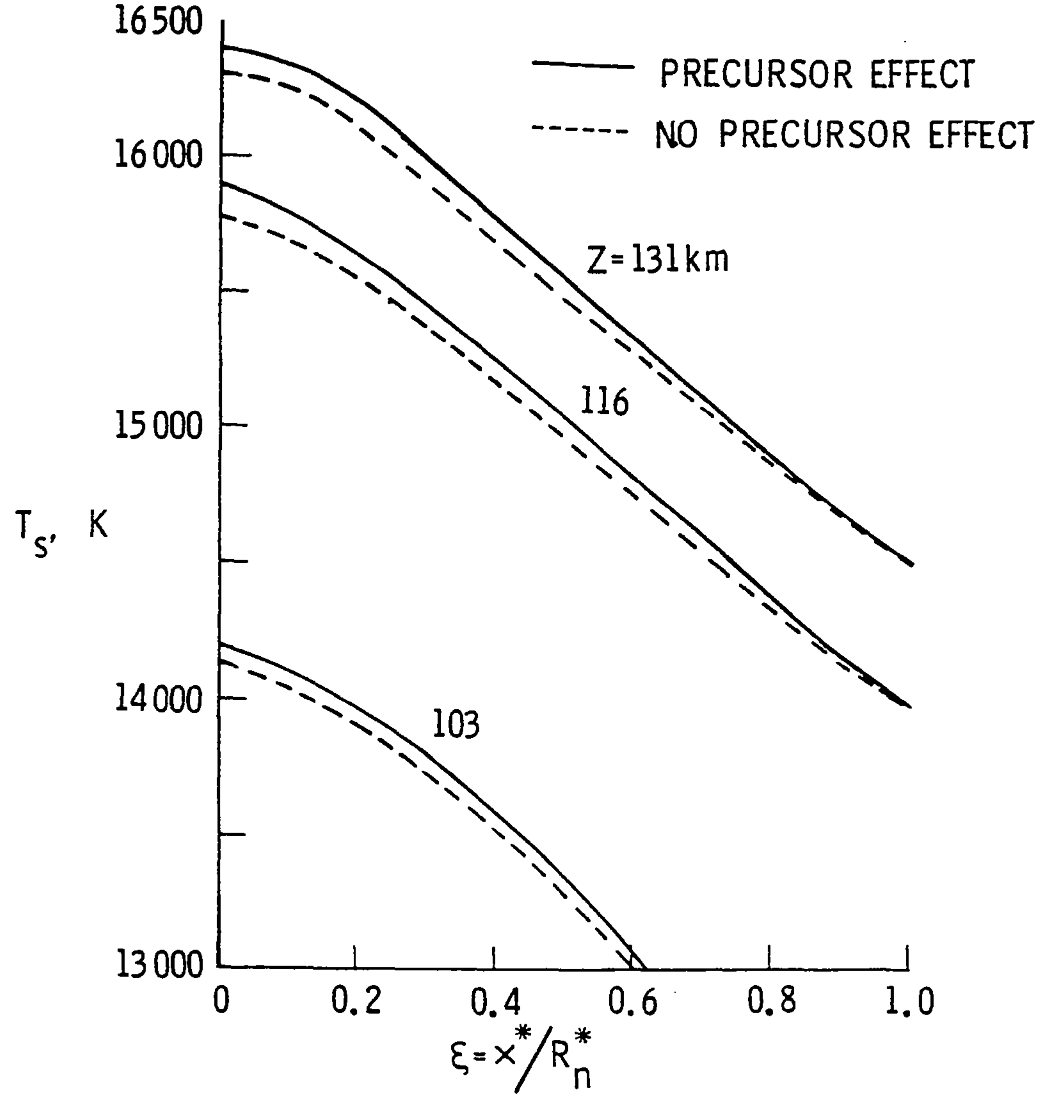

Figure 6.4. Temperature variation just behind the shock with distance along the body surface.

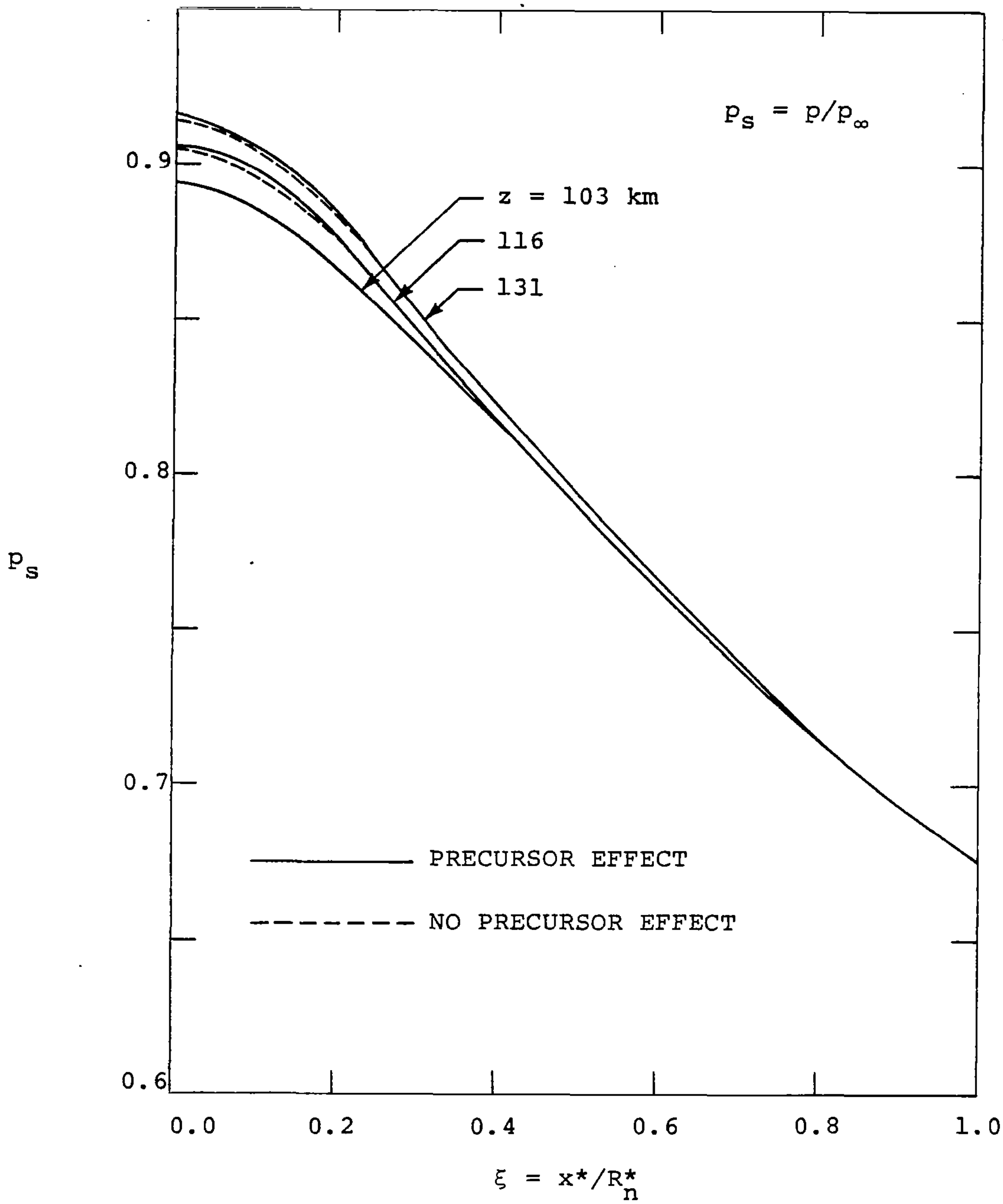

Figure 6.5. Pressure variation just behind the shock with distance along the body surface.

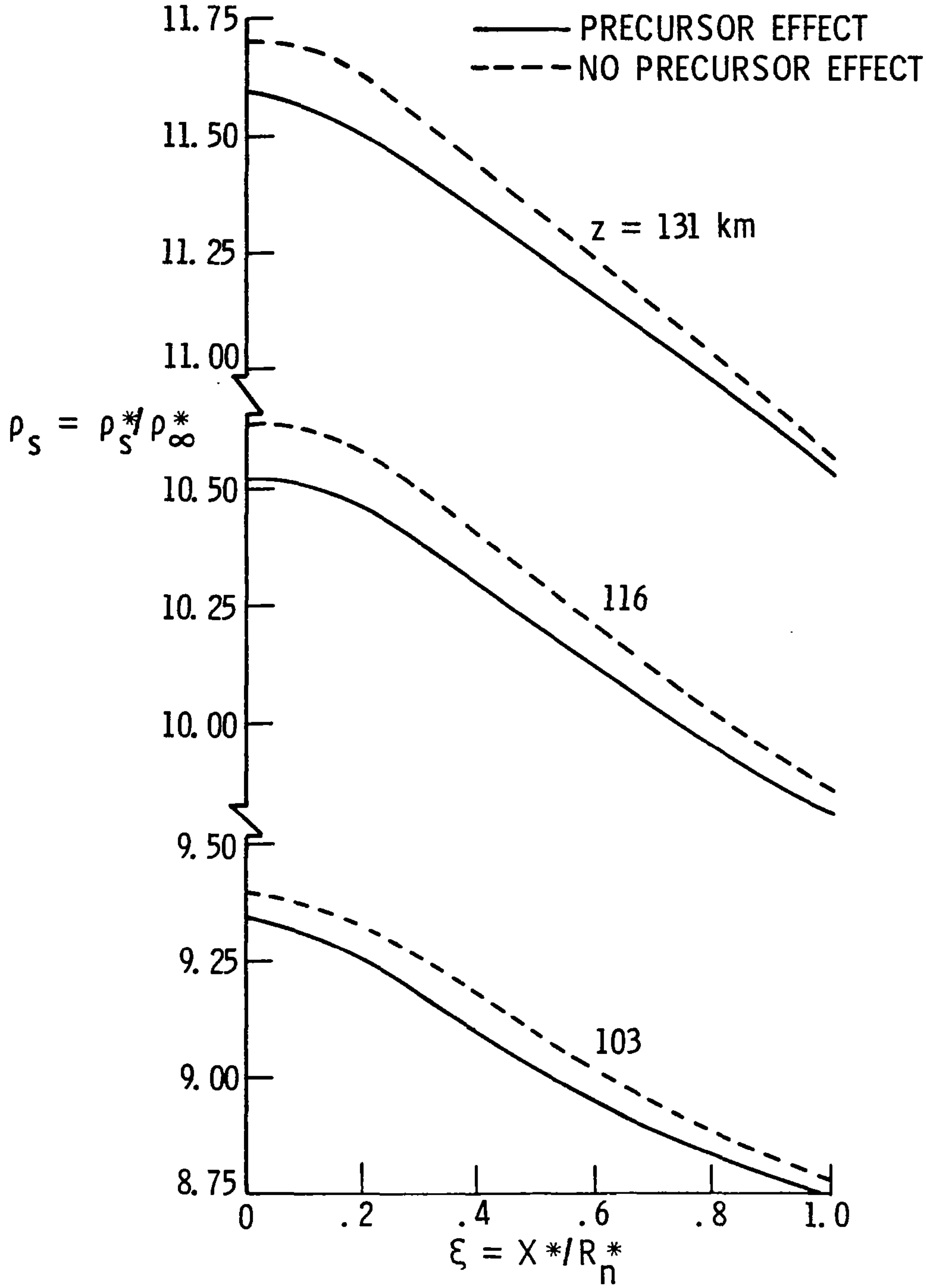

Figure 6.6. Density variation just behind the shock with distance along the body surface.

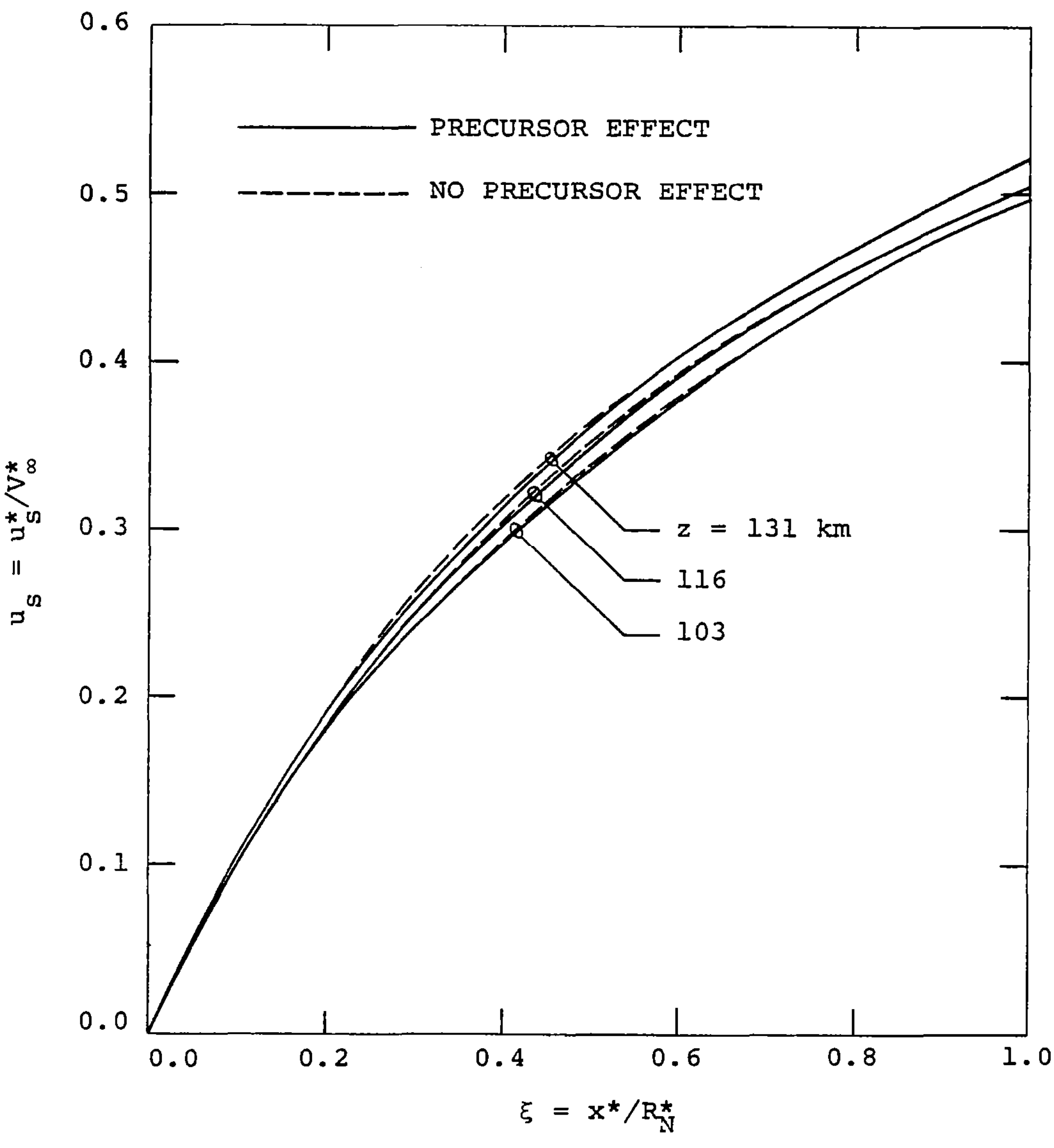

Figure 6.7. Variation of u-velocity component just behind the shock with distance along the body surface.

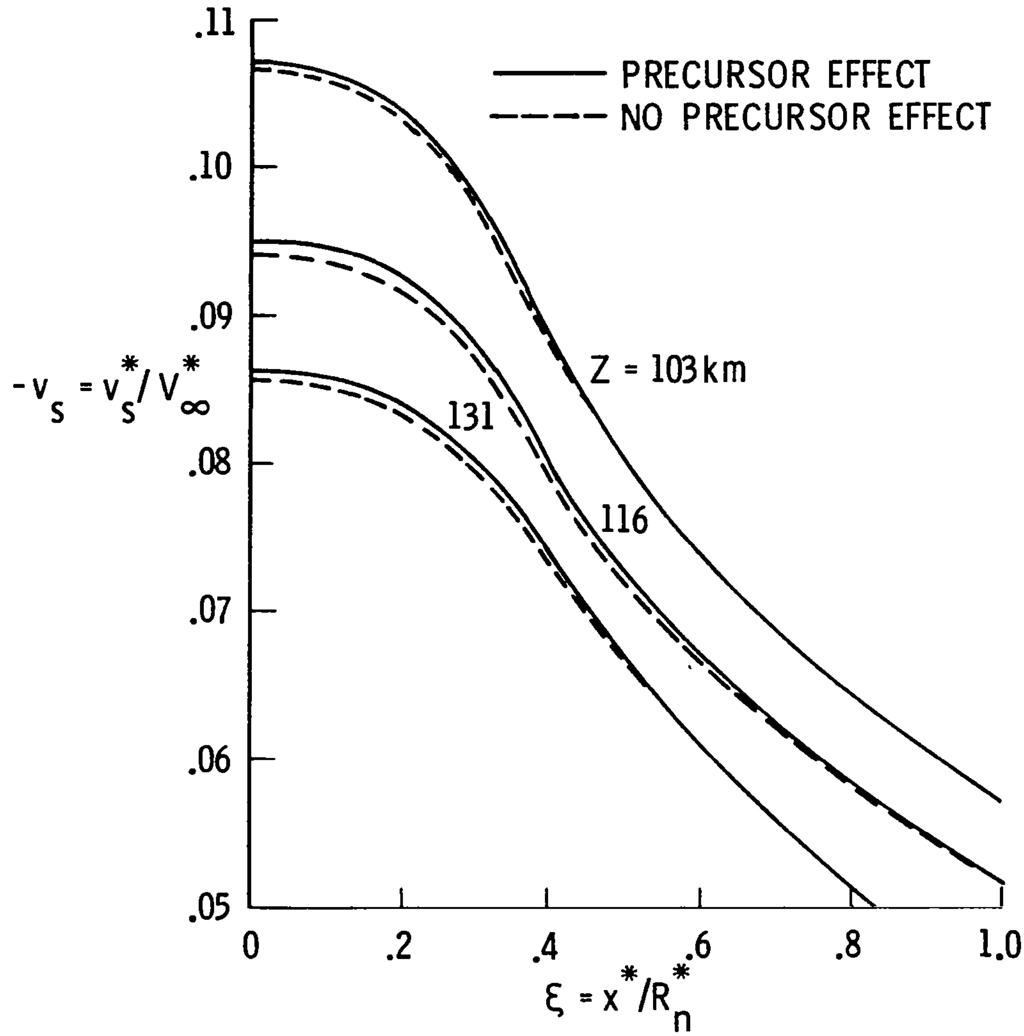

Figure 6.8. Variation of v-velocity component just behind the shock with distance along the body surface.

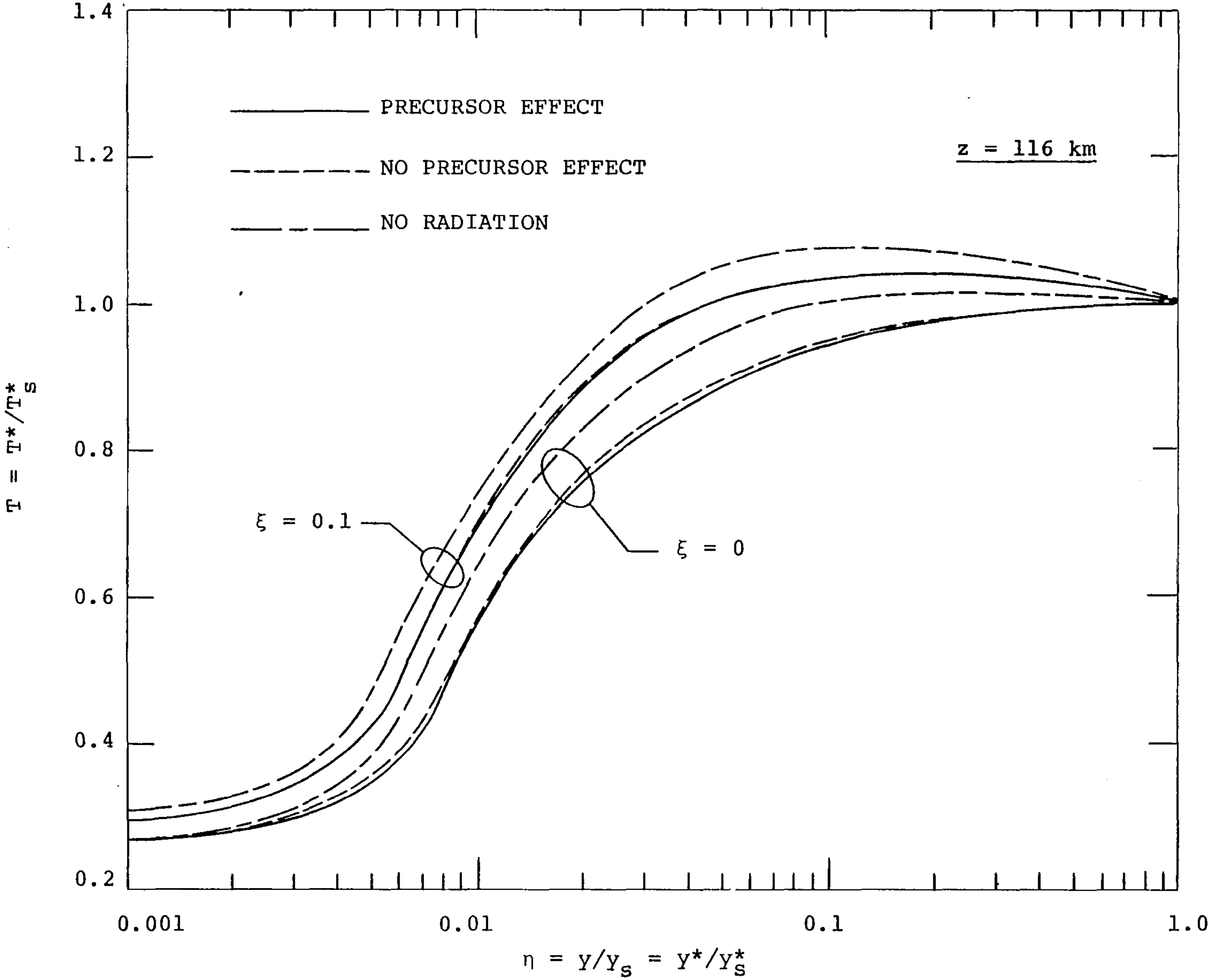

Figure 6.9. Variation of temperature in the shock layer for two body locations (ξ = 0 and 1).

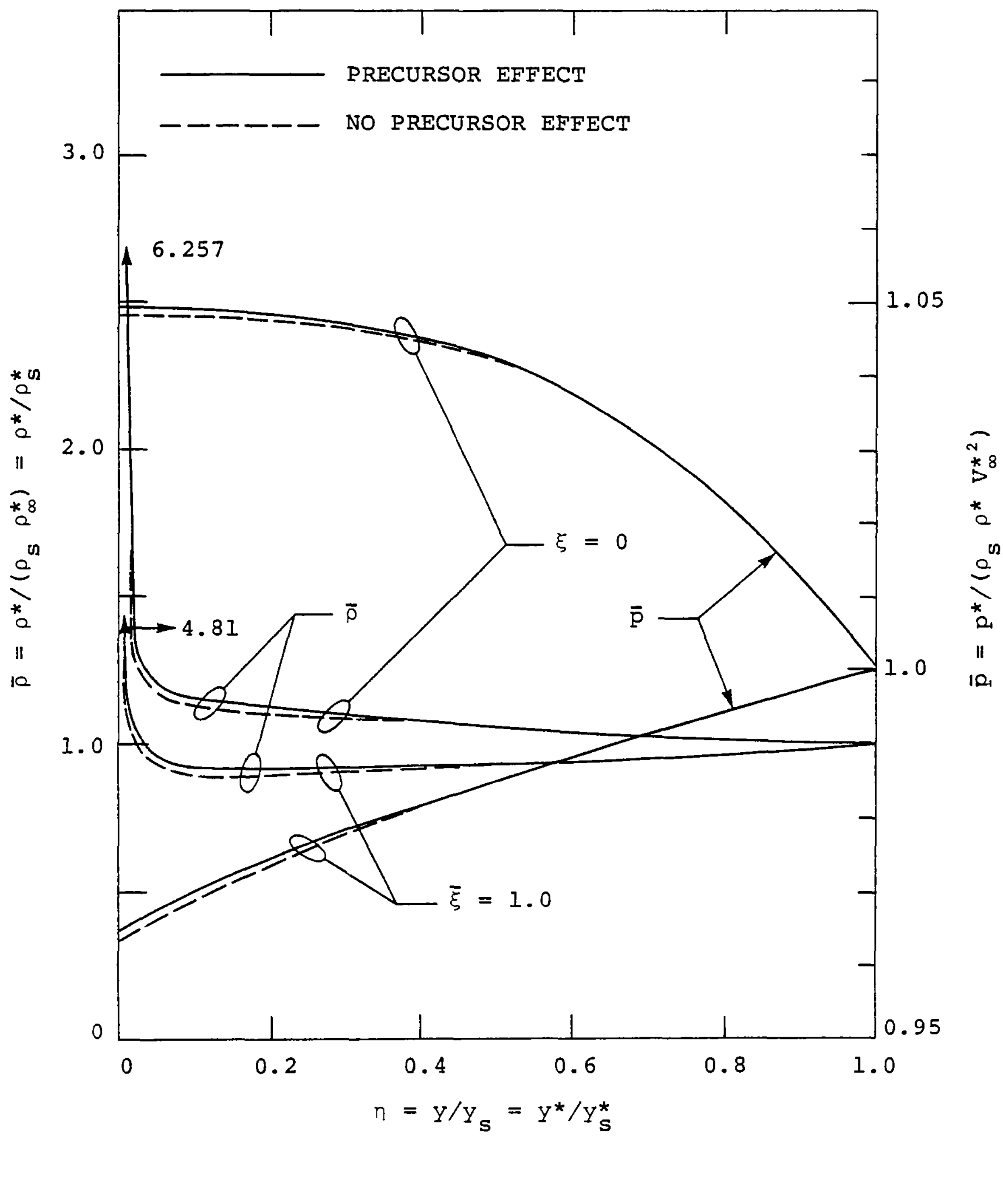

Figure 6.10. Variation of pressure and density in the shock layer for two body locations (ξ = 0 and 1).

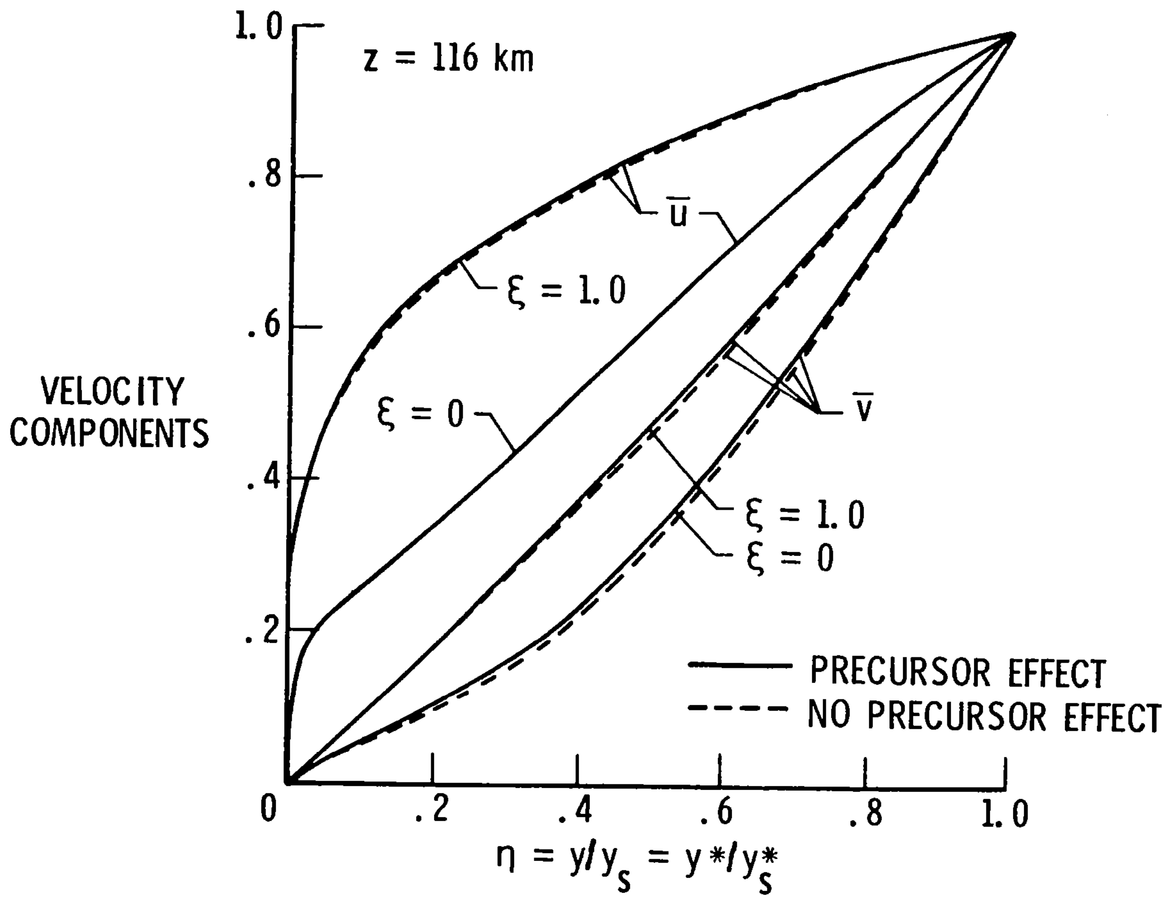

Figure 6.11. Variation of velocity components in the shock layer for two body locations (ξ = 0 and 1).

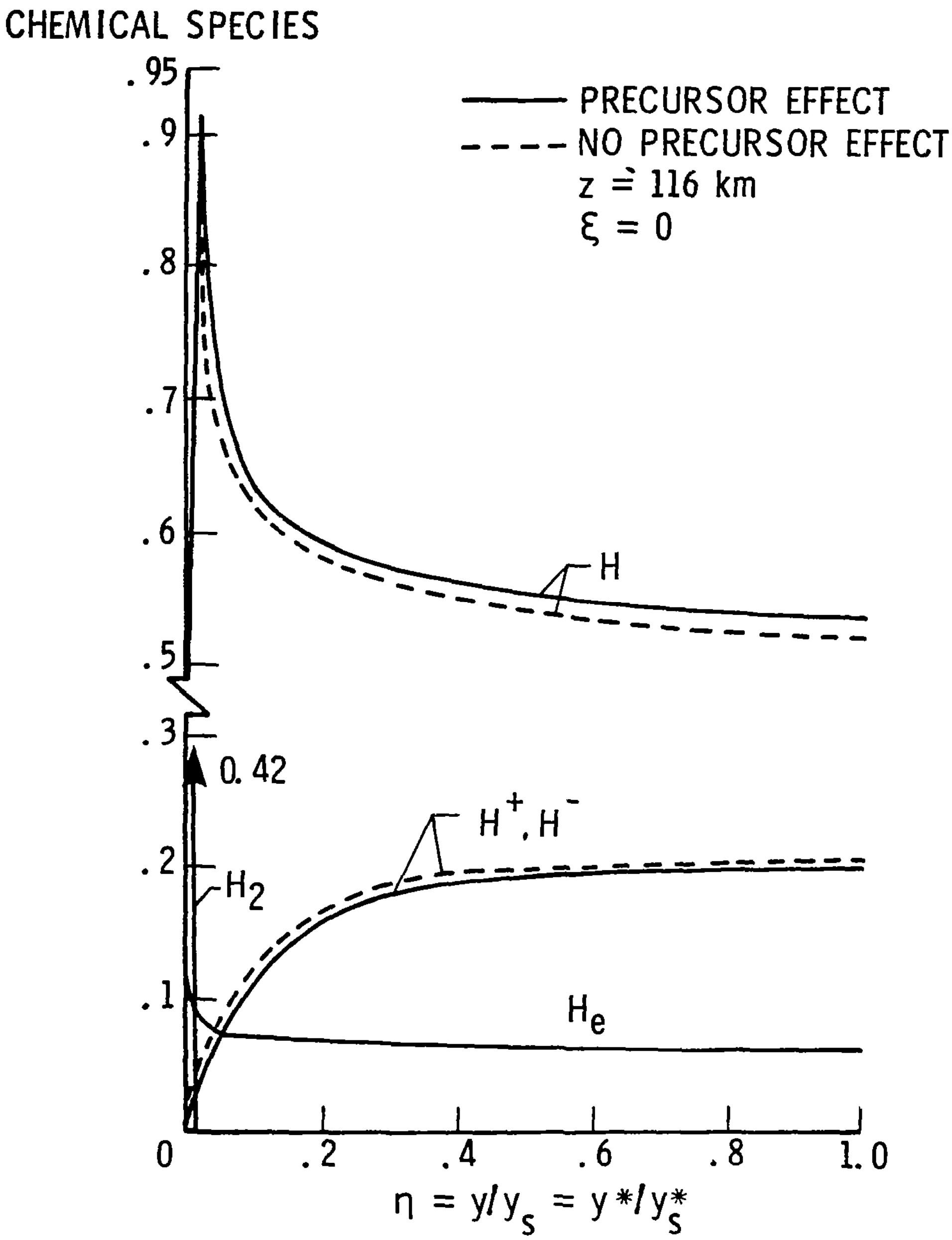

Figure 6.12. Species concentration in the shock layer for $\xi = 0$.

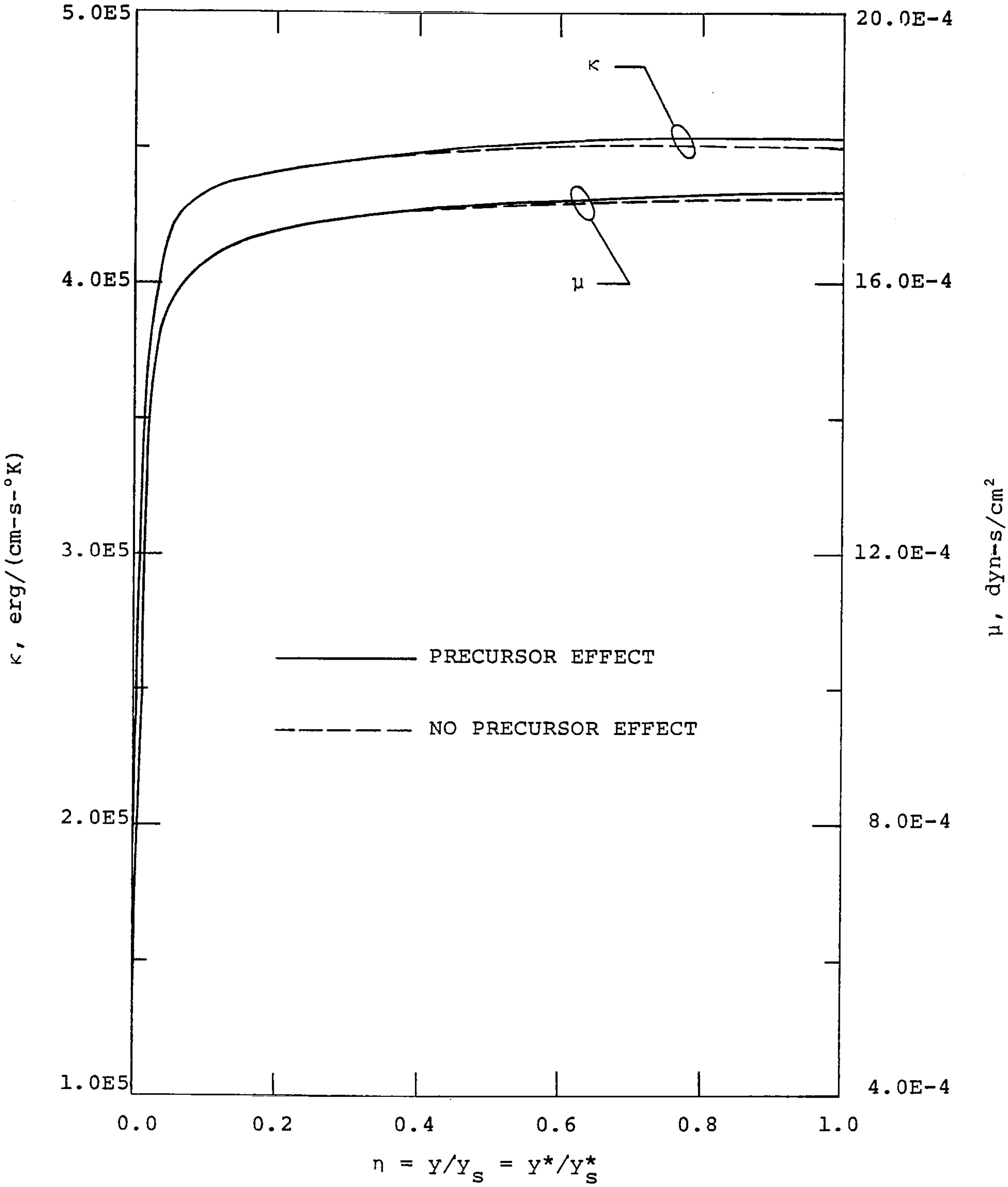

Figure 6.13. Variation of thermal conductivity and viscosity in the shock layer for ξ = 0.

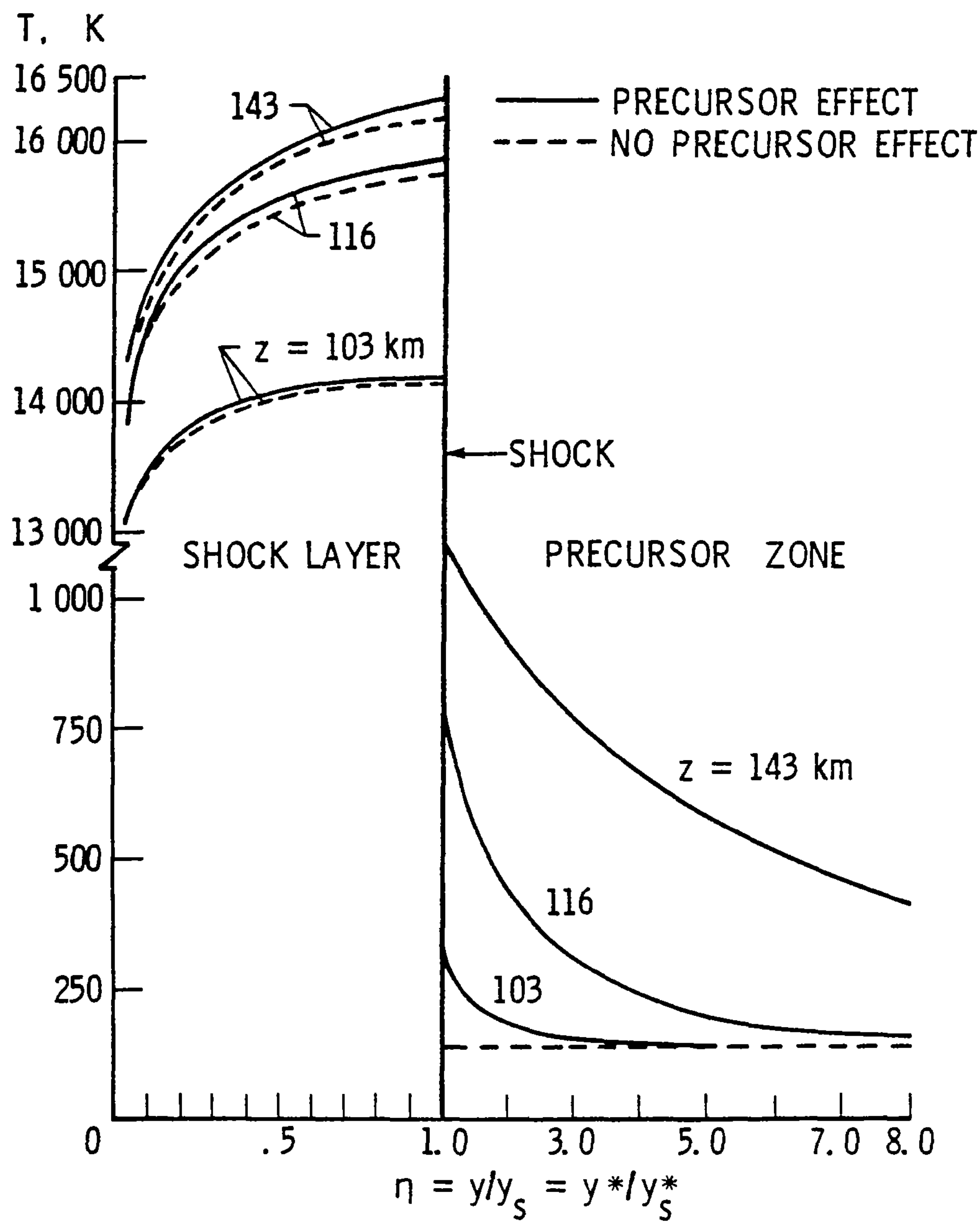

Figure 6.14. Temperature variation in the shock/precursor region along the stagnation streamline.

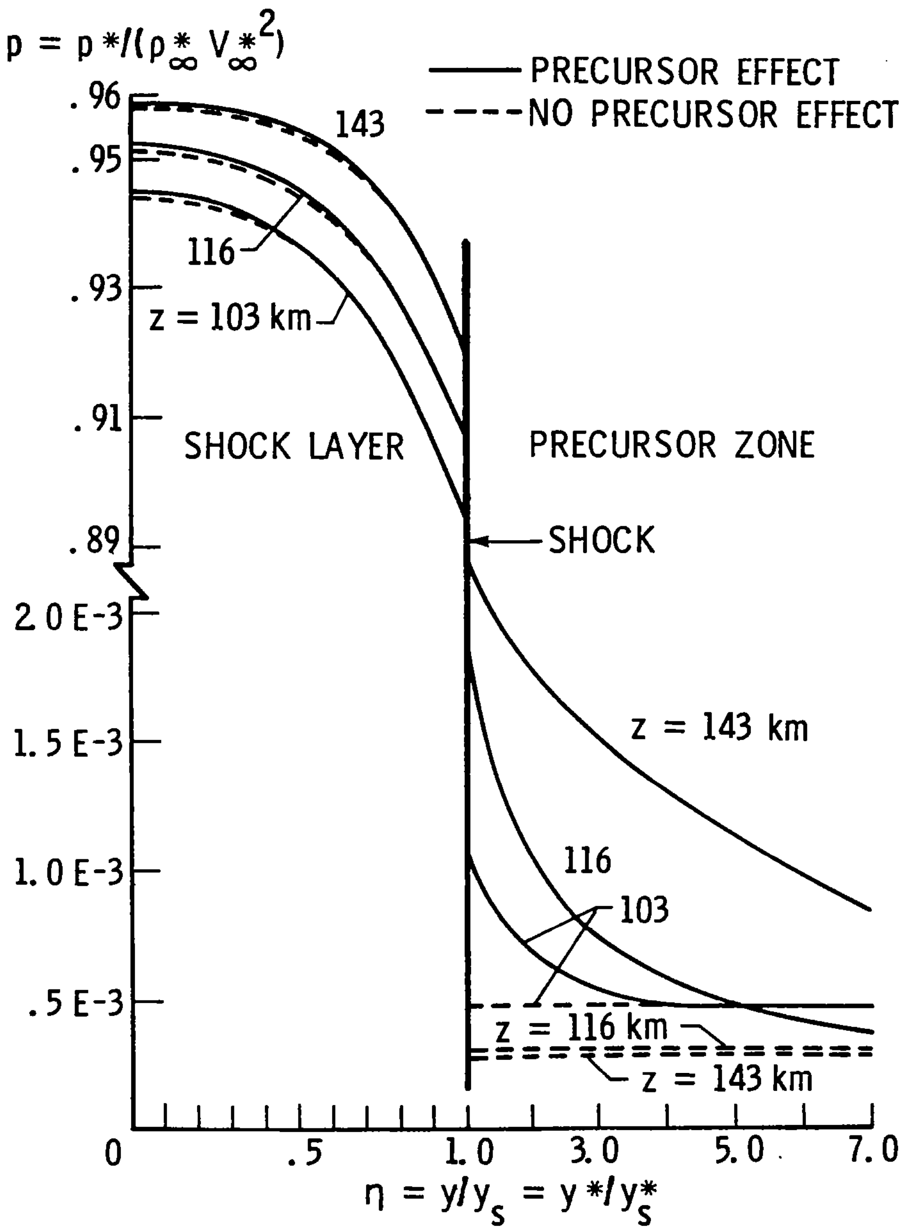

Figure 6.15. Pressure variation in the shock/precursor region along the stagnation streamline.

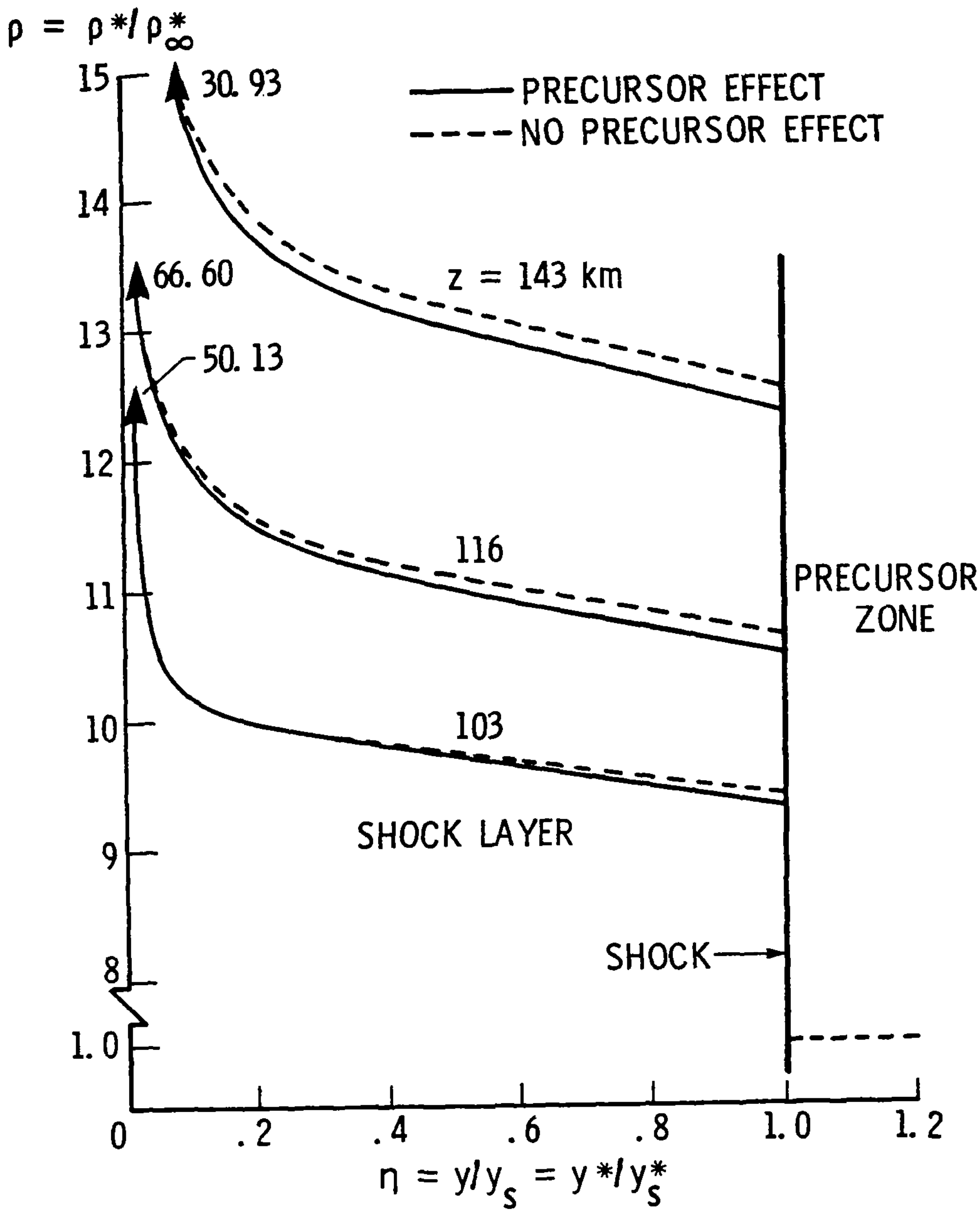

Figure 6.16. Density variation in the shock/precursor region along the stagnation streamline.

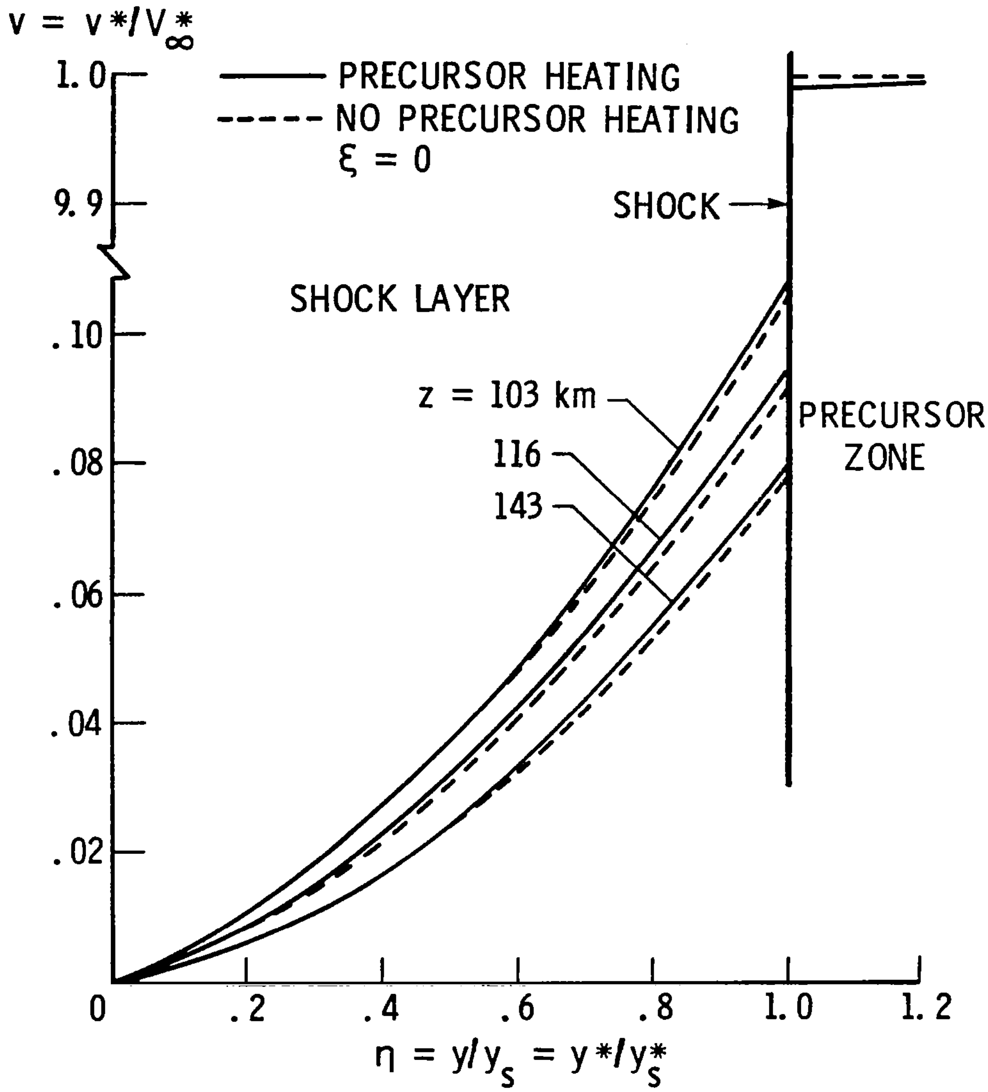

Figure 6.17. Variation of v-velocity component in the shock/precursor region along the stagnation streamline.

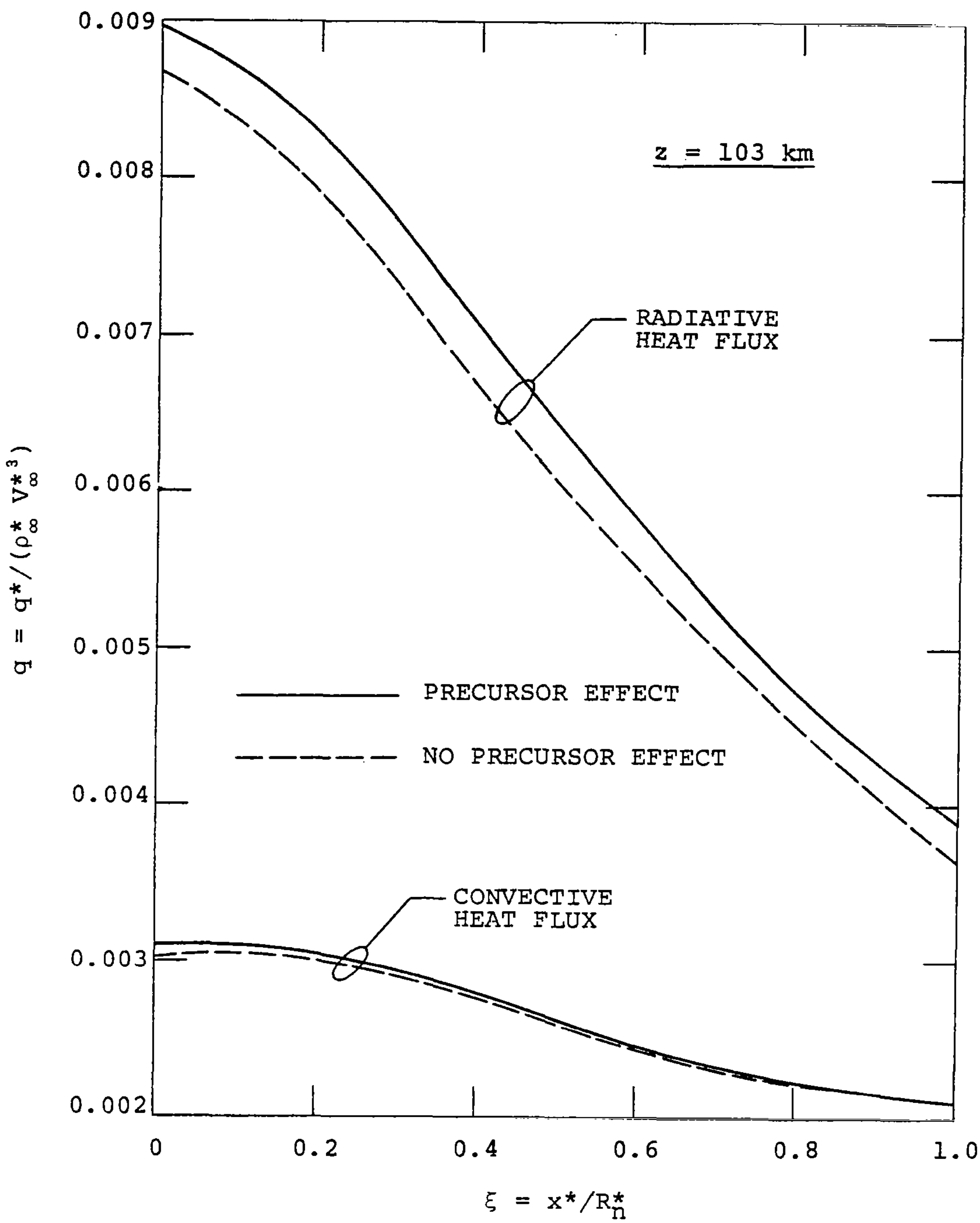

Figure 6.18. Variation of radiative and convective heat flux with distance along the body surface for z = 103 km.

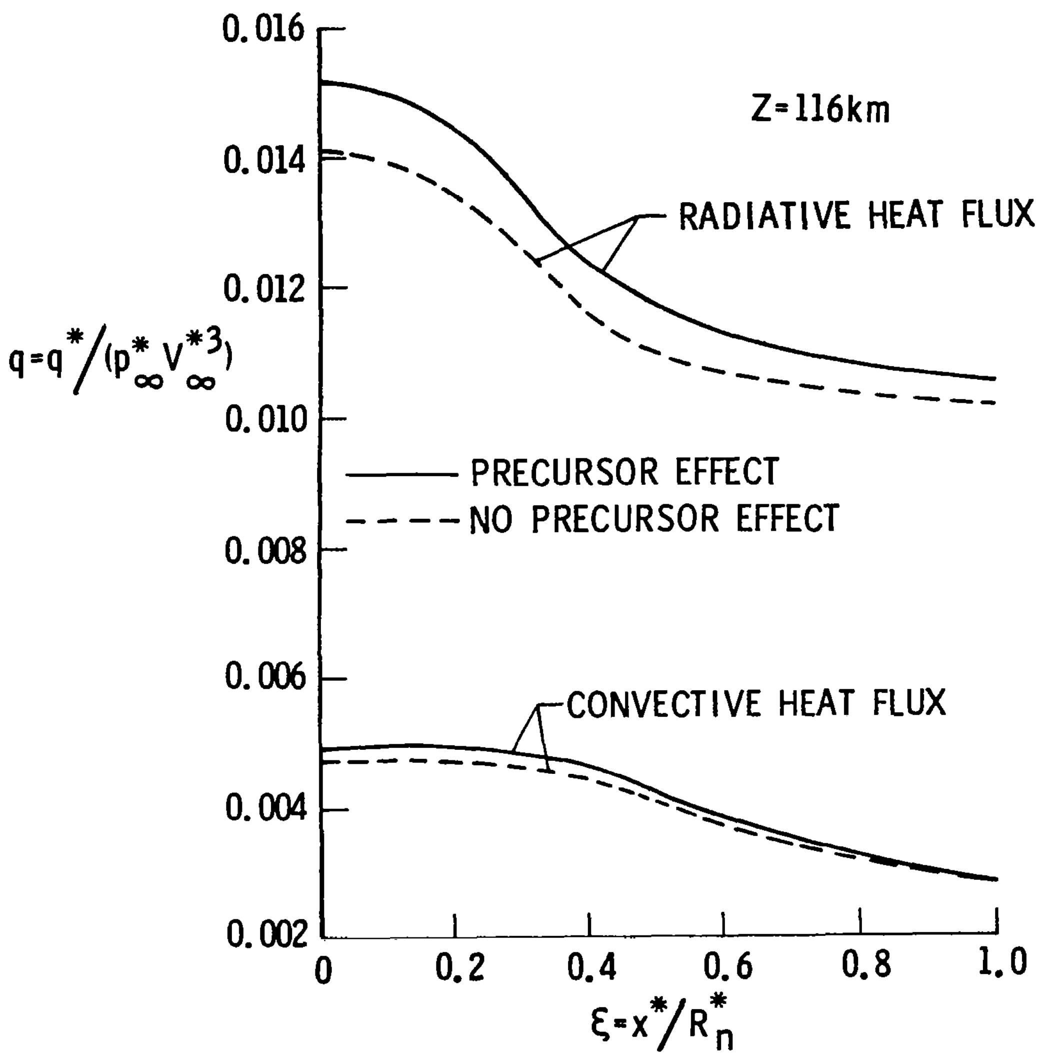

Figure 6.19. Variation of radiative and convective heat flux with distance along the body surface for z = 116 km.

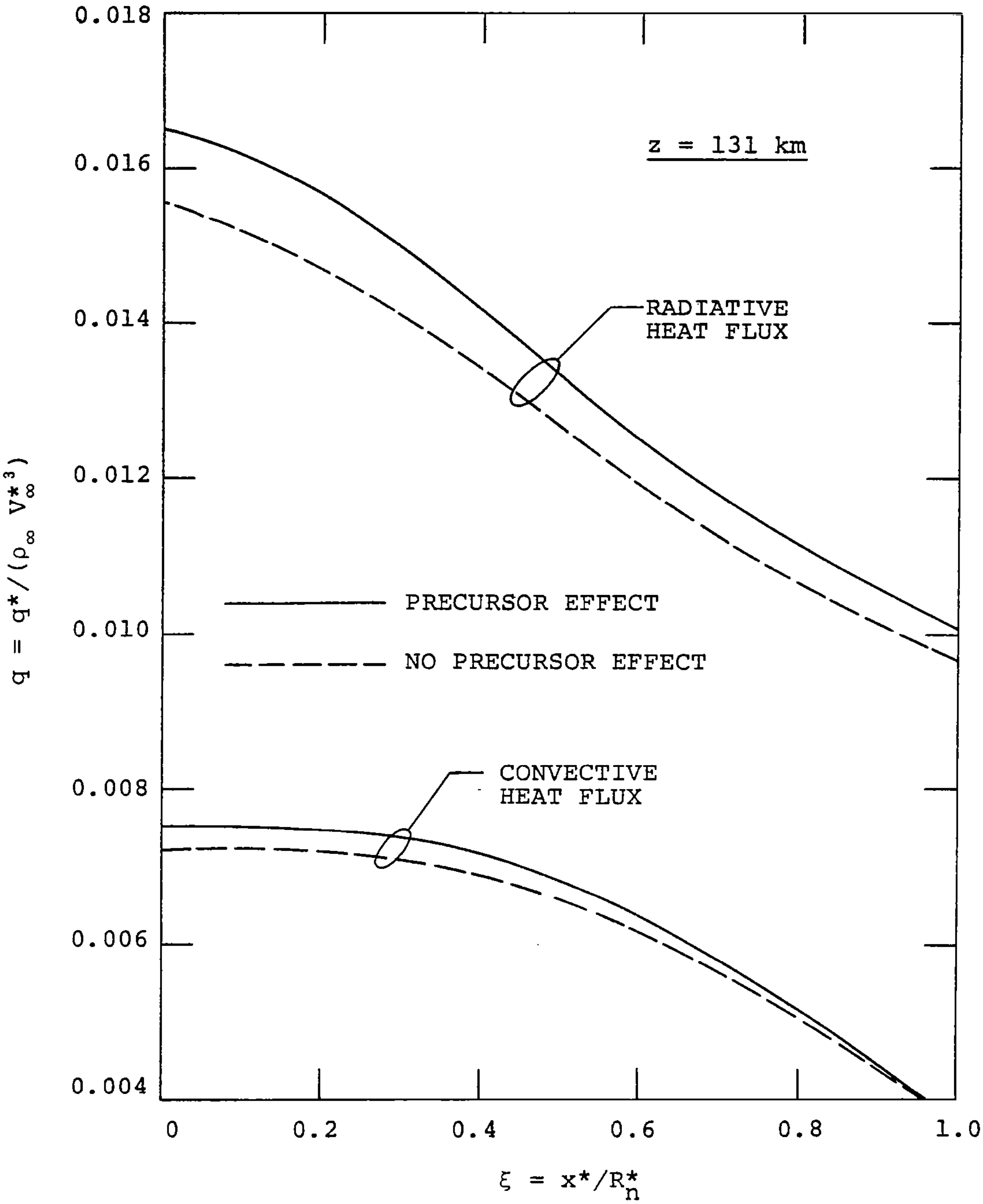

Figure 6.20. Variation of radiative and convective heat flux with distance along the body surface for z = 131 km.

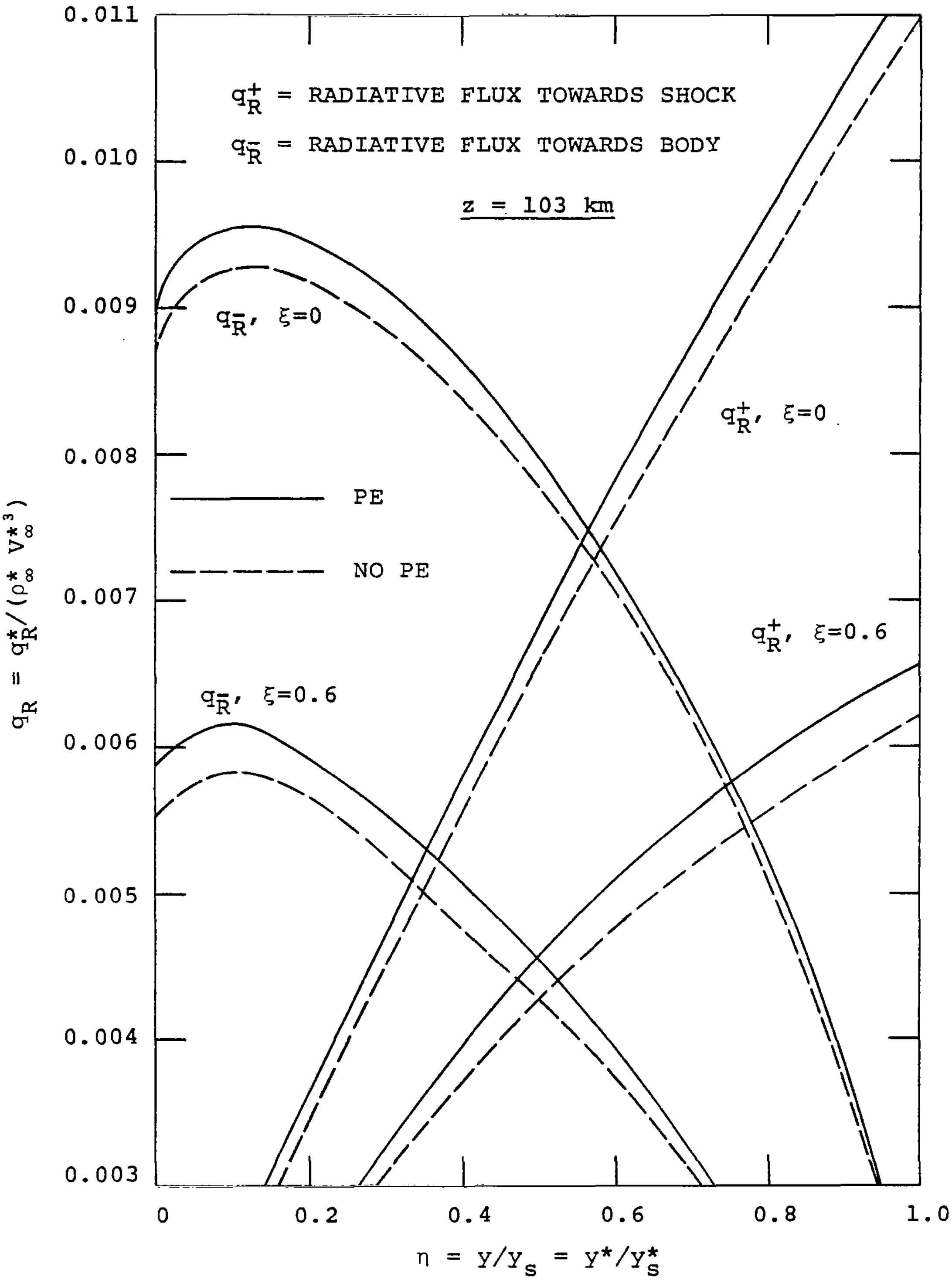

Figure 6.21. Variation of radiative heat flux in the shock layer for two body locations (ξ = 0 and 0.6), z = 103 km.

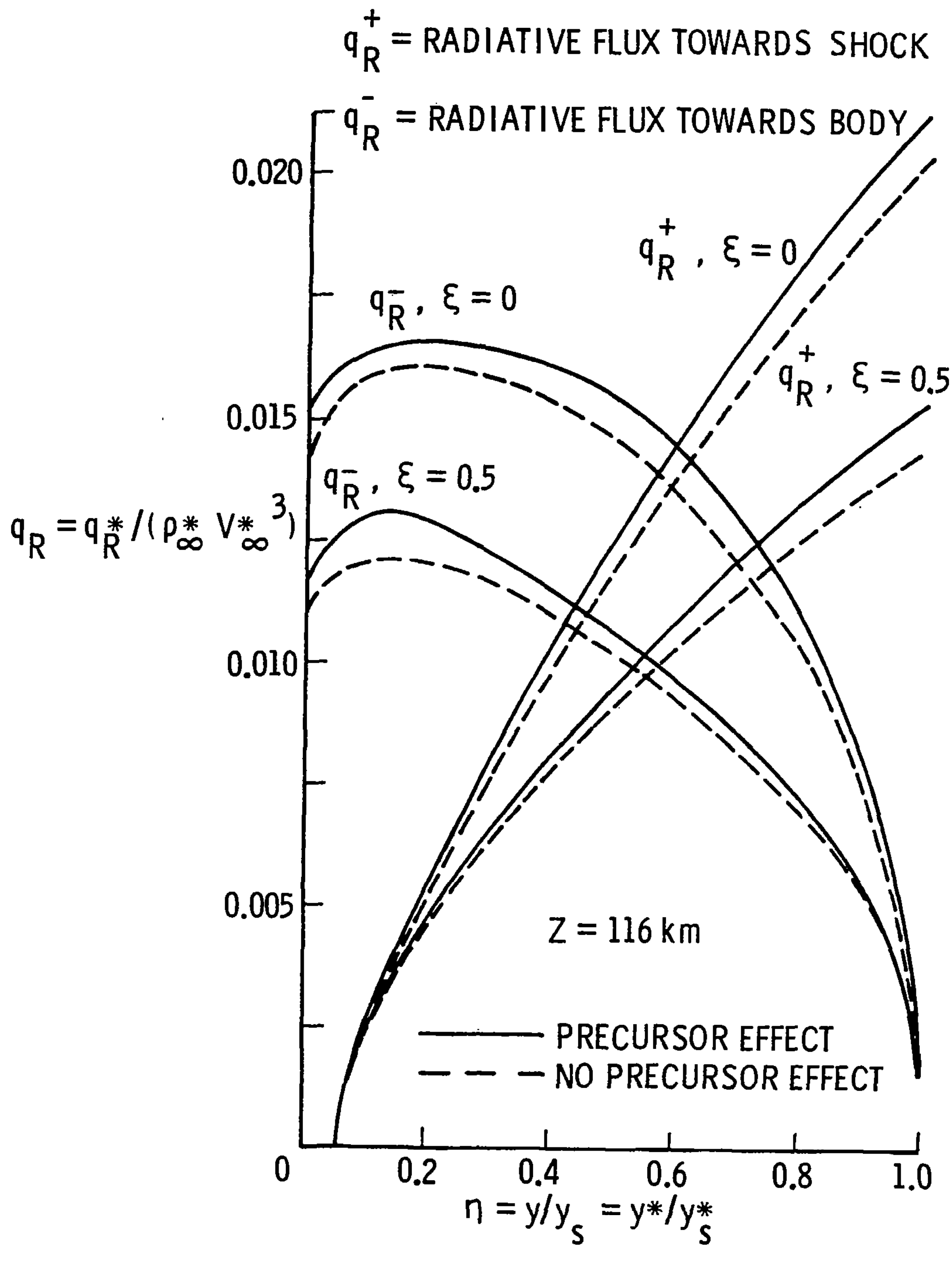

Figure 6.22. Variation of radiative heat flux in the shock layer for two body locations (ξ = 0 and 0.5), z = 116 km.

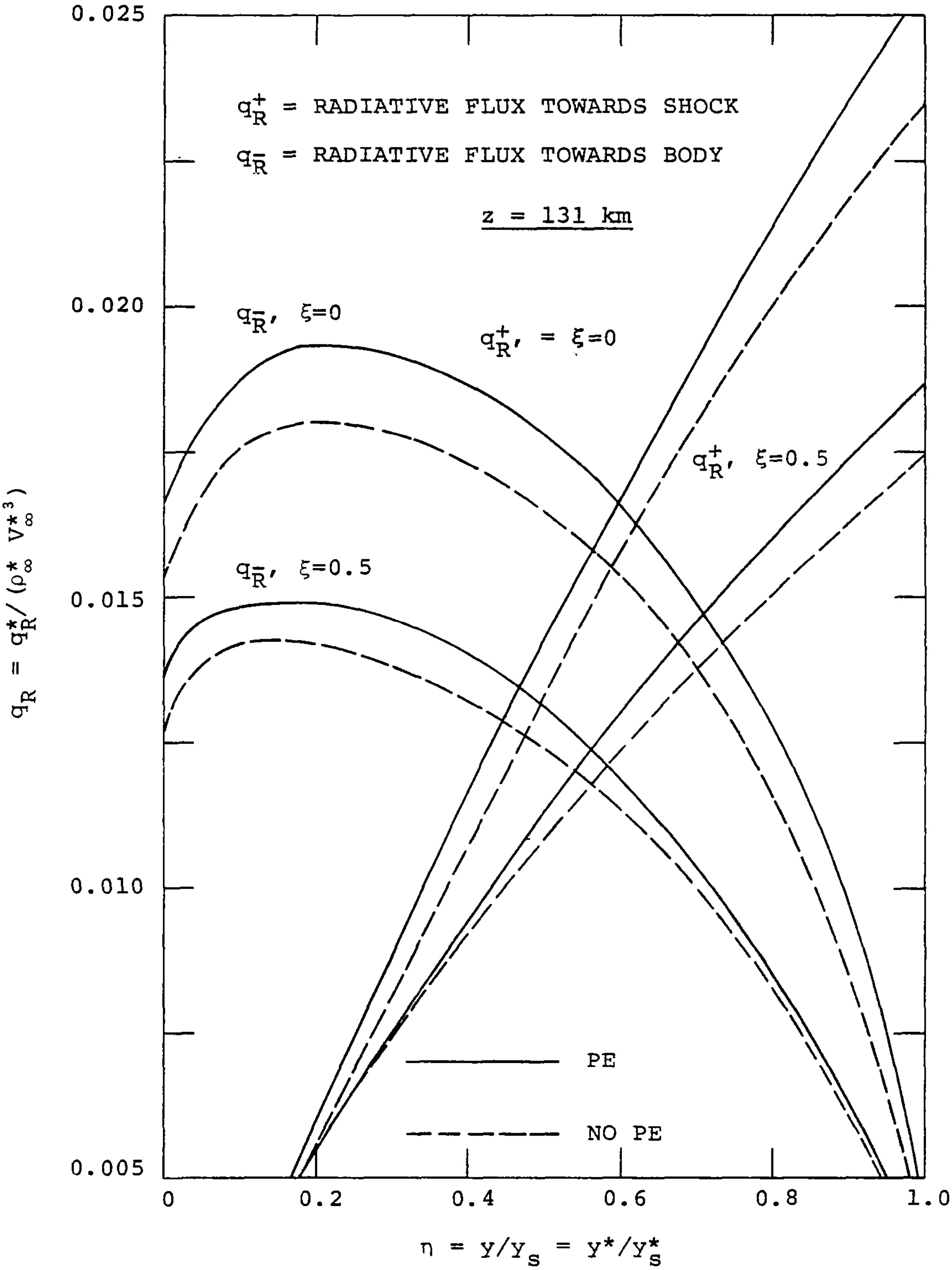

Figure 6.23. Variation of radiative heat flux in the shock layer for two body locations (ξ = 0 and 0.5), z = 131 km.

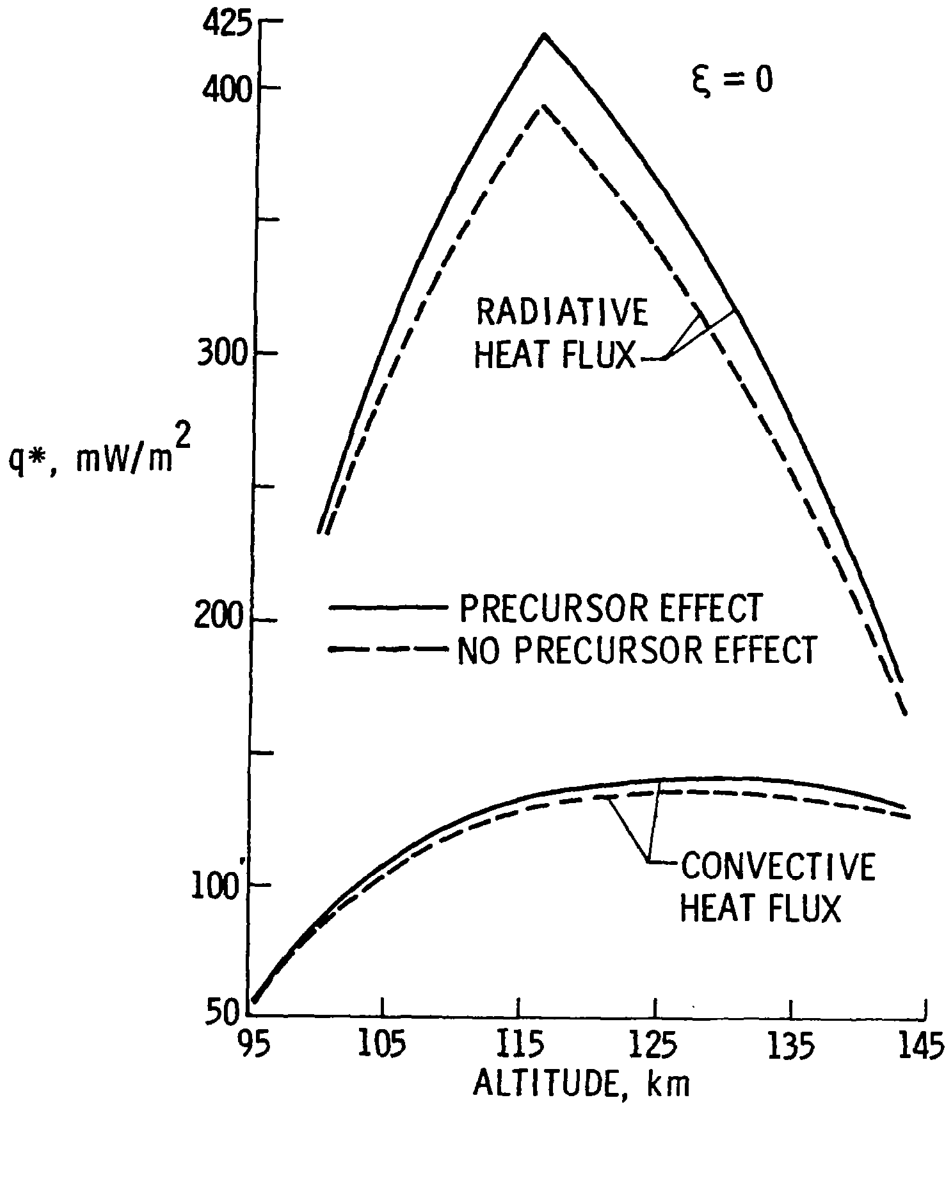

Figure 6.24. Radiative and convective heat flux to the body (at $\xi = 0$, $\eta = 0$) for different entry altitudes.

APPENDIX A

EXPLANATION OF SYMBOLS USED IN COMPUTER PROGRAM OF THE SHOCK-LAYER REGION

APPENDIX A

EXPLANATION OF SYMBOLS USED IN COMPUTER PROGRAM OF THE SHOCK-LAYER REGION

ARFA	shock angle defined in figure 2.1
CH	mass fraction of H
CHE	mass fraction of He
CHP	mass fraction of H^+
CHZ	mass fraction of Hz
CH2P	mass fraction of H_2^+
CE	mass fraction of e^-
CPII	free-stream specific heat
CPL	specific heat just ahead of shock, nondimensonal
CPS	specific heat just behind the shock, nondimensional
D	density, nondimensional
DD	coordinate measured normal to the body, cm
DENI	free-stream density, cm/sec
DI	density just ahead of the shock, g/cm^3
DS	density just behind the shock, nondimensional
DX	step distance between two nodal points along the body surface
DY	step distance between two nodal points normal to the body surface
EPS	Reynolds number parameter, nondimensional
ETHC	enthalpy, erg/g
E2	second exponential integral function
E3	third exponential integral function
F1	defined function of temperature

H2	number density of Hz, number/m^3
H	number density of H, number/m^3
HPLUS	number density of H^+, number/m^3
HE	number density of He, number/m^3
HE2PLUS	number density of He_2^+, number/m^3
M	molecular weight
MACI	Mach number
MV	viscosity
MVS	viscosity at shock
MUREF	refrance vicosity
NOPER	1 without precursor effect 2 with precursor effect
NORAD	1 without radiation 2 with radiation
NS	shock stand-off distance
P	pressure, nondimensional
PERI	free-stream pressure
PINF	pressure just ahead of the shock
PS	pressure just behind the shock
QO	radiative heat flux which come out from the shock toward the precursor region
QFXM	radiative heat flux toward body
QFXP	radiative heat flux toward shock
QTOTAL	net radiative heat flux between body and shock
RAT	the ratios of dy(N + 1)/dy(N)
T	temperature, nondimensional
TB	body temperature, °K
TH	enthalpy, nondimensional

THS	enthalpy at the shock, nondimensional
TINF	free-stream temperature, °K
TK	thermal conductivity of mixture, nondimensional
TS	temperature at the shock, nondimensional
V	velocity component tangent to the body surface, nondimensional
VS	shock velocity ocmponent tangent to the body surface, nondimensional
V	velocity component normal to the body surface, nondimensional
VELΦI	free-stream velocity
VS	shock velocity component normal to the body surface, nondimensional
VT	velocity at precursor region
XH	mole fraction of H between shock and body
XH2	mole fraction of H_2 between shock and body
XHE	mole fraction of He between shock and body
XH2I	mole fraction of Hz at free stream
XHEP	mole fraction of He^+ between shock and body
XHE2P	mole fraction of He_2^+ between shock and body
Y	normal coordinate, nondimensional
YH	Planck constant, erg/s
YK	Boltzmann constant, erg/°K
ZTA	body angle

APPENDIX B

COMPLETE COMPUTER PROGRAM

```
      PROGRAM COMPLET (INPUT,OUTPUT,TAPE5=INPUT,TAPE6=OUTPUT)
      COMMON /CONST1/ AL,AK,CT,K,K11,MBP,MA1,MA2
      COMMON /PERC/ VI(20),PINF(20), ETHP(20), DI(20),CPL(20), Q01(20),
     1        PINFN(20)
      COMMON /INFI/ TINF, PREI, VELOI, DENI, J, ALT, I111, CPII,XH2I
     1       ,NORAD,NOPRE
      COMMON /RAD/ COF1(58,51), QFXP(51),QFXM(51),QFX(51),DQY(51)
      COMMON /SHOCK/ DS(20), TS(20), VS(20), US(20), PS(20),MUS(20),TKS(
     120),ARFA(20),CPS(20) ,THS(20)
      COMMON /SDFDIS/ NS(20),NS1,NS2,PS1,AS(20) ,NSS2
      DIMENSION Q0(20),SPEC(6)
      REAL NS
      DATA (SPEC(I),I=1,6) / -1,-1,-1,0,-1,-1 /
      CALL SYSTEMC (115,SPEC)
C
C     ****  XH2I-- MOLE FRACTION OF H2 ***
C     *** NORAD=1   -- NO RADIATION ****
C     *** NORAD=2 --  WITH RADIATION ****
C     *** NOPRE=1--  NO      PRECURSOR EFFECT   ***
C     *** NOPRE=2--  WITH    PRECURSOR EFFECT   ***
C
      NOPRE=2
      NORAD=2
      XH2I=0.85
      CH2=XH2I*2/(XH2I*2+(1-XH2I)*4)
      CHE=1.-CH2
      CH=0.
      CH2P=0.
      CHP=0.
      CE=0.
      READ (5,1) TINF,PREI,VELOI,DENI,Z,CPII
    1 FORMAT (6E10.3)
      DO 2 M=1,20
      DI(M)=DENI
      VI(M)=VELOI
      PINF (M)=PREI
      ETHP(M)=-1.412E-3/VI(M)**2
      CPL(M)=19.52E7
      Q0(M)=0.
    2 CONTINUE
      KDD=1
    6 CALL SHOKLY
      IF (KDD.EQ.2) GO TO 3
      IF ((Q01(1)-Q0(1))/Q01(1).LT.0.03) GO TO 3
```

```
      QO(1)=QO1(1)
      QO1(MBP)=QO1(MA2)
      DO 5 M=1,MBP
      Y1=0.
      S=M*1.
      VELOI=ABS(VELOI)
      TSDIM=TS(M)*VELOI**2/CPII
      CALL PREC2 (M,Y1,TSDIM,PREI, ARFA(M), QO1(M), VELOI,DENI,TP,PP,VP,
     1  UI, VT, DP,  CHM, CH2M, HEI  ,CPC)
      VI(M)=VT
      DI(M)=DP
      PINF (M)=PP
      ETHP(M)=HEI    /VI(M)**2
    5 CONTINUE
      KDD=2
      GO TO 6
    3 CONTINUE
      WRITE (6,332)
  332 FORMAT (/,3X,*TEMP*,12X,*PRE*,12X,*V-VELO*,10X,*U-VELO*,9X,*DEN*,1
     1  2X,*CH*, 12X, *CH2+*,12X,*ENTH*,  4X,*Y2*, 5X,*M*)
      DO 11 M=1,MA2
      Y1=0.
      TSDIM=TS(M)*VELOI**2/CPII
    9 VELOI=ABS(VELOI)
      CALL PREC2 (M,Y1,TSDIM,PREI, ARFA(M), QO1(M), VELOI,DENI,TP,PP,VP,
     1  UI, VT, DP,  CHM, CH2M, ENTHC,CPC)
      Y2=Y1/(NS(M)*23)
      WRITE (6,331) TP, PP, VP, UI, DP, CHM,CH2M,ENTHC,  Y2,M
  331     FORMAT (  2X,8E14.4,3X,E12.4,3X,I2)
      IF (Y1.GT.10.0) GO TO 11
      IF (Y1.GT.3.0) GO TO 16
      IF (Y1.GT.1.0) GO TO 15
      Y1=Y1+0.2
      GO TO 9
   15 Y1=Y1+0.5
      GO TO 9
   16 Y1=Y1+1.0
      GO TO 9
   11 CONTINUE
      STOP
      END
C
C
      SUBROUTINE PREC2(S, Y, TS, PREI, ZTA, QO, VELOI, DENI, TP, PP, VP,
```

```
     1   UI, VT,DP, CHM, CH2M, HEI   , CPC)
      COMMON ARF(3),SUM(12), I1,T(50),TT,YI(3),YD(3), NA,ROH(3),IERR(12)
     1,VF(3,2), DH,CK,C,K,QQ,Y1,S1, E3(3),J,VE,DE
      DIMENSION  V(50),U(50),P(50),PHT(50),PH(50),CH2(50),CH(50),DEN(50)
      REAL NA,NB,NA1,MH2,MHH,MH,MHE
      TT=TS
      QQ=Q0
      Y1=Y
      S1=S
      VELOI=-VELOI
      VE=VELOI
      DE=DENI
      ROH(1)=4.1E-18
      ROH(2)=8.2E-18
      ROH(3)=2.1E-18
      DH=6.6256E-27
      CK=1.38054E-16
      C=3.0E10
      VF(1,1)=8.7E15
      VF(2,2)=3.75E15
      VF(3,1)=3.75E15
      VF(3,2)=1.15E15
      VF(1,2)=5.02E15
      VF(2,1)=5.02E15
      VI=VELOI*SIN(ZTA)
      UI=VELOI*COS(ZTA)   *(-1)
      V(1)=VI
      U(1)=UI
      P(1)=PREI
      DEN(1)=DENI
      CH2(1)=0.
      CH(1)=0.
      A=14.8E12
      D=4.5E12/2.
      YI(1)=1.0
      YI(2)=0.875
      YI(3)=0.
      YD(1)=0.0
      YD(2)=0.125
      YD(3)=1.
      R=8.3413E7
      PHT(1)=(VELOI**2)/2.+1.527*R*145.
      PH(1)=1.527*145.*R
      T(1)=145.
```

```
   20 DO 111  I=1,49
      I1=I
      NA=(7.2431122E22*0.85)*P(1)/(T(1)*10.)
      NA1=NA*1.0E-6
      ARF(1)=ROH(1)*NA1
      ARF(2)=ROH(2)*NA1
      ARF(3)=ROH(3)*NA1
      DEN(I+1)=DENI*VI/V(I)
      V(I+1)=(DENI*(VI**2)-P(I)+P(1))/(DENI*VI)
      U(I+1)=UI
      CALL QRADIA(Y,S,QR)
      PHTI=1.458*R*145.+(VELOI**2)/2.
      PHT(I+1)=(DENI*VI*PHTI-QR)/(DENI*VI)
      PH(I+1)=PHT(I+1)-(V(I+1)**2+U(I+1)**2)/2.
      T(I+1)=(PH(I+1)-(5./4.*R*T(I)+A/2.)*CH2(I)-(3./4.*R*T(I)+D)*CH(I))
     1/(1.458*R)
      CALL PCH2(PCHI,PCHD)
      NB=1.
      CH(I+1)=NB*PCHD
      CH2(I+1)=NB*PCHI
      P(I+1)=DEN(I+1)*R*T(I+1)*(176.17/400.+0.5*(CH2(I+1)+CH(I+1)))
      IF (ABS((V(I+1)-V(I))/V(I)).GT.0.01) GO TO 59
      IF (ABS((T(I+1)-T(I))/T(I)).GT.0.01) GO TO 59
      IF (ABS((P(I+1)-P(I))/P(I)).GT.0.01) GO TO 59
      IF (ABS((PH(I+1)-PH(I))/PH(I)).GT.0.01) GO TO 59
      IF (ABS((PHT(I+1)-PHT(I))/PHT(I)).GT.0.01) GO TO 59
      IF (ABS((CH(I+1)-CH(I))/CH(I)).GT.0.01) GO TO 59
      IF (ABS((CH2(I+1)-CH2(I))/CH2(I)).GT.0.01) GO TO 59
      IF (ABS((DEN(I+1)-DEN(I))/DEN(I)).GT.0.01) GO TO 59
      GO TO 75
   59 GO TO 111
  111 CONTINUE
   75 CHH=0.8019-CH2(I+1)-CH(I+1)
      CHE=0.1981
      CHM=CH(I+1)
      CH2M=CH2(I+1)
      HEI=PH(I+1)
      TP=T(I+1)
      PP=P(I+1)
      VP=-V(I+1)
      DP=DEN(I+1)
      VT=(VP**2+UI**2)**0.5
      RETURN
      END
```

```
      SUBROUTINE  QRADIA(Y,S,QR)
      COMMON ARF(3),SUM(12),I,T(50),TS,YI(3),YD(3),NA,ROH(3),IERR(12),VF
     1(3,2),DH,CK,C,K1,Q0,YY,SS,E3(3)
      COMMON /FFF/ Z
      DIMENSION E2(3),ARY(3),E1(3),V1(3,2)
      EXTERNAL FX5,FX2,FX3
      F1=6.256E-27/(1.3805E-16*TS)
      V1(1,1)=VF(1,1)*F1
      V1(1,2)=VF(1,2)*F1
      V1(2,1)=VF(2,1)*F1
      V1(2,2)=VF(2,2)*F1
      V1(3,1)=VF(3,1)*F1
      V1(3,2)=VF(3,2)*F1
      EPS=0.002
      DO 50 K=1,3
      K1=K
   30 CALL ROMBS (V1(K,2),V1(K,1),FX2,EPS,SUM(K+3),IERR(K+3))
      IF (IERR(K+3).EQ.0) GO TO 50
      K3=K+3
      PRINT 31, K3, IERR(K+3)
   31 FORMAT (*K=*,I2,*IERR=*,I3)
   50 CONTINUE
      QR1=0
      DO 100 K=1,3
      GR=0.5772
      ARY(K)=ARF(K)*Y
      IF (Y.LT.0.001) GO TO 35
      A0=0.26777343
      A1=8.6347608925
      A2=18.0590169730
      A3=8.5733287401
      B0=3.958469228
      B1=21.09965308
      B2=25.63295614
      B3=9.5733223454
      IF (ARY(K).LT.1.) GO TO 200
      X=ARY(K)
      E1(K)=EXP(-X)*(A0+A1*X+A2*X**2+A3*X**3+X**4)/(X*(B0+B1*X+B2*X**2+B
     13*X**3+X**4))
      GO TO 220
  200 X=ARY(K)
      E1(K)=-0.57721566-ALOG(X)+X-X**2./4.+X**3./18.-X**4./96.+X**5./600
     1.-X**6./4320.+X**7./35280.-X**8./322560.+X**9./3265920.-X**10./362
     288000.
```

```
220 E2(K)=(EXP(-X)-X*E1(K))
    E3(K)=(EXP(-X)-X*E2(K))/2.
    GO TO 35
 33 E2(K)=1.
    E3(K)=0.5
 35 QR4=E3(K)*SUM(K+3)*15.*Q0/(3.14159**5)
    QR1=     QR4+QR1
100 CONTINUE
    QR=QR1*2.*3.14159
    RETURN
    END
    FUNCTION FX2(X)
    COMMON ARF(3),SUM(12),I,T(50),TS,YI(3),YD(3),NA,ROH(3),IERR(12),VF
   1(3,2),DH,CK,C,K,Q0
    DAT=5.6697E-5
    FX2=X**3/(EXP(X)-1.)
    RETURN
    END
    SUBROUTINE PCH2 (PCHI,PCHD)
    COMMON ARF(3),SUM(12),I,T(50),TS,YI(3),YD(3),NA,ROH(3),IERR(12),VF
   1(3,2),DH,CK,C,K,Q0,Y,S,E3(3),J1,VELOI,DENI
    DIMENSION V1(3,2),CH1(3),CH2(3)
    EXTERNAL FX4
    F1=6.256E-27/(1.3805E-16*TS)
    V1(1,1)=VF(1,1)*F1
    V1(1,2)=VF(1,2)*F1
    V1(2,1)=VF(2,1)*F1
    V1(2,2)=VF(2,2)*F1
    V1(3,1)=VF(3,1)*F1
    V1(3,2)=VF(3,2)*F1
    EPS=0.001
    DO 59 J=1,3
    J1=J
    CALL ROMBS (V1(J,2),V1(J,1), FX4, EPS, SUM(J+9),IERR(J+9))
    CH1(J)=YI(J)*E3(J)*SUM(J+9)/(1.3805E-16*TS)
    CH2(J)=YD(J)*E3(J)*SUM(J+9)/(1.3805E-16*TS)
 59 CONTINUE
    PDHI=CH1(1)+CH1(2)+CH1(3)
    PDHD=CH2(1)+CH2(2)+CH2(3)
    X1=Q0*15.*2.*3.28E-24/(DENI*VELOI*3.14159**4)*(-1.)
    PCHI=PDHI*X1
    PCHD=PDHD*X1
    RETURN
    END
```

```
      FUNCTION FX4(X)
      COMMON ARF(3),SUM(12),I,T(50),TS,YI(3),YD(3),NA,ROH(3),IERR(12),VF
     1(3,2),DH,CK,C,K,Q0,Y,S,E3(3),J
      FX4=X**2/(EXP(X)-1)
      RETURN
      END
C
C
      SUBROUTINE SHOKLY
      COMMON / BODY/ ZTA(20), CK(20), X(20), DX,R(20),BATA(20),MUREF,EPS
      COMMON /CONST/ GAMA,DY(51),Y(51),CC3(20,51) ,CCC1,ICONT
      COMMON /CONST1/ AL,AK,CT,K,K11,MBP,MA1,MA2
      COMMON /CONST3/    AH2(3,7),AHP(3,7),AH2P(3,7),AHE(3,7),AHEP(3,7),
     1          AE(3,7) ,AH(3,7),KE
      COMMON /CONST6/ YH,YK,TB
      COMMON /DEPEND/ T(20,51),P(20,51),D(20,51),U(20,51),V(20,51),XHE(5
     11),XHH(51), XH(51),XHP(51),CP(51),XHEP(51),XHE2P(51),XEMIN(51)
     1   ,THP1(51),TH(51)
      COMMON /HEAT/ QCON,DIFU,RAT,QTOTL
      COMMON /INF/ VINF, DINF,CPI
      COMMON /INFI/ TINF, PREI, VELOI, DENI, M, ALT, I111, CPII,XH2I
     1      ,NORAD,NOPRE
      COMMON /PERC/ VI(20),PINF(20), ETHP(20), DI(20),CPL(20), Q01(20),
     1       PINFN(20)
      COMMON /RAD/ COF1(58,51), QFXP(51),QFXM(51),QFX(51),DQY(51)
      COMMON /R1/ A(58),B(58),F1(58),F3(58),F(58), V0(10),W1(58)
      COMMON /SDFDIS/ NS(20),NS1,NS2,PS1,AS(20) ,NSS2
      COMMON /SHOCK/ DS(20), TS(20), VS(20), US(20), PS(20),MUS(20),TKS(
     120),ARFA(20),CPS(20) ,THS(20)
      COMMON /SPHT/ CH2(51),CH(51),CHP(51),CHE(51)
      COMMON /TRANS/ TK(51),MU(51),TKDI
      REAL MUREF, MUHH,MUHE,MACI,MU,MUS,NS,NS1,NS2 ,MUU1
      INTEGER HIST
      RAT=1.10
      MBP=11
      MA1=MBP+1
      MA2=MBP-1
      TB=4000
      CALL DATAIN
      ICONT=1
      DO 43 I3=1,20
      PINFN(I3)=PINF(I3)/(DI(I3)*VI(I3)**2)
   43 CONTINUE
      NS2=0.
```

```
      K=51
      K11=K-1
      I111=1
      DIFU=0.005
      VELOI=ABS(VELOI)
      CALL BODY
   10 M=1
      IF (I111.GT.1) GO TO 2
   32 IF (M.EQ.1) GO TO 5
      NS(M)=NS(M-1)
      GO TO 15
    5 NS(1)=0.1
   15 CALL SHOCK
      M=1
   33 CONTINUE
      VINF=VI(M)
      DINF=DI(M)
      CPI=CPL(M)
      IF (I111.GT.1) GO TO 81
      IF (M.EQ.1) GO TO 6
      NS(M)=NS(M-1)
      GO TO 16
    6 NS(1)=0.1
   16 IF (I111.GT.1) GO TO 2
      ZTAA=ARFA(M)
      VENF=VINF*1.E-5
      UT=VENF*SIN(ZTAA   )*(1.+0.7476*(1.-XH2I))
      CTU=-545.37+61.608*UT-2.2459*UT**2+0.039922*UT**3-0.00035148*UT**4
     1+0.0000012361*UT**5
      CHT=5.661-0.52661*UT+0.020376*UT**2-0.00037861*UT**3+0.0000034265*
     1UT**4-0.000000012206*UT**5
      CH=CHT-0.3167*(1.-XH2I)
      CT=CTU+61.2*(1.-XH2I)
      IF (M.GT.1) GO TO 4
      DO 21 N=1,51
      P(M,N)=1.
      N2=N-1
      U(M,N)=1./50.*N2
      V(M,N)=1./50.*N2
      T(M,N)=(0.75/50.)*N2+0.25
      TSS=T(M,N)*TS(M)*VINF**2/CPI
      PSS=P(M,N)*PS(M)*DINF*VINF**2
      TSS1=(PSS/1013250.)**AL
      DSS=0.001292*(CT*TSS1/TSS)**(1./AK)
```

```
      D(M,N)=DSS/(DS(M)*DINF)
   21 CONTINUE
      GO TO 8
    4 DO 22 N=1,51
      T(M,N)=T(M-1,N)
      P(M,N)=P(M-1,N)
      D(M,N)=D(M-1,N)
      U(M,N)=U(M-1,N)
      V(M,N)=V(M-1,N)
      NS(M)=NS(M-1)
   22 CONTINUE
      GO TO 8
    2 CONTINUE
      CALL SHOCK
      M=1
   81 NST=NS(9)
    8 UST=U(M,20)
      ZTAA=ARFA(M)
      UT=VENF*SIN(ZTAA   )*(1.+0.7476*(1.-XH2I))
      CTU=-545.37+61.608*UT-2.2459*UT**2+0.039922*UT**3-0.00035148*UT**4
     1+0.0000012361*UT**5
      CHT=5.661-0.52661*UT+0.020376*UT**2-0.00037861*UT**3+0.0000034265*
     1UT**4-0.000000012206*UT**5
      CH=CHT-0.3167*(1.-XH2I)
      CT=CTU+61.2*(1.-XH2I)
      DST=D(M,20)
      TST=T(M,2 )
      DEFU=DIFU
      HIST=1
  105 DO 23 N1=1,51
      N=52-N1
      TSS=T(M,N)*TS(M)*VINF**2/CPI
      RHO=D(M,N)*DS(M)*DINF*1000.
      P11=TSS*(RHO/(1000.*0.001292))**AK
      P12=1013250.*(P11/CT)**(1./AL)
      P13=0.1*P12
      CALL NOBDEN (TSS,RHO,H2,H,HPLUS,HE,HEPLUS,HE2PLUS,EMINUS,XH2I)
      AA1=1./( H2+H+HPLUS+HE+HEPLUS+ HE2PLUS+EMINUS)
      R1=1.98726
      EMINS=EMINUS
      ND=ICONT/2
      ND=ND*2
      IF (NORAD .EQ.1) GO TO 902
      IF (ND.NE.ICONT) GO TO 902
```

```
      IF (HIST.EQ.2) GO TO 902
  901 CALL ABSOCOF (TSS,RHO,P12,H2,H,HPLUS,HE,HEPLUS,HE2PLUS,EMINS)
  903 DO 900 KCD=1,58
      COF1(KCD,N)=A(KCD)
  900 CONTINUE
  902 XHH(N)=H2*AA1
      XH(N)=H*AA1
      XHE(N)=HE*AA1
      XHP(N)=HPLUS*AA1
      XHEP(N)=HEPLUS*AA1
      XHE2P(N)=HE2PLUS*AA1
      XEMIN(N)=EMINUS*AA1
      C11=R1*2.5
      IF (TSS.LT.6000.) GO TO 51
      CPH2=R1*(3.363+4.656E-4*TSS-5.127E-8*TSS**2+2.802E-12*TSS**3-4.905
     1E-17*TSS**4)
      CPH=R1*(2.475164+7.366387E-5*TSS-2.537593E-8*TSS**2+2.386674E-12*T
     1SS**3-4.551431E-17*TSS**4)
      CEMIN=R1*(2.508-6.332E-6*TSS+1.364E-9*TSS**2-1.094E-13*TSS**3+2.93
     14E-18*TSS**4)
      GO TO 52
   51 CPH2=R1*(3.100190+5.111946E-4*TSS+5.26442E-8*TSS**2-3.490997E-11*T
     1SS**3+3.69453E-15*TSS**4)
      CPH=C11
      CEMIN=C11
   52 CPHE=C11
      CPHPL=C11
      CHEP=C11
      CX=CPH2*XHH(N)+CPHE*XHE(N)+CPH*XH(N)+CPHPL*XHP(N)+CEMIN*XEMIN(N)+C
     1HEP*XHEP(N)
      CX2=XHH(N)*2.+XH(N)+XHE(N)*4.+XHP(N)+XEMIN(N)*0.5486E-3
      CX1=CX/CX2*4.181E7
      IF (N.EQ.51) GO TO 9
      CP(N)=CX1/(CPI*CPS(M))
      GO TO 23
    9 CPS(M)=CX1/CPI
      CP(51)=1.
   23 CONTINUE
      IF ( HIST.EQ.2) GO TO 905
      IF (NORAD .EQ.1) GO TO 905
      IF  (ND.EQ.ICONT) GO TO 904
      IF (ICONT.NE.1.) GO TO 905
      IF (M.NE.1) GO TO 905
      DO 93 N4=1,51
```

```
      QFX(N4)=0.
      DQY(N4)=0.
   93 CONTINUE
      GO TO 905
  904 CALL RADAT
  905 CALL TRANSP
      IF ( HIST.EQ.2) GO TO 83
      CALL ENERGY
      HIST=2
      GO TO 105
   83 CALL MOMENTM
       ICONT=ICONT+1
      IF (ABS((U(M,20)-UST)/UST).GT.0.040) GO TO 8
      IF (ABS((D(M,20)-DST)/DST).GT.0.030) GO TO 8
      IF (ABS((T(M,2 )-TST)/TST).GT.0.015) GO TO 8
      IF (ABS ((DIFU-DEFU)/DIFU) .GT.0.10) GO TO 8
      IF (ICONT .LT.4) GO TO 8
      WRITE (6,113) M,NS(M),ICONT   ,X(M)
  113 FORMAT (////,3X,*STATION M=*,I2,5X, *NS(M)=*, E12.4, 5X, *ITERATIO
     1   N=*, I2,5X,*X(M)=*,F4.1)
      WRITE (6,112) QCON,DIFU ,QTOTL,ETHP(M)
  112 FORMAT (//,2X,*QCON=*,E11.4,5X,*DIFU=*,E11.4,*     QTOT=*,E11.4,
     1   *   ETHP(M)=*,E11.4,/)
      WRITE (6,72)
   72 FORMAT (/,2X,*U-VELOCITY*,6X,*V-VELOCITY*,8X, *PRE*,11X,*TEMP*,10X
     1,*DENSITY*, 9X,* TDIM*,9X,*QFXP   *,6X,*QFXM*, 9X,*Y*,10X,*N*,/)
      DO 79 N=1,51
      TT=T(M,N)*TS(M)
      TT1=TT*VINF**2/CPI
      WRITE (6,75) U(M,N),V(M,N), P(M,N), T(M,N), D(M,N),TT1,QFXP(N),QFX
     1   M(N),Y(N),N
   75 FORMAT (  1X,9E14.4,3X,I2        )
   79 CONTINUE
      WRITE (6,62)
   62 FORMAT (//,8X, *XH2*,12X,*XHE*,12X,*XH*,12X,*XH+*,11X,*XE-*,11X,*C
     1P*,12X,* TK*,12X,*MU*,5X,*N*,/)
      DO 65 N=1,51
      TKK1=TK(N)*TKS(M)*CPI*MUREF
      MUU1=MU(N)*MUS(M)*MUREF
      WRITE (6,61) XHH(N), XHE(N),XH(N),XHP(N),XEMIN(N),CP(N),TKK1,MUU1
     1    ,N
   61 FORMAT (  1X,8E14.3,3X,I2)
      THP1(N)=TH(N)
   65 CONTINUE
```

```
      IF (NOPRE.EQ.1) GO TO 24
      Q01(M)=QFXP(51)*CCC1
   24 M=M+1
  123 ICONT=1
      IF (I111.EQ.2) GO TO 66
      IF (M.LT.MA1) GO TO 33
      GO TO 67
   66 IF (M.LT.MBP) GO TO 33
   67 ASS=(NS(4)-NS(1)) /6
      AS(1)=NS(1)
      AS(2)=AS(1)+ASS
      AS(3)=AS(2)+2*ASS
      DO 7 M1=4,MBP
   90 AS(M1)=NS(M1)
    7 CONTINUE
      IF (I111.EQ.1) GO TO 111
      GO TO 60
  111 NST=NS(3)
      I111=2
      GO TO 10
   60 CONTINUE
      IF (NORAD .EQ.1) GO TO 201
      IF (NOPRE.EQ.1) GO TO 201
      RETURN
      GO TO 202
  201 STOP
  202 END
C
C
      SUBROUTINE DATAIN
      COMMON /R1/ A(58),B(58),F1(58),F3(58),F(58), V0(10),W1(58)
      DATA(F1(I),I=1,58)/ 14.595,13.595,13.215,13.086,13.016,12.765,
     A      12.725,12.545,12.284,12.106,12.086,12.082,12.064,11.884,
     B      11.196,10.696,10.246,10.201,10.1965,10.1955,10.191,10.146,
     C       9.696, 9.000, 7.000, 5.000, 4.000, 3.400, 3.020, 2.875,
     D       2.835, 2.655, 2.579, 2.552, 2.546, 2.519, 2.249, 1.988,
     E       1.898, 1.889, 1.887, 1.878, 1.788, 1.511, 1.131,  .987,
     F        .947,  .850,  .731,  .668,  .654,  .591,  .470,  .396,
     G        .315,  .297,  .216, 0.000/
      DATA (F3(I),I=1,58)/ .482E-3,.716E-3,.831E-3,.879E-3,.900E-3,
     A     .934E-3,.966E-3,.992E-3,.105E-2,.110E-2,.113E-2,.113E-2,
     B     .114E-2,.117E-2,.130E-2,.153E-2,.174E-2,.187E-2,.189E-2,
     C     .189E-2,.189E-2,.190E-2,.205E-2,.246E-2,.403E-2,.980E-2,
     D     .225E-1,.400E-1,.609E-1,.782E-1,.860E-1,.969E-1,.112E+0,
```

```
E      .118E+0,.121E+0,.123E+0,.149E+0,.212E+0,.273E+0,.295E+0,
F      .297E+0,.300E+0,.325E+0,.452E+0,.905E+0,.170E+1,.221E+1,
G      .277E+1,.410E+1,.587E+1,.693E+1,.833E+1,.138E+2,.250E+2,
H      .457E+2,.699E+2,.125E+3,.159E+4/
 DATA (F(I),I=1,58)/ 1.19,1.04,.986,.967,.960,.948,.937,.929,.913,
A      .897,.890,.889,.888,.881,.849,.805,.770,.752,.750,.750,.750,
B      .748,.730,.688,.588,.441,.331,.272,.236,.217,.210,.202,.192,
C      .189,.187,.186,.175,.156,.143,.139,.139,.138,.135,.121,.0972,
D      .0779,.0711,.0661,.0581,.0515,.0486,.0458,.0390,.0318,.0261,
E      .0225,.0189,.00794/
 DATA  (VO(I), I=1,10)/ 10.196,12.084,12.745,13.051,1.888,2.549,
A         2.855,.661,.967,.306/
 DATA (W1(I),I=1,58)/ 35.4,14.595,13.595,13.215,13.086,13.016,12.76
A    5,12.725,12.545,12.284,12.106,12.086,12.082,12.046,11.884,
B     11.196,10.696,10.246,10.201,10.1965,10.1955,10.191,10.146,
C     9.696,9.000,7.000,5.000,4.000,3.400,3.020,2.875,2.835,2.655,
D     2.579,2.552,2.546,2.519,2.249,1.988,1.898,1.889,1.887,1.878,
E     1.788,1.511,1.131,0.987,0.947,0.850,0.731,0.688,0.654,0.591,
F     0.470,0.396,0.315,0.297,0.216/
 RETURN
 END
C
 SUBROUTINE ENTHALP ( TEMP,  CH2,CH,CHE,CH2P,CE,CHP,CPC,ENTHC)
 COMMON /ENTH/ THH2, THH, THHE, THHP, THE
 COMMON /CONST3/    AH2(3,7),AHP(3,7),AH2P(3,7),AHE(3,7),AHEP(3,7),
1           AE(3,7) ,AH(3,7),KE
 IF (KE.NE.1) GO TO 15
 DATA (AH(1,I),I=1,7)/2.5,0.,0.,0.,0.,2.547162E4,-4.601176E-1/
 DATA (AH(2,I),I=1,7)/2.5,0.,0.,0.,0.,2.547162E4,-4.601176E-1/
 DATA (AH(3,I),I=1,7)/2.475164,7.366387E-5,-2.537593E-8,2.386674E-1
1       2,-4.551431E-17,2.523626E4,-3.749137E-1/
 DATA (AH2(1,I),I=1,7)/3.057445,2.676520E-3,-5.809916E-6,5.521039E-
1      9,-1.812273E-12,-9.889047E2,-2.299705/
 DATA (AH2(2,I),I=1,7)/3.100190,5.111946E-4,5.264421E-8,-3.490997E-
1      11,3.694534E-15,-8.773804E2,-1.962942/
 DATA (AH2(3,I),I=1,7)/3.36300,4.65600E-4,-5.12700E-8,2.80200E-12,-
1      4.905E-17,-1.01800E3,-3.716/
 DATA (AHP(1,I),I=1,6)/2.5,0.,0.,0.,0.,1.840334E5/
 DATA (AH2P(1,I),I=1,6)/2.817375,3.657610E-3,-7.965548E-6,8.26140E-
1     9,-3.090228E-12,1.80027389E5/
 DATA (AH2P(2,I),I=1,6)/ 3.32817562,2.50506781E-4,1.42245209E-7,-4.
1     45902420E-11,3.733756E-15,1.7997470E5/
 DATA (AHE(1,I),I=1,7)/2.5,0.,0.,0.,0.,-7.453749E2,9.153488E-1/
 DATA (AHEP(1,I),I=1,7)/2.5,0.0,0.0,0.0,0.0,2.853426E5,1.608404/
```

```
      DATA (AE(1,I),I=1,7)/2.5,0.,0.,0.,0.,-7.453750E2,-1.173402E1/
      DATA (AE(3,I),I=1,7)/2.508,-6.3320E-6,1.3640E-9,-1.094E-13,2.9340E
     1    -18,-7.450E2,-1.208E1/
      DO 1 I=1,6
      AHP(2,I)=AHP(1,I)
      AHP(3,I)=AHP(1,I)
      AH2P(3,I)=AH2P(2,I)
      AHE(2,I)=AHE(1,I)
      AHE(3,I)=AHE(1,I)
      AHEP(2,I)=AHEP(1,I)
      AHEP(3,I)=AHEP(1,I)
      AE(2,I)=AE(1,I)
    1 CONTINUE
   15 R=1.98726
      IF (TEMP.GT.1000.) GO TO 2
      J=1
      GO TO 10
    2 IF (TEMP.GT.6000.)GO TO 3
      J=2
      GO TO 10
    3 J=3
   10 CPH=R*(AH(J,1)+AH(J,2)*TEMP+AH(J,3)*TEMP**2+AH(J,4)*TEMP**3+AH(J,5
     1        )*TEMP**4)
      CPH2=R*(AH2(J,1)+AH2(J,2)*TEMP+AH2(J,3)*TEMP**2+AH2(J,4)*TEMP**3+
     1        AH2(J,5)*TEMP**4)
      CPHP=R*(AHP(J,1)+AHP(J,2)*TEMP+AHP(J,3)*TEMP**2+AHP(J,4)*TEMP**3+
     1        AHP(J,5)*TEMP**4)
      CPH2P=R*(AH2P(J,1)+AH2P(J,2)*TEMP+AH2P(J,3)*TEMP**2+AH2P(J,4)*TEMP
     1        **3+AH2P(J,5)*TEMP**4)
      CPHE=R*(AHE(J,1)+AHE(J,2)*TEMP+AHE(J,3)*TEMP**2+AHE(J,4)*TEMP**3+
     1        AHE(J,5)*TEMP**4)
      CPE=R*(AE(J,1)+AE(J,2)*TEMP+AE(J,3)*TEMP**2+AE(J,4)*TEMP**3+AE(J,5
     1       )*TEMP**4)
      R1=R*TEMP
      THH=R1*(AH(J,1)+AH(J,2)/2.*TEMP+AH(J,3)/3.*TEMP**2+AH(J,4)/4.*TEMP
     1        **3+AH(J,5)/5.*TEMP**4.+AH(J,6)/TEMP)
      THH2=R1*(AH2(J,1)+AH2(J,2)/2.*TEMP+AH2(J,3)/3.*TEMP**2+AH2(J,4)/4.
     1         *TEMP**3+AH2(J,5)/5.*TEMP**4+AH2(J,6)/TEMP)
      THHP=R1*(AHP(J,1)+AHP(J,2)/2.*TEMP+AHP(J,3)/3.*TEMP**2+AHP(J,4)/4.
     1         *TEMP**3+AHP(J,5)/5.*TEMP**4+AHP(J,6)/TEMP)
      THH2P=R1*(AH2P(J,1)+AH2P(J,2)/2.*TEMP+AH2P(J,3)/3.*TEMP**2+AH2P(J,
     1      4)/4.*TEMP**3+AH2P(J,5)/5.*TEMP**4+AH2P(J,6)/TEMP)
      THHE=R1*(AHE(J,1)+AHE(J,2)/2.*TEMP+AHE(J,3)/3.*TEMP**2+AHE(J,4)/4.
     1         *TEMP**3+AHE(J,5)/5.*TEMP**4+AHE(J,6)/TEMP)
```

```
      THE=R1*(AE(J,1)+AE(J,2)/2.*TEMP+AE(J,3)/3.*TEMP**2+AE(J,4)/4*TEMP*
     1     *3 +AE(J,5)/5.*TEMP**4+AE(J,6)/TEMP)
      CP=CPH*CH+CPH2*CH2/2.+CPHP*CHP+CPH2P*CH2P/2.+CPHE*CHE/4.+CPE*CE/0.
     1   5486E-3
      CPC=CP/(2.3901E-8)
      ENTH=THH*CH+THH2*CH2/2.+THHP*CHP+THH2P*CH2P/2.+THHE*CHE/4.+THE*CE/
     1     0.5486E-3
      ENTHC=ENTH/(2.3901E-8)
C
C     CP..CAL/GM   K     CPC..CM2/SEC2 K
C     ENTH..CAL/GM       ENTHC..CM2/SEC2 K
C     CH2..CH..CH2P..CHP...ETC......MASS FRACTION
      RETURN
      END
C
C
      SUBROUTINE BODY
      COMMON / BODY/ ZTA(20), CK(20), X(20), DX,R(20),BATA(20),MUREF,EPS
      COMMON /CONST/ GAMA,DY(51),Y(51),CC3(20,51)
      COMMON /INFI/ TINF, PREI, VELOI, DENI, M, ALT, I111, CPII,XH2I
      COMMON /INF/ VINF, DINF,CPI
      COMMON /HEAT/ QCON,DIFU,RAT,QTOTL
      REAL MUREF, MUHH,MUHE,MACI,MU,MUS,MUH
      WRITE (6,11)
   11 FORMAT (/,5X,*ZTA*,9X,*BODY CURVE*, 6X,*R*,9X,*MUREF*,7X,*EPS*,
     1 8X,*M*,/)
      RN=23.
      TREF=VELOI**2/CPII
      MUREF=0.66E-6*(TREF**1.5/(TREF+70.5))*10.
      EPS=MUREF/(DENI*VELOI*RN)
      EPS=EPS**0.5
      PI=3.14159
      X(1)=0.
      ZTA(1)=PI/2.
      BATA(1)=0.
      CK(1)=1.
      R(1)=0.
      DX=0.1
      A=1.
      M1=20
      DO 5 M=2,M1
    7 F1=DX*SQRT((A**2+R(M-1)**2)/(A**2+2.*R(M-1)**2))
      F2=DX*SQRT((A**2+(R(M-1)+F1/2.)**2)/(A**2+2.*(R(M-1)+F1/2.)**2))
      F3=DX*SQRT((A**2+(R(M-1)+F2/2.)**2)/(A**2+2.*(R(M-1)+F2/2.)**2))
```

```
      F4=DX*SQRT((A**2+(R(M-1)+F3)**2)/(A**2+2.*(R(M-1)+F3)**2))
      R(M)=R(M-1)+(F1+2.*F2+2.*F3+F4)/6.
      W=SQRT(A**2+R(M)**2)
      CK(M)=A**2/(R(M)**2+W**2)**1.5
      ZTA(M)=ATAN(W/SQRT(W**2-A**2))
      BATA(M)=PI/2.-ZTA(M)
      X(M)=X(M-1)+DX
      WRITE (6,89)ZTA(M),CK(M),R(M),MUREF,EPS,M
   89 FORMAT (3X,5E12.4,4X,I2   )
    5 CONTINUE
      YY=1.00*(1-RAT)/(1-RAT**50)
      DY(1)=YY
      Y(1)=0.
      DO 99 N=1,49
      DY(N+1)=RAT*DY(N)
      Y(N+1)=Y(N)+DY(N)
   99 CONTINUE
      Y(51)=Y(50)+DY(50)
      DX=0.1
      RETURN
      END
C
C
      SUBROUTINE SHOCK
      COMMON / BODY/ ZTA(20), CK(20), X(20), DX,R(20),BATA(20),MUREF,EPS
      COMMON /CONST1/ AL, AK, CT,K,K11,MBP,MA1
      COMMON /CONST3/     AH2(3,7),AHP(3,7),AH2P(3,7),AHE(3,7),AHEP(3,7),
     1           AE(3,7) ,AH(3,7),KE
      COMMON /INFI/ TINF, PREI, VELOI, DENI, M, ALT, I111, CPII,XH2I
      COMMON /PERC/ VI(20),PINF(20), ETHP(20), DI(20),CPL(20), Q01(20),
     1        PINFN(20)
      COMMON /SDFDIS/ NS(20),NS1,NS2,PS1,AS(20)
      COMMON /SHOCK/ DS(20), TS(20), VS(20), US(20), PS(20),MUS(20),TKS(
     120),ARFA(20),CPS(20) ,THS(20)
      REAL MUREF, MUHH,MUHE,MACI,MU,MUS,NS,NS1,NS2
      DIMENSION HS(20),HSS(20),EH(20) ,DNS(20)
      HX2I= XH2I
      MBB=MBP-1
      W=8.3143E7
      AL=0.67389-0.04637*ALOG(XH2I)
      AK=0.65206-0.04407*ALOG(XH2I)
      AM=0.95252-0.1447*ALOG(XH2I)
      AN=0.97556-0.16149*ALOG(XH2I)
      WRITE (6,39)
```

```
39 FORMAT (9X,*PS*,15X,*DEN*,15X,*TEMP*, 14X,*HS*, 16X,*US*,16X,*VS*,
  110X,*M*,8X,*T (K)*,/)
   IF (I111.GT.1) GO TO 1
   DO 11 I=1,20
   ARFA(I)=ZTA(I)
11 CONTINUE
   GO TO 4
 1 DO 12 I=2,MBB
   IF (I.EQ.MBP) GO TO 2
   DNS(I)=(AS(I+1)-AS(I-1))/(2.*DX)
   GO TO 30
 2 DNS(MBP)=(AS(MBP)-AS(MBB))/DX
30 ARFA(I)= ZTA(I)+ATAN(DNS(I)/(1.+CK(I)*NS(I)))
12 CONTINUE
   ARFA(1)=ZTA(1)
 4 CONTINUE
   VINF=VI(M)
   DINF =DI(M)
   CPI=CPL(M)
   VENF=VINF*1.E-5
   ZTAA=ARFA(M)
   UT=VENF*SIN(ZTAA   )*(1.+0.7476*(1.-HX2I))
   CTU=-545.37+61.608*UT-2.2459*UT**2+0.039922*UT**3-0.00035148*UT**4
  1+0.0000012361*UT**5
   CHT=5.661-0.52661*UT+0.020376*UT**2-0.00037861*UT**3+0.0000034265*
  1UT**4-0.000000012206*UT**5
   CH=CHT-0.3167*(1.-HX2I)
   CT=CTU+61.2*(1.-HX2I)
   IF (M.EQ.1) GO TO 3
   DS1=DS(M-1)
   DS2=DS1+1.
27 D9=DS2
   EH1=ETHP(M)                    +SIN(ARFA(M))**2*(1.-1./DS1**2)/2.
   P1=PINFN(M)            +SIN(ARFA(M))**2*(1.-1./DS1)
   GO TO 301
 9 EH2=ETHP(M)                    +SIN(ARFA(M))**2*(1.-1./DS2**2)/2.
   P2=PINFN(M)            +SIN(ARFA(M))**2*(1.-1./DS2)
   GO TO 302
 3 DS1=6
   DS2=9
28 D9=DS2
   NS1=NS(1)
   EH1=ETHP(M)                    +0.5*(1.-1./DS1**2)
   PP=PINFN(M)            +(1.-1./DS1)
```

```
      PP1=BATA(M)**2*((1.-1./DS1)*(1.-NS2/(1.+NS1))**2)
      P1=PP-PP1
  301 DSS=DS1*DINF
      PSS=P1*DINF*VINF**2
      XA=PSS/1013250.
      YA=DSS/0.001292
      TSS=CT*(XA**AL/YA**AK)
      RHO=DSS*1000
      CALL NOBDEN (TSS , RHO, H2,H,HPLUS,HE, HEPLUS, HE2PLUS,EMINUS,
     1             XH2I)
      CALL VOLMAS (H2,H, HPLUS,HE, HEPLUS,HE2PLUS,EMINUS,YH2, YH, YHP,
     1         YHE, YHEP,YHE2P, YE)
      YH2P=0
      KE=1
      CALL ENTHALP (TSS ,YH2,YH,YHE,YH2P,YE,YHP,CPC,ENTHC)
      KE=2
      EHH1=ENTHC
      DH1=EHH1/(VINF**2)-EH1
      IF (M.NE.1) GO TO 9
   19 EH2=ETHP(M)                      +0.5*(1.-1./DS2**2)
      PS1=PINFN(M)             +(1.-1./DS2)
      PP1=BATA(M)**2*((1.-1./DS2)*(1.-NS2/(1.+NS1))**2)
      P2=PS1-PP1
  302 PSS=P2*DINF*VINF**2
      DSS=DS2*DINF
      XA=PSS/1013250.
      YA=DSS/0.001292
      Z=W*273.15/2.304
      TSS=CT*(XA**AL/YA**AK)
      RHO=DSS*1000
      CALL NOBDEN (TSS , RHO, H2,H,HPLUS,HE, HEPLUS, HE2PLUS,EMINUS,
     1             XH2I)
      CALL VOLMAS (H2,H, HPLUS,HE, HEPLUS,HE2PLUS,EMINUS,YH2, YH, YHP,
     1         YHE, YHEP,YHE2P, YE)
      CALL ENTHALP (TSS ,YH2,YH,YHE,YH2P,YE,YHP,CPC,ENTHC)
      EHH2=ENTHC
      EH3=EHH2/(VINF**2)
      IF (ABS((EH3-EH2)/EH2).LT.0.005) GO TO 100
      DH2=EH3-EH2
      SLOP=(DH2-DH1)/(DS2-DS1)
      D3=DS2-DH2/SLOP
      DH1=DH2
      IF (D3.LT.5.) GO TO 8
      IF (D3.LT.14.) GO TO 18
```

```
    8 DS2=D9+0.1
      IF (M.NE.1) GO TO 27
      GO TO 28
   18 DS2=D3
      IF (N.NE.1) GO TO 9
      GO  TO 19
  100 PS(M)=P2
      DS(M)=DS2
      TSS=CT*(XA**AL/YA**AK)
      TS(M)=TSS*CPI/(VINF**2)
      EH(M)=EHH2/(VINF*VINF)
      VSP=-SIN(ARFA(M))/DS(M)
      USP=COS(ARFA(M))
      US(M)=USP*SIN(ARFA(M)+BATA(M))+VSP*COS(ARFA(M)+BATA(M))
      VS(M)=-USP*COS(ARFA(M)+BATA(M))+VSP*SIN(ARFA(M)+BATA(M))
      THS(M)=EH(M)+US(M)**2/2
      WRITE (6,29) PS(M), DS(M), TS(M), EH(M), US(M),VS(M), M,TSS
   29 FORMAT (  4X,6E17.4,4X,I2,4X,E11.4)
      M=M+1
      IF (M.GT. MBP) GO TO 69
      GO TO 4
   69 RETURN
      END
C
      SUBROUTINE NOBDEN (TSS,RHO, H2,H,HPLUS, HE, HEPLUS,HE2PLUS,EMINUS,
     1      XH2I)
      XH2=XH2I
      XHE=1.-XH2
      ALPHAH=2.*XH2
      ALPHAHE=XHE
      ALPHAC=0.
      T=TSS
      AMO=1.008*ALPHAH+4.003*ALPHAHE+12.011*ALPHAC
      R=8.31441E3
C COMPUTE EQUILIBRIUM CONSTANTS - NATURAL LOGS
3     A=ALOG(T)
      STARN=6.02252E26*(RHO/AMO)
      B=1./T
      C1=69.939357-51964.*B
      C2=-49.234384-(1.5*A)+157810.*B
      AKK=ALPHAHE*STARN
      IF(ALPHAHE.EQ.0.)GOTO4
      C3=-50.620678-(1.5*A)+285287.*B
      C4=-99.161915-(3.*A)+916687.*B
```

```
      IF(C4.GT.741.)C4=741.
4     IF(ALPHAC-0.)5,7,5
5     C5=292.632558-(1.25*A)-197547.4*B
      C6=218.091512-A-146258.4*B
      C7=144.311945-(.5*A)-102732.0*B
      C8=68.629830-40279.5*B
      C9=-49.522066-1.5*A+130774.8*B
      C10=-97.657838-3.*A+413782.3*B
6     FORMAT(1H //)
C COMPUTE SPECIES NUMBER DENSITIES
7     AK=ALPHAH*STARN
      AK1=EXP(C1)/(4.*AK)
      AK2=2.*AK*EXP(C2)
      E1=1.-AK1*(SQRT(1.+(2./AK1))-1.)
      E2=(1./AK2)*(SQRT(1.+2.*AK2)-1.)
      IF(ALPHAHE.EQ.0.)GOTO8
      AK3=AKK*EXP(C3)
      AK4=AKK*EXP(C4)
      AK34=EXP(C3)/AK4
      A1=ALPHAH/ALPHAHE
      E2AL=E2*A1
      D=(1./AK3)+(E2AL)
      A2=1.+E2AL+AK34
      E4=.5*A2*(SQRT(1.+((4.*AK34)/(A2**2)))-1.)
      E3=.5*D*(SQRT(1.+((4./AK3)/D**2))-1.)-E4
      E12=E3+2.*E4
8     IF(ALPHAC-0.)9,99,9
9     AKA=AK*SQRT(2.*E1*AK1)
      AK5=(AKA**4)/EXP(C5)
      AK6=(AKA**3)/EXP(C6)
      AK7=(AKA**2)/EXP(C7)
      AK8=(AKA)/EXP(C8)
      ACNSTR=ALPHAC*STARN
      AK9=ACNSTR*EXP(C9)
      AK19=1./AK9
      EA=1./(1.+AK5+AK6+AK7+AK8)
      E5=AK5*EA
      E6=AK6*EA
      E7=AK7*EA
      E8=AK8*EA
      AA=(4.*E5)+(3.*E6)+(2.*E7)+E8
      IF(ALPHAHE.EQ.0.)GOTO10
      E11=((E2*ALPHAH)+((E12)*ALPHAHE))/ALPHAC
      E10=1./(1.+((E2*AK)+(E12*AKK))*EXP(C10-C9))
```

```
      E9=.5*(E11+AK19)*(SQRT(1.+((4.*AK19)/(E11+AK19)**2))-1.)-E10
      GOTO99
10    E10=1./(1.+(E2*AK)*(EXP(C10-C9)))
      EE=E2*(ALPHAH/ALPHAC)+AK19
      E9=.5*EE*(SQRT(1.+4.*AK19/(EE*EE))-1.)-E10
99    CONTINUE
      H2=.5*E1*AK
      H=(1.-E1-E2)*AK
      HPLUS=E2*AK
      IF(HPLUS.LT.0.)HPLUS=0.
      IF(ALPHAHE.EQ.0.)GOTO11
      HE=(1.-E3-E4)*AKK
      HEPLUS=E3*AKK
      HE2PLUS=E4*AKK
      EMINUS=HPLUS+(E12*AKK)
      Z=((1.-(E1/2.)+E2)*ALPHAH)+((1.+E12)*ALPHAHE)
      GOTO50
11    Z=(1.-(E1/2.)+E2)*ALPHAH
      HE=0.
      EMINUS=HPLUS
      HEPLUS=0.
      HE2PLUS=0.
50    IF(ALPHAC-0.)12,14,12
12    H2=H2-((E1/(1.+E1))*AA*ACNSTR)
      H=H-((((1.-E1)/(1.+E1))*AA)-(E9*((1.-E2)/(2.-E2))))*ACNSTR
      HPLUS=HPLUS-(E9*((1.-E2)/(2.-E2))*ACNSTR)
      IF(HPLUS.LT.0.)HPLUS=0.
      IF(ALPHAHE.EQ.0.)GOTO77
      BBB=(E3*(1.-E3)*(1.+E10))/((E3*(2.-E3))+A1)
      CC=(2.*E4*(1.-E4))/((1.+(2.*E4)-(E4**2))+A1)
      HE=HE+(BBB*ACNSTR)
      HEPLUS=HEPLUS-((BBB-CC)*ACNSTR)
      HE2PLUS=HE2PLUS-(CC*ACNSTR)
      EMINUS=EMINUS+((E9/(2.-E2))+(2.*E10)-BBB-CC)*ACNSTR
      Z=Z+(1.-AA/(1.+E1)+E9/(2.-E2)+2.*E10-(E3*(1.-E3)*(1.+E10))/(E3+A1)
     1-CC)*ALPHAC
      GOTO13
77    HE=0.
      HEPLUS=0.
      HE2PLUS=0.
      DD=E9/(2.-E2)+2.*E10
      EMINUS=EMINUS+DD*ACNSTR
      Z=Z+(1.-AA/(1.+E1)+DD)*ALPHAC
13    CH4=E5*ACNSTR
```

```
      CH3=E6*ACNSTR
      CH2=E7*ACNSTR
      CH=E8*ACNSTR
      CN=(1.-E5-E6-E7-E8-E9-E10)*ACNSTR
      CPLUS=E9*ACNSTR
      C2PLUS=E10*ACNSTR
      GOTO88
14    CH4=0.
      CH3=0.
      CH2=0.
      CH=0.
      CN=0.
      CPLUS=0.
      C2PLUS=0.
88    CONTINUE
   39 RETURN
      END
C
      SUBROUTINE TRANSP
      COMMON / BODY/ ZTA(20), CK(20), X(20), DX,R(20),BATA(20),MUREF,EPS
      COMMON /CONST/ GAMA,DY(51),Y(51),CC3(20,51)
      COMMON /CONST1/ AL, AK, CT
      COMMON /DEPEND/ T(20,51),P(20,51),D(20,51),U(20,51),V(20,51),XHE(5
     11),XHH(51), XH(51),XHP(51),CP(51),XHEP(51),XHE2P(51),XEMIN(51)
      COMMON /INF/ VINF, DINF,CPI
      COMMON /INFI/ TINF, PREI, VELOI, DENI, M, ALT, I111, CPII
      COMMON /SDFDIS/ NS(20),NS1,NS2
      COMMON /SHOCK/ DS(20), TS(20), VS(20), US(20), PS(20),MUS(20),TKS(
     120),ARFA(20)
      COMMON /TRANS/ TK(51),MU(51),TKDI
      REAL MUHH, MUH, MUHE, MUD, MUREF, MSD, MU,MUS
      K=51
      DO 10 N1=1,51
      N=52-N1
      NNN=N
      TEMP=T(M,N)*TS(M)*VINF**2/CPI
      MUHH=0.66E-6*TEMP**1.5/(TEMP+70.5)*10.
      MUHE=1.55E-6*(TEMP)**1.5/(TEMP+97.8)*10.
      TKHH=3.211E-5+5.344E-8*TEMP/(6.718E-2)
      TKH =2.496E-5+5.129E-8*TEMP/(6.718E-2)
      MUH= TKH*4./(15.*1.987)
      TKHE=MUHE*15.*1.987/16.
      PC11=1.
      PC22=1.
```

```
      PC33=1.
      PC12=(1.+(MUHH/MUH)**0.5*(0.5)**0.25)**2/SQRT(24.)
      PC13=(1.+SQRT(MUHH/MUHE)*2.**0.25)**2/SQRT(12.)
      PC21=(1.+SQRT(MUH/MUHH)*2.**0.25)**2/SQRT(12.)
      PC23=(1.+SQRT(MUH/MUHE)*4.**0.25)**2/SQRT(10.)
      PC31=(1.+SQRT(MUHE/MUHH)*(0.50)**0.25)**2/SQRT(24.)
      PC32=(1.+SQRT(MUHE/MUH)*(0.25)**0.25)**2/SQRT(40.)
      PCHH=XHH(NNN)*PC11+XH(NNN)*PC12+XHE(NNN)*PC13
      PCH=XHH(NNN)*PC21+XH(NNN)*PC22+XHE(NNN)*PC23
      PCHE=XHH(NNN)*PC31+XH(NNN)*PC32+XHE(NNN)*PC33
      PC=PCHH+PCH+PCHE
      MUD=(XHH(NNN)*MUHH)/PCHH +(XH(NNN)*MUH)/PCH +(XHE(NNN)*MUHE)/PCHE
      TKD=(XHH(NNN)*TKHH)/PCHH +(XH(NNN)*TKH)/PCH +(XHE(NNN)*TKHE)/PCHE
      TKD=TKD*4.18E7
      IF (N.GT.1) GO TO 5
      TKDI=TKD
    5 IF (N.NE.K) GO TO 2
      MSD=MUD/MUREF
      TKSD=TKD/(MUREF*CPI)
      MUS(M)=MSD
      TKS(M)=TKSD
    2 CONTINUE
      MU(N)=MUD/(MUREF*MSD)
      TK(N)=TKD/(MUREF*CPI*TKSD)
   10 CONTINUE
      RETURN
      END
C
C
      SUBROUTINE ABSOCOF (TSS,RHO,P12,H2,H, HPLUS,HE ,HEPLUS, HE2PLUS, E
     1MINS)
C
C     ***  CALCULATION OF ABSORPTION COEFFICIENTS  ***
      COMMON /R1/ A(58),B(58),F1(58),F3(58),F(58), V0(10)
      DIMENSION S(10),G(10)
      REAL NH2,NH,NHP,NHN,NE,NHE,NHEP,NHE2P
      NH2=H2/1000000.
      NH=H/1000000.
      NHP=HPLUS/1000000.
      NHN=0.
      NHE=HE/1000000.
      NHEP=HEPLUS/1000000.
      NHE2P=HE2PLUS/1000000.
      NE=EMINS/1000000.
```

```
      P=P12
      T=TSS
      ST = 157780./T
C
C     *** FREE-FREE AND BOUND-FREE TRANSITIONS FOR HYDROGEN  ***
C
      C1 = 9.93E-15*NH
      C2 = 1.23E-15*NH*EXP(-.75*ST)
      C3 = 3.67E-16*NH*EXP(-.8888*ST)
      C4 = 1.55E-16*NH*EXP(-.9374*ST)
      D1 = 1.0E-6*(NE**.286)
      IF(D1.GT..38) D1=.38
      A1 = 3.16E-20*NH*T*EXP(-(1.0-D1/13.595)*ST)*(EXP((.04-D1/13.595)*
     1ST)-1.0)
      CD = 1.35E-35*NHP*NE/SQRT(T)
      A(1) = F3(1)*C1
      A(2) = F3(2)*C1
      CC = CD+C2+C3+C4
      W = (1.0-.0736*D1)**2
      A(3) = F3(3)*CC + .014*C1*(1.0-W)/W
      DO 20  I=4,28
   20 A(I) = F3(I)*CC
      CC = CC-C2+A1
      W = (1.0-.294*D1)**2
      A(29) = F3(29)*CC + .23*C2*(1.0-W)/W
      DO 30  I=30,44
   30 A(I) = F3(I)*CC
      CC = CC-C3
      W = (1.0-.662*D1)**2
      A(45) = F3(45)*CC + 1.153*C3*(1.0-W)/W
      DO 40  I=46,48
   40 A(I) = F3(I)*CC
      CC = CC-C4
      X = .85-D1
      DO 45  I=49,53
      IF(F1(I)-X) 46,47,48
   46 W = (X/F1(I-1))**2
      W1 = W*F1(I-1)*F1(I-1)*(F1(I-1)-F1(I))
      A(I) = F3(I)*CC + C4*W/W1
      K1 = I+1
      GO TO 49
   47 A(I) = F3(I)*(CC+C4)
      K1 = I+1
      GO TO 49
```

```
   48 A(I) = F3(I)*(CC+C4)
   45 CONTINUE
      K1 = 54
   49 CONTINUE
      DO 50  I=K1,58
   50 A(I) = F3(I)*CC
C
C     ***  BOUND-BOUND TRANSITIONS FOR HYDROGEN  ***
C
      S1 = 1.098E-16*NH
      S(1) = .4160*S1
      S(2) = .0791*S1
      S(3) = .0290*S1
      S(4) = .0139*S1
      S2 = S1*EXP(-.75*ST)
      S(5) = 2.560*S2
      S(6) = 0.447*S2
      S(7) = 0.179*S2
      S2 = S1*EXP(-.8888*ST)
      S(8)  = 7.578*S2
      S(9)  = 1.355*S2
      S2 = S1*EXP(-.9374*ST)
      S(10) = 16.61*S2
      G(1) = 4.53E-15*(NE**.6667)
      G(1) = .42*G(1)
      G(2) = 4.30*G(1)
      G(3) = 8.12*G(1)
      G(4) = 13.4*G(1)
      G(5) = 1.80*G(1)
      G(6) = 6.44*G(1)
      G(7) = 11.5*G(1)
      G(8) = 2.58*G(1)
      G(9) = 8.63*G(1)
      G(10)= 3.33*G(1)
      DO 300  I=3,25
      PS = 0.
      DO 200  J=1,4
      PS = PS + (.3183*S(J)*(ATAN((F1(I-1)-V0(J))/G(J))-ATAN((F1(I)-
     1V0(J))/G(J)))/(F1(I-1)-F1(I)))
  200 CONTINUE
      A(I) = A(I) + PS
  300 CONTINUE
      DO 301  I=29,44
      PS = 0.
```

```
      DO 201  J=5,7
      PS = PS + (.3183*S(J)*(ATAN((F1(I-1)-V0(J))/G(J))-ATAN((F1(I)-
     1V0(J))/G(J)))/(F1(I-1)-F1(I)))
  201 CONTINUE
      A(I) = A(I) + PS
  301 CONTINUE
      DO 302  I=45,48
      PS = 0.
      DO 202  J=5,9
      PS = PS + (.3183*S(J)*(ATAN((F1(I-1)-V0(J))/G(J))-ATAN((F1(I)-
     1V0(J))/G(J)))/(F1(I-1)-F1(I)))
  202 CONTINUE
      A(I) = A(I) + PS
  302 CONTINUE
      DO 303  I=49,58
      PS = 0.
      DO 203  J=5,10
      PS = PS + (.3183*S(J)*(ATAN((F1(I-1)-V0(J))/G(J))-ATAN((F1(I)-
     1V0(J))/G(J)))/(F1(I-1)-F1(I)))
  203 CONTINUE
      A(I) = A(I) + PS
  303 CONTINUE
  990 CONTINUE
C
C     ***   CORRECTIONS FOR INDUCED EMISSION   ***
      M = 58
      DO 500  I=1,M
      A(I) = A(I)*(1.0-EXP(-F(I)*ST))
  500 CONTINUE
      RETURN
      END
      SUBROUTINE BLBODY
C
C     ***  CALCULATION OF BLACKBODY FUNCTION  ***
C
      COMMON/T1/T,RHO,XH2,XHE,P,NH2,NH,NHP,NHN,NE,NHE,NHEP,NHE2P
      COMMON /R1/ A(58),B(58),F1(58),F3(58),F(58), V0(10),W1(58)
      REAL NH2,NH,NHP,NHN,NE,NHE,NHEP,NHE2P
      BL(X) = .15399*(6.*(X+1.)+X*X*(X+3.))*EXP(-X)
      ST = 157780.0/T
      M = 58
      N = M-1
      N1 = M+1
      DO 10  I=1,N
```

```
      Y = F1(I)*ST/13.595
      IF(Y.LT.2.0) GO TO 5
      B(I) = BL(Y) +.0625*BL(2.*Y) +.01235*BL(3.*Y)
      GO TO 10
    5 CONTINUE
      B(I) = 1.0 -.05133*Y*Y*Y*(1.0-.375*Y+.05*Y*Y)
   10 CONTINUE
      B(M) = 1.0000
      DO 20  I=1,N
      J = N1-I
      K = J-1
      B(J) = B(J)-B(K)
   20 CONTINUE
      RETURN
      END
C
C
      SUBROUTINE RADAT
      COMMON /CONST/ GAMA,DY(51),Y(51),CC3(20,51) ,CCC1
      COMMON /CONST6/ YH,YK,TB
      COMMON /DEPEND/ T(20,51),P(20,51),D(20,51),U(20,51),V(20,51),XHE(5
     11),XHH(51), XH(51),XHP(51),CP(51),XHEP(51),XHE2P(51),XEMIN(51)
      COMMON /SHOCK/ DS(20), TS(20), VS(20), US(20), PS(20),MUS(20),TKS(
     120),ARFA(20),CPS(20)
      COMMON /INF/ VINF, DINF,CPI
      COMMON /INFI/ TINF, PREI, VELOI, DENI, M, ALT, I111, CPII
      COMMON /RAD/ COF1(58,51), QFXP(51),QFXM(51),QFX(51),DQY(51)
      COMMON /R1/ Q(58),B(58),F1(58),F3(58),F(58), V0(10),W1(58)
      COMMON /SDFDIS/ NS(20),NS1,NS2,PS1,AS(20)
      DIMENSION V1(58),V2(58),        COF3(58,51),COF2(58,51),
     1  EI2(51),EI1(51),E2(51),QP1(51),A(51),E3(51),QPT2(51),EJ1(51),EJ2
     2(51),EM2(51),QM1(51),W1(58),W2(58) ,DD(50),W3(58),W4(58)
      REAL NS
      EXTERNAL FX ,FX1
      IQW=0
      K11=50
      CCC1=DINF*VINF**3
      A0=0.26777343
      A1=8.6347608925
      A2=18.0590169730
      A3=8.5733287401
      B0=3.958469228
      B1=21.09965308
      B2=25.63295614
```

```
      B3=9.5733223454
      DO 21 N=1,50
      DD(N)=DY(N)*23*NS(M)
   21 CONTINUE
      YE=0.8
      YH=6.625E-27
      YK=1.380E-16
      XX=2.*YH*(YK/YH)**4/(3.E10**2)
      M5=58
      EPS=0.011
      DO 66 N=1,51
  301 TSS=T(M,N)*TS(M)*VINF**2/CPI
      DO 2 I=1,57
      W2(I)=W1(I+1)
    2 CONTINUE
      W2(58)=0.01
      DO 19 I=1,58
      V1(I)=YH*W1(I)/(YK*TSS)*3.E18/1.2402115E4
      V2(I)=YH*W2(I)/(YK*TSS)*3.E18/1.2402115E4
      W3(I)=W1(I)*3.E18/1.2402115E4
      W4(I)=W2(I)*3.E18/1.2402115E4
   19 CONTINUE
      DO 67 K=1,M5
      XX1=XX*TSS**4
   93 CALL ROMBS (V2(K),V1(K),FX,EPS,SUM    ,IERR)
      COF2(K,N)=XX1*SUM
      IF (IQW.EQ.0) GO TO 67
      CALL ROMBS(W4(K),W3(K),FX1,EPS,SUN      ,IERR)
      XX2=YE*YH/(3.E10**2)
      COF3(K,N)=XX2*SUN
   67 CONTINUE
   66 CONTINUE
      DO 1 N=2,51
      IF (N.GT.40) GO TO 302
      ND=N/2
      ND=ND*2
      IF (ND.NE.N) GO TO 1
  302 N1=N-1
      N2=N+1
      QPPP=0
      QMMM=0
      DO 10 K=1,M5
      DO 9 I=1,N1
      J=I+1
```

```
      EI1(J)=DD(I)*(COF1(K,I)+COF1(K,I+1))/2.
    9 CONTINUE
      DO 3 I=1,N
      EI2(I)=0.
      J=I
    4 IF (J.EQ.N ) GO TO 3
      EI2(I)=EI1(J+1)+EI2(I)
      J=J+1
      GO TO 4
    3 CONTINUE
      EI2(N) =0.04*DD(N1)*COF1(K,N)
      DO 5 I=1,N
      IF (EI2(I).GT.1.) GO TO 70
      E2(I)=1.+(0.5772-1.+ALOG(EI2(I)))*EI2(I)-EI2(I)**2/2.+EI2(I)**3/12
     1.
      GO TO 5
   70 X=EI2(I)
      IF (X.GT.200) GO TO 152
      E111=EXP(-X)*(A0+A1*X+A2*X**2+A3*X**3+X**4)/(X*(B0+B1*X+B2*X**2+B3
     1*X**3+X**4))
      E2(I)=EXP(-X)-X*E111
      GO TO 5
  152 E2(I)=0.
    5 CONTINUE
      QP1(1)=0.
      DO 7 I=2,N
      QP1(I)=DD(I-1)/2*(COF1(K,I-1)*COF2(K,I-1)*E2(I-1)+COF1(K,I)*COF2(K
     1,I)*E2(I))+QP1(I-1)
      QPP=QP1(I)
    7 CONTINUE
      QPPP=QPP+QPPP
   10 CONTINUE
      QPT2(N)=0.
      IF (IQW.EQ.0) GO TO 210
      DO 100 K=1,M5
      A(1)=0.
      DO 101 I=2,N
      A(I)=DD(I-1)/2.*(COF1(K,I-1)+COF1(K,I))+A(I-1)
      AII=A(I)
  101 CONTINUE
      IF (AII.GT.1.) GO TO 71
      E3(N)=0.5-AII+0.5*(-0.5772+1.5-ALOG(AII))*AII**2+AII**3/6.
      GO TO 72
   71 X=AII
```

```
      IF (X.GT.200) GO TO 151
      E111=EXP(-X)*(A0+A1*X+A2*X**2+A3*X**3+X**4)/(X*(B0+B1*X+B2*X**2+B3
     1*X**3+X**4))
      E222=EXP(-X)-X*E111
      E3(N)=(EXP(-X)-X*E222)/2.
      GO TO 72
  151 E3(N)=0.
   72 CONTINUE
      QPT2(N)=E3(N)*COF3(K,N)+QPT2(N)
  100 CONTINUE
  210 QMMM=0.
      IF (N.EQ.51) GO TO 190
      DO 112 K=1,M5
      DO 113 I=N1,50
      J=I+1
      EJ1(J)=DD(I)/2.*(COF1(K,I)+COF1(K,I+1))
  113 CONTINUE
      EJ1(N1)=0.040*DD(N1)*COF1(K,N)
      EJ2(N   )=0.
      DO 114 I=N2,51
      IF (N2.EQ.52) GO TO 114
      EJ2(I)=EJ1(I)+EJ2(I-1)
  114 CONTINUE
      EJ2(N)=EJ1(N1)
      DO 115 I=N ,51
      IF (N2.EQ.52) GO TO 115
      IF (EJ2(I).GT.1.) GO TO 74
      EM2(I)=1.+(.5772-1.+ALOG(EJ2(I)))*EJ2(I)-EJ2(I)**2/2.+EJ2(I)**3/12
     1.
      GO TO 115
   74 X=EJ2(I)
      IF (X.GT.200) GO TO 150
      E111=EXP(-X)*(A0+A1*X+A2*X**2+A3*X**3+X**4)/(X*(B0+B1*X+B2*X**2+B3
     1*X**3+X**4))
      EM2(I)=EXP(-X)-X*E111
      GO TO 115
  150 EM2(I)=0.
      GO TO 115
  115 CONTINUE
      QM1(N-1)=0.
      DO116 I=N2,51
      IF (N2.EQ.52) GO TO 116
      IP=I-1
      QM1(IP)=DD(I-1)/2*(COF1(K,I-1)*COF2(K,I-1)*EM2(I-1)+COF1(K,I)*COF2
```

```
     1(K,I)*EM2(I))+QM1(IP-1)
 160 QMM=QM1(IP)
 116 CONTINUE
 103 QMMM=QMM+QMMM
 112 CONTINUE
 190 QFXP(N)=(QPPP+QPT2(N))*6.2831/CCC1
     QFXM(N)=QMMM*6.28318/CCC1
     QFX(N)=QFXP(N)-QFXM(N)
   1 CONTINUE
     DO 303 N=3,39,2
     QFXP(N)=(QFXP(N+1)+QFXP(N-1))/2
     QFXM(N)=(QFXM(N+1)+QFXM(N-1))/2
     QFX(N)=(QFX(N+1)+QFX(N-1))/2
 303 CONTINUE
     QFXM(1)=QFXM(2)
     QFXP(1)=0.8*5.668E-5*(TB    **4)/CCC1
     QFX(1)=QFXP(1)-QFXM(1)
     DQY(1)=(QFX(2)-QFX(1))/DY(1)/NS(M)
     DQY(51)=-(QFX(50)-QFX(51))/DY(50)/NS(M)
     DO 888 I=2,K11
     AA1=DY(I-1)/(DY(I)*(DY(I-1)+DY(I)))
     AA2=DY(I)/(DY(I-1)*(DY(I-1)+DY(I)))
     AA3=(DY(I)-DY(I-1))/(DY(I)*DY(I-1))
     DQY(I)=AA1*QFX(I+1)-AA2*QFX(I-1)+AA3*QFX(I)
 889 DQY(I)=DQY(I)/NS(M)
 888 CONTINUE
     RETURN
     END
     FUNCTION FX(X)
     FX=X**3/(EXP(X)-1.)
     RETURN
     END
     FUNCTION FX1(X)
     COMMON /CONST6/ YH,YK,TB
     FX1=X**3/(EXP(YH*X/(YK*TB))-1)
     RETURN
     END
C
C
     SUBROUTINE ENERGY
     COMMON / BODY/ ZTA(20), CK(20), X(20), DX,R(20),BATA(20),MUREF,EPS
     COMMON /CONST/ GAMA,DY(51),Y(51),CC3(20,51) ,CCC1,ICONT
     COMMON /CONST1/ AL,AK,CT,K,K11,MBP,MA1,MA2
     COMMON /CONST3/     AH2(3,7),AHP(3,7),AH2P(3,7),AHE(3,7),AHEP(3,7),
```

```
     1          AE(3,7) ,AH(3,7),KE
      COMMON /CONST6/ YH,YK,TB
      COMMON /DEF/ DVY(51), DK(51), DMU(51), DPY(51), DUY(51), DP1(51)
      COMMON /DEPEND/ T(20,51),P(20,51),D(20,51),U(20,51),V(20,51),XHE(5
     11),XHH(51), XH(51),XHP(51),CP(51),XHEP(51),XHE2P(51),XEMIN(51)
     1    ,THP1(51),TH(51)
      COMMON /ENTH/ THH2, THH, THHE, THHP, THE
      COMMON /HEAT/ QCON,DIFU,RAT,QTOTL
      COMMON /INF/ VINF, DINF,CPI
      COMMON /INFI/ TINF, PREI, VELOI, DENI, M, ALT, I111, CPII,XH2I
     1       ,NORAD,NOPRE
      COMMON /PERC/ VI(20),PINF(20), ETHP(20), DI(20),CPL(20), Q01(20),
     1        PINFN(20)
      COMMON /RAD/ COF1(58,51), QFXP(51),QFXM(51),QFX(51),DQY(51)
      COMMON /SDFDIS/ NS(20),NS1,NS2,PS1,AS(20)
      COMMON /SHOCK/ DSN(20),TSN(20),VSN(20),USN(20),PSN(20), MUSN(20),
     1    TKSN(20),ARFA(20),CPSN(20),THS(20)
      COMMON /SPHT/ CH2(51),CH(51),CHP(51),CHE(51)
      COMMON /TRANS/ TK(51),MU(51),TKDI
      DIMENSION        A2(51),A3(51),A4(51),AN(51),BN(51),CN(51),DN(51),
     1E(51),F(51)                    ,DPX(51),DNS(20),DTS(20),DPS(51),A1(51)
     2      ,DHP(51), DHE(51), DH(51), DH2(51), PR(51),DPR(51) ,DE(51)
     3     ,CH2P(51),CE(51),          DPCI(51),DTH(51) ,PCI(51),DTHS(20)
      REAL MUHH, MUHE, MUH,MUD,MSD,MU,MACI,MUREF,MUSN,NS,NS1,NS2
      IF (NORAD.NE.1) GO TO 31
      DO 32 N=1,51
      QFXP(N)=0
      QFXM(N)=0
      QFX(N)=0.
      DQY(N)=0
   32 CONTINUE
   31 HX2I=XH2I
      V(M,51)=1.
      U(M,51)=1.
      D(M,51)=1.
      P(M,51)=1.
      TH(51)=1.
      T(M,51)=1.
      T(M,1)=TB*CPI/(VINF*VINF*TSN(M))
      PRS=CPSN(M)*MUSN(M)/TKSN(M)
      DO 131 N=1, 51
      AAA=XHH(N)*2+XH(N)+XHP(N)+XHE(N)*4+XEMIN(N)*0.5486E-3
      CH2(N)=XHH(N)*2/AAA
      CH(N)= XH(N)/AAA
```

```
      CHP(N)=XHP(N)/AAA
      CHE(N)=XHE(N)/AAA*4.
      CE(N)=XEMIN(N)*0.5486E-3/AAA
      PR(N)=CP(N)*MU(N)/TK(N)
      CH2P(N)=0.
  131 CONTINUE
      DO 2 N1=1,49
      N=51-N1
      AA4=DY(N)*( DY(N-1)+DY(N))
      AA1=DY(N-1)/AA4
      AA2=-DY(N)/(DY(N-1)*(DY(N-1)+DY(N)))
      AA3=+(DY(N)-DY(N-1))/(DY(N)*DY(N-1))
      DMU(N)=AA1*MU(N+1)+AA2*MU(N-1)+AA3*MU(N)
      DK(N)=AA1*TK(N+1)+AA2*TK(N-1)+AA3*TK(N)
      DPY(N)=AA1*P(M,N+1)+AA2*P(M,N-1)+AA3*P(M,N)
      DUY(N)=AA1*U(M,N+1)+AA2*U(M,N-1)+AA3*U(M,N)
      DVY(N)=AA1*V(M,N+1)+AA2*V(M,N-1)+AA3*V(M,N)
      DHP(N)=AA1*CHP(N+1)+AA2* CHP(N-1)+AA3*CHP(N)
      DHE(N)=AA1*CHE(N+1)+AA2* CHE(N-1)+AA3*CHE(N)
      DE  (N)=AA1*CE  (N+1)+AA2* CE  (N-1)+AA3*CE  (N)
      DH2(N)=AA1*CH2(N+1)+AA2* CH2(N-1)+AA3*CH2(N)
      DH  (N)=AA1*CH  (N+1)+AA2* CH  (N-1)+AA3*CH  (N)
      DPR(N)=AA1*PR  (N+1)+AA2* PR  (N-1)+AA3*PR  (N)
    2 CONTINUE
      DHE(1)=((CHE(2)-CHE(1))/DY(1)  +DHE(2))/2
      DHP(1)=((CHP(2)-CHP(1))/DY(1)  +DHP(2))/2
      DH2(1)=((CH2(2)-CH2(1))/DY(1)  +DH2(2))/2
      DH  (1)=((CH  (2)-CH  (1))/DY(1)  +DH(2))/2
      DE  (1)=((CE  (2)-CE  (1))/DY(1)  +DE(2))/2
      DPR(1)=(PR(2)-PR(1))/DY(1)
      DPR(51)=0.
      DMU(1)=(MU(2)-MU(1))/DY(1)
      DK(1)=(TK(2)-TK(1))/DY(1)
      DPY(1)=(P(M,2)-P(M,1))/DY(1)
      DUY(1)=(U(M,2)-U(M,1))/DY(1)
      DK(51)=-(TK(50)-TK(51))/DY(50)
      DPY(51)=-(P(M,50)-P(M,51))/DY(50)
      DUY(51)=-(U(M,50)-U(M,51))/DY(50)
      DVY(1)=(V(M,2)-V(M,1))/DY(1)
      DMU(51)=(MU(51)-MU(50))/DY(50)
      DVY(51)=(V(M,51)-V(M,50))/DY(50)
      KE=1
      DO 101 N=1,K11
      TEMP=T(M,N)*TSN(M)*VINF**2/CPI
```

```
      CALL ENTHALP (TEMP,CH2(N),CH(N),CHE(N),CH2P(N),CE(N),CHP(N),CPC,
     1              ENTHC)
      KE=2
      IF (N.NE.1) GO TO 106
      TH(1)=(ENTHC/(VINF**2)              )/THS(M)
  106 ANDO=        VINF**2
      THH2=THH2/(2*ANDO)
      THHE=THHE/(4*ANDO)
      THE=THE/(0.5486E-3*ANDO)
      THH=THH/ANDO
      THHP=THHP/ANDO
      SGM=DH2(N)*THH2+DH(N)*THH+DHE(N)*THHE+DHP(N)*THHP   +DE(N)*THE
      SGM=SGM/(2.3901E-8)
      IF (N .NE. 1) GO TO 54
      DIF=-1.1*MU(N)*MUSN(M)*SGM/NS(M)/PR(N)
   54 PC1=MU(N)/PR(N)*0.1*SGM
      PC2=MUSN(M)*USN(M)**2*CK(M)*MU(N)*U(M,N)**2/(1+NS(M)*Y(N)*CK(M))
      PC3=MU(N)*U(M,N)*USN(M)**2*(PRS*PR(N)-1)*DUY(N)/PR(N)
      PCI(N)=MUSN(M)/(NS(M)*PRS)*(PC1+PC3)-PC2
  101 CONTINUE
      KK=K11-1
      DO 102 N=2,KK
      AA4=DY(N)*( DY(N-1)+DY(N))
      AA1=DY(N-1)/AA4
      AA2=-DY(N)/(DY(N-1)*(DY(N-1)+DY(N)))
      AA3=+(DY(N)-DY(N-1))/(DY(N)*DY(N-1))
      DPCI(N)=AA1*PCI(N+1)+AA2*PCI(N-1)+PCI(N)*AA3
  102 CONTINUE
      DPCI(K11)=DPCI(KK)
      DPCI(1)=(PCI(2)-PCI(1))/DY(1)
      IF (M.GT.1) GO TO 5
      NS1=NS(1)
      PS1=PINFN(M)          +(1.-1./DSN(M))
      DO 6 N=1,K11
      AB1=DMU(N)/MU(N)-DPR(N)/PR(N)+2*NS1/(1+NS1*Y(N))
      A1(N)=AB1-NS1*DSN(M)*PRS*VSN(M)*D(M,N)*PR(N)*V(M,N)/(EPS**2*MUSN(M
     1)*MU(N))
      A4(N)=0
      A2(N)=0.
      AB2=PRS*NS1**2*PR(N)/(MUSN(M)*THS(M)*MU(N))
      A3(N)=AB2*(DPCI(N)/NS1+2*PCI(N)/(1+NS1*Y(N)) )
      A3(N)=A3(N)-(AB2/EPS**2)*(DQY(N)+QFX(N)*(2/(1+ NS1   *Y(N))) )
      A3(N)=A3(N)+DPY(N)*VS N(1)*V(1,N)*PSN(1)*AB2/(EPS**2*NS1)
    6 CONTINUE
```

```
      GO TO 10
    5 DO 11 N=1,K11
      DPX(N)=(P(M,N)-P(M-1,N))/DX
   11 CONTINUE
      IF (M.EQ.MBP) GO TO 59
      DTHS(M)=(THS(M+1)-THS(M-1))/(2*DX)
      IF (I111.EQ.1) GO TO 50
      DNS(M)=(NS(M+1)-NS(M-1))/(2.*DX)
      GO TO 52
   59 IF (I111.EQ.1) GO TO 50
      DNS(MBP)=(AS(MBP)-AS(MA2))/DX
      DTHS(MBP)=(THS(MBP)-THS(MA2))/DX
      GO TO 52
   50 DNS(M)=0
      IF (M.NE.MBP ) GO TO 52
      DTHS(MBP)=(THS(MBP)-THS(MA2))/DX
   52 DO 12 N=1,K11
      TC1=1+     Y(N)*CK(M)*NS(M)
      TC2=EPS**2*MUSN(M)*MU(N)
      TC3=COS(ZTA(M))/(R(M)+NS(M)*Y(N)*COS(ZTA(M)))
      AB3=DMU (N)/MU(N)-DPR(N)/PR(N)+NS(M)*(CK(M)/TC1+TC3)
      AB4=(DNS(M)*USN(M)*Y(N)*U(M,N)*D(M,N)/TC1-VSN(M)*D(M,N)*V(M,N))
      A1(N)=AB3+DSN(M)*PRS*PR(N)*NS(M)/TC2*AB4
      AB5=PRS*PR(N)*NS(M)**2/(MUSN(M)*MU(N)*THS(M) )
      A3(N)=AB5*(DPCI(N)/NS(M)+(CK(M)/TC1+TC3)*PCI(N))
      A3(N)=A3(N)-(AB5/EPS**2)*(DQY(N)+QFX(N)*(CK(N)/TC1+TC3) )
      A3(N)=A3(N)+DPY(N)*AB5*VSN(M)*V(M,N)/NS(M)*PSN(M) /EPS**2
   66 A4(N)=PRS*NS(M)**2*DSN(M)*USN(M)*PR(N)*U(M,N)*D(M,N)/(TC1*TC2)
      A4(N)=-A4(N)
      A2(N)=A4(N)*DTHS(M)/THS(M)
   12 CONTINUE
   10 DO 20 N=2,K11
      AN(N)=(2.+A1(N)*DY(N-1))/(DY(N)+DY(N-1))/DY(N)
      BN(N)=(2.-A1(N)*(DY(N)-DY(N-1)))/(DY(N)*DY(N-1))-A4(N)/DX-A2(N)
      BN(N)=-BN(N)
      CN(N)=(2.-A1(N)*DY(N))/(DY(N-1)*(DY(N)+DY(N-1)))
      IF (M.GT.1) GO TO 18
      DN(N)=A3(N)
      DN(N)=-DN(N)
      GO TO 20
   18 DN(N)=A4(N)/DX*THP1(N) *(-1)+A3(N)
      DN(N)=-DN(N)
   20 CONTINUE
      E(1)=0.
```

```
      F(1)=TH(1)
      DO 22 N=2,K11
      E(N)=-AN(N)/(BN(N)+CN(N)*E(N-1))
      F(N)=(DN(N)-CN(N)*F(N-1))/(BN(N)+CN(N)*E(N-1))
   22 CONTINUE
      DO 24 N1=1,49
      N=51-N1
      TH(N)=E(N)*TH(N+1)+F(N)
   24 CONTINUE
      YH2P=0.
      DO 108 N4=2,50
      N=52-N4
      RHO=D(M,N)*DSN(M)*DINF*1000
  145 TSS2=T(M,N)*TSN(M)*VINF**2/CPI
  146 CALL NOBDEN (TSS2, RHO, H2,H,HPLUS,HE, HEPLUS, HE2PLUS,EMINUS,
     1              XH2I)
      CALL VOLMAS (H2,H, HPLUS,HE, HEPLUS,HE2PLUS,EMINUS,YH2, YH, YHP,
     1          YHE, YHEP,YHE2P, YE)
      CALL ENTHALP (TSS2,YH2,YH,YHE,YH2P,YE,YHP,CPC,ENTHC)
      THO=(ENTHC/VINF**2+U(M,N)**2/2*USN(M)**2)
  137 DTHO=THO-TH(N)*THS(M)
      TSS3=           TSN(M)*VINF**2/CPI*(T(M,N +1)-0.05)
  110 CALL NOBDEN (TSS3, RHO, H2,H,HPLUS,HE, HEPLUS, HE2PLUS,EMINUS,
     1              XH2I)
      CALL VOLMAS (H2,H, HPLUS,HE, HEPLUS,HE2PLUS,EMINUS,YH2, YH, YHP,
     1          YHE, YHEP,YHE2P, YE)
      CALL ENTHALP (TSS3,YH2,YH,YHE,YH2P,YE,YHP,CPC,ENTHC)
      TH1=(ENTHC/VINF**2+U(M,N)**2/2*USN(M)**2)
  136 DTH1=TH1-TH(N)*THS(M)
  111 IF (ABS(DTH1/TH1).LT.0.01) GO TO 109
      SL=(DTH1-DTHO)/(TSS3-TSS2)
      TSS2=TSS3
      DTHO=DTH1
      TSS3=TSS2-DTHO/SL
      GO TO 110
  109 T(M,N)=TSS3*CPI/(VINF*VINF*TSN(M))
  108 CONTINUE
      DT1=(T(M,2)-T(M,1))/DY(1)
      DT2=DT1*TSN(M)/NS(M)
      QCON=TK(1)*TKSN(M)*    DT2*EPS**2*(-1)
      DIFU=DIF*EPS**2
      QTOTL=-1*(QCON+DIFU)
      RETURN
      END
```

```
      SUBROUTINE VOLMAS ( H2,H,HPLUS,HE,HEPLUS,HE2PLUS,EMINUS,CH2,CH,CHP
     1          ,CHE,CHEP,CHE2P,CE)
      AA1=H2+H+HPLUS+HE+HEPLUS+HE2PLUS+EMINUS
      XH2=H2/AA1
      XH=H/AA1
      XHP=HPLUS/AA1
      XHE=HE/AA1
      XHEP=HEPLUS/AA1
      XE=EMINUS/AA1
      AA2=XH2*2+XHE*4+XH+XHP+XHEP*4+XE*0.5486E-3
      CH2=XH2*2/AA2
      CH=XH/AA2
      CHP=XHP/AA2
      CHE=XHE*4/AA2
      CHEP=XHEP*4/AA2
      CE=XE*0.5486E-3/AA2
      RETURN
      END
C
C
      SUBROUTINE MOMENTM
      COMMON / BODY/ ZTA(20), CK(20), X(20), DX,R(20),BATA(20),MUREF,EPS
      COMMON /CONST/ GAMA,DY(51),Y(51),CC3(20,51) ,CCC1,ICONT
      COMMON /CONST1/ AL,AK,CT,K,K11,MBP,MA1,MA2
      COMMON /DEF/ DVY(51), DK(51), DMU(51), DPY(51), DUY(51), DP1(51)
      COMMON /DEPEND/ T(20,51),P(20,51),D(20,51),U(20,51),V(20,51),XHE(5
     11),XHH(51), XH(51),XHP(51),CP(51)
      COMMON /INFI/ TINF, PREI, VELOI, DENI, M, ALT, I111, CPII
      COMMON /INF/ VINF, DINF,CPI
      COMMON /PERC/ VI(20),PINF(20), ETHP(20), DI(20),CPL(20), Q01(20),
     1        PINFN(20)
      COMMON /SDFDIS/ NS(20),NS1,NS2,PS1,AS(20) ,NSS2
      COMMON /TRANS/ TK(51),MU(51)
      COMMON /SHOCK/ DS(20), TS(20), VS(20), US(20), PS(20),MUS(20),TKS(
     120),ARFA(20)
      DIMENSION P1(51),P2(51),U1(51),E1(51),F1(51),B1(51),B2(51),B3(51),
     1B4(51),DPX(51),    AN1(51),BN1(51),CN1(51),DN1(51),DNS(20),
     2                 DPS(20),         DVS(20),DVX(51),DUS(20)
      REAL MUREF, MUHH,MUHE,MACI,MU,MUS,MUH,NSS1,NSS2,NSS3
      REAL      NS,NS1,NS2,INTGA,INTGB,INTGC,INTGD,INTGE,INTGF
      IF(M.GT.1)GO TO 1
      P1(51)=1.
      PS1=PINFN(M)           +(1.-1./DS(M))
      IF (I111.GT.1) GO TO 2
```

```
      NS2=0
      NS1=NS(1)
      PS2=-(1.-1./DS(M))
      P2(51)=0.
      US1=1.
      DO 5 N1=1,50
      N=52-N1
      P2(N-1)=-DY(N-1)*(DS(M)*US1**2*NS1*D(M,N)*U(1,N)**2/(PS1*(1.+Y(N)*
     1NS1)))+P2(N)
      P1(N-1)=1.
    5 CONTINUE
      GO TO 24
    2 NS2=(AS(3)-AS(1))/(4.*DX**2)
      NS1=NS(1)
      US1=1.-2.*NS2/(1.+NS1)*(1.-1./DS(1))
      PS2=(1.-(1./DS(1)))*(1.-2.*NS2/(1.+NS1))**2*(-1.)
      P2(51)=0.
      DO 23 N1=1,50
      N=52-N1
      C11=DS(M)*US1**2*NS1*D(M,N)*U(M,N)**2/(PS1*(1.+Y(N)*NS1))
      C12=2*DS(M)*US1*NS2*VS(M)*D(M,N)*U(M,N)*Y(N)*DVY(N)/(PS1*(1.+Y(N)*
     1NS1))
      C13=PS2*DS(1)          *D(1,N)*VS(1)**2*V(1,N)/(PS1**2)*DVY(N)
      P2(N-1)=-DY(N-1)*(C11+C12+C13)+P2(N)
   23 CONTINUE
      DO 99 N1=1,50
      N=52-N1
      I=N-1
      P1(N-1)=(-VS(1)**2*DS(1)*D(1,I)*V(1,I)*DVY(I)/PS1)*(-DY(I))+P1(N)
   99 CONTINUE
   24 DO 7 N=1,K11
      B1(N)=DMU(N)/MU(N)+2.*NS1/(1.+NS1*Y(N))-NS1*DS(1)*VS(1)*D(1,N)*V(1
     1,N)/(EPS**2*MUS(1)*MU(N))
    7 CONTINUE
      DO 8 N=1,K11
      BB1=DMU(N)/MU(N)+NS1/(1+NS1*Y(N))*2.
      BB2=DS(M)*NS1*US1   *MU(N)*D(M,N)/(EPS**2*MUS(1)*MU(N))
      BB3=NS1*DS(1)*VS(1)*D(1,N)*V(1,N)/(EPS**2*MUS(1)*MU(N))
      B2(N)=-(NS1/(1+NS1*Y(N)))*(BB1+BB2+BB3)
    8 CONTINUE
      DO 9 N=1,K11
      DP1(N)=(P1(N+1)-P1( N ))/DY(N)
    9 CONTINUE
      DO 10 N=1,K11
```

```
      CC1=P2(N)+PS2*P1(N)/PS1-NS2*Y(N)*DP1(N)/NS1
      CC2=-2.*PS1*NS1**2/(EPS**2*MUS(1)*(1.+NS1*Y(N))*US1*MU(N))
      B3(N)=CC2*CC1
   10 CONTINUE
      DO 11 N=2,K11
      AN1(N)=(2.+B1(N)*DY(N-1))/(DY(N)*(DY(N)+DY(N-1)))
      BN1(N)=-(2.-B1(N)*(DY(N)-DY(N-1)))/(DY(N)*DY(N-1))+B2(N)
      CN1(N)=(2.-B1(N)*DY(N))/(DY(N-1)*(DY(N)+DY(N-1)))
      DN1(N)=B3(N)
      DN1(N)=-DN1(N)
   11 CONTINUE
      E1(1)=0.
      F1(1)=0.
      DO 12 N=2,K11
      E1(N)=-AN1(N)/(BN1(N)+CN1(N)*E1(N-1))
      F1(N)=(DN1(N)-CN1(N)*F1(N-1))/(BN1(N)+CN1(N)*E1(N-1))
   12 CONTINUE
      U(M,51)=1.
      U(M,1)=0.
      DO 13 N1=1,49
      N=51-N1
      U(M,N)=-AN1(N)/(BN1(N)+CN1(N)*E1(N-1))*U(M,N+1)+(DN1(N)-CN1(N)*F1(
     1N-1))/(BN1(N)+CN1(N)*E1(N-1))
   13 CONTINUE
      INTGA=0.
      INTGB=0.
      DO 14 N=1,K11
      INTGA=DY(N)/2.*(D(M,N+1)*U(M,N+1)+D(M,N)*U(M,N))+INTGA
      INTGB=DY(N)/2.*(D(M,N+1)*U(M,N+1)*Y(N+1)+D(M,N)*U(M,N)*Y(N))+INTGB
   14 CONTINUE
      VS11=VS(M)
      A11=(VS11 +2.*US1*INTGB)
      B11=(2.*VS11 +2.*INTGA*US1)
      NS1=(-B11+(B11**2-4.*A11*VS11) **0.5)/(2.*A11)
      NS(1)=NS1+NS2*BATA(1)**2
      DA=1.
      DO 330 N=2,50
      DB=(1.+NS1*Y(N))
      DC=(DB*D(1,N)*U(1,N)+DA*D(1,N-1)*U(1,N-1))/2.*DY(N-1)
      V(1,N)=1./(DB**2*VS(M)*D(M,N))* (DA**2*VS(M)*D(M,N-1)*V(1,N-1)-2.
     1*NS1*US1*DC)
      DA=DB
  330 CONTINUE
      DO 26 N=1,K
```

```
      P(1,N)=P1(N)+P2(N)*BATA(1)**2
   26 CONTINUE
      GO TO 28
    1 IF (I111.GT.1) GO TO 40
      DNS(M)=0
      GO TO 42
   40 IF (M.EQ.MBP) GO TO 33
      DNS(M)=(AS(M+1)-AS(M-1))/(2.*DX)
      GO TO 42
   33 DNS(MBP)=(AS(MBP)-AS(MA2))/DX
   42 DO 44 N=1,K11
      D11=DMU(N)/MU(N)+NS(M)*CK(M)/(1.+NS(M)*Y(N)*CK(M))+NS(M)*COS(ZTA(M
     1))/(R(M)+NS(M)*Y(N)*COS(ZTA(M)))
      D12=NS(M)*DS(M)*US(M)*DNS(M)*D(M,N)*U(M,N)*Y(N)/(EPS**2*MUS(M)*(1.
     1+NS(M)*Y(N)*CK(M))*MU(N))
      B1(N)=D11+D12-NS(M)*DS(M)*VS(M)*D(M,N)*V(M,N)/(EPS**2*MUS(M)*MU(N)
     1)
   44 CONTINUE
      DUS(M)=(US(M)-US(M-1))/DX
      DO 45 N=1,K11
      D21=-CK(M)*NS(M)*DMU(N)/((1.+NS(M)*Y(N)*CK(M))*MU(N))-CK(M)**2*NS(
     1M)**2/(1.+NS(M)*Y(N)*CK(M))**2
      D22=-COS(ZTA(M))*NS(M)**2*CK(M)/(R(M)+NS(M)*Y(N)*COS(ZTA(M)))/(1.+
     1NS(M)*CK(M)*Y(N))
      D23=-DS(M)*NS(M)**2*DUS(M)*U(M,N)*D(M,N)/(EPS**2*MUS(M)*(1+NS(M)*Y
     1(N)*CK(M))*MU(N))
      D24=-NS(M)**2*DS(M)*VS(M)*CK(M)*D(M,N)*V(M,N)/(EPS**2*MUS(M)*(1.+
     1NS(M)*Y(N)*CK(M))*MU(N))
      B2(N)=D21+D22+D23+D24
   45 CONTINUE
      DO 46 N=1,K11
      DPX(N)=(P(M,N)-P(M-1,N))/DX
   46 CONTINUE
      DPS(M)=(PS(M)-PS(M-1))/DX
      DNS(M)=(NS(M)-NS(M-1))/DX
      DPY(K)=-(P(M,K-1)-P(M,K))/DY(K-1)
      DO 48 N=1,K11
      D31=(DPX(N)+DPS(M)*P(M,N)/PS(M)-DNS(M)*Y(N)*DPY(N)/NS(M))
      D32=-PS(M)*NS(M)**2/(EPS**2*MUS(M)*(1.+NS(M)*Y(N)*CK(M))*MU(N)*US(
     1M))
      B3(N)=D31*D32
   48 CONTINUE
      DO 49 N=1,K11
      B4(N)=DS(M)*US(M)*NS(M)**2*D(M,N)*U(M,N)        /(EPS**2*MUS(M)*(1.
```

```
     1+NS(M)*Y(N)*CK(M))*MU(N))
      B4(N)=-B4(N)
   49 CONTINUE
      DO 50 N=2,K11
      AN1(N)=(2.+B1(N)*DY(N-1))/(DY(N)*(DY(N)+DY(N-1)))
      BN1(N)=-(2.-B1(N)*(DY(N)-DY(N-1)))/(DY(N)*DY(N-1))+B2(N)+B4(N)/DX
      CN1(N)=(2.-B1(N)*DY(N))/(DY(N-1)*(DY(N)+DY(N-1)))
      DN1(N)=B3(N)-B4(N)/DX*U(M-1,N)
      DN1(N)=-DN1(N)
   50 CONTINUE
      E1(1)=0.
      F1(1)=0.
      DO 52 N=2,K11
      E1(N)=-AN1(N)/(BN1(N)+CN1(N)*E1(N-1))
      F1(N)=(DN1(N)-CN1(N)*F1(N-1))/(BN1(N)+CN1(N)*E1(N-1))
   52 CONTINUE
      U(M,K)=1
      DO 54 N1=1,49
      N=51-N1
      U(M,N)=-AN1(N)/(BN1(N)+CN1(N)*E1(N-1))*U(M,N+1)+(DN1(N)-CN1(N)*F1(
     1N-1))/(BN1(N)+CN1(N)*E1(N-1))
   54 CONTINUE
      INTGD=0.
      INTGE=0.
      ANTGM=0.
      ANTGN=0.
      DO 56 N=1,K11
      INTGD=DY(N)/2.*(D(M,N+1)*U(M,N+1)+D(M,N)*U(M,N))+INTGD
      INTGE=DY(N)/2.*(D(M,N+1)*U(M,N+1)*Y(N+1)+D(M,N)*U(M,N)*Y(N))+INTGE
      ANTGM=DY(N)*(D(M-1,N+1)*U(M-1,N+1)*Y(N+1)+D(M-1,N)*U(M-1,N)*Y(N))/
     12.+ANTGM
      ANTGN=DY(N)*(D(M-1,N+1)*U(M-1,N+1)+D(M-1,N)*U(M-1,N))/2.+ANTGN
   56 CONTINUE
      CC1=INTGE*COS(ZTA(M))*DS(M)*US(M)
      CC2=INTGD*R(M)*DS(M)*US(M)
      CC8=ANTGM*COS(ZTA(M-1))*DS(M-1)*US(M-1)
      CC9=ANTGN*R(M-1)*DS(M-1)*US(M-1)
      IF(I111.EQ.1) GO TO 83
      IF (M.EQ.MBP) GO TO 101
      DNS(M)=(AS(M+1)-AS(M-1))/(2.*DX)
      GO TO 59
  101 DNS(MBP)=(AS(MBP)-AS(MA2))/DX
   59 I=M-1
      DNS(I)=(AS(I+1)-AS(I-1))/(2.*DX)
```

```
      GO TO 84
   83 DNS(M)=0.
      I=M-1
      DNS(I)=0.
   84 AA1=CC1
      BB1=CC2
      CCI=-(CC8*NS(I)**2+CC9*NS(I))
      CCI=CCI+(R(I)+NS(I)*COS(ZTA(I))) *( (1.+NS(I)*CK(I))*DS(I)*VS(I)
     1   -DNS(I)*DS(I)*US(I))*DX
      XX1=CC1                 +DX*DS(M)*VS(M)*COS(ZTA(M))*CK(M)
      XX2=CC2                               +DX*DS(M)*VS(M)*R(M)*CK(M)
     1                       +DX*DS(M)*VS(M)*COS(ZTA(M))-COS(ZTA(M))*DS(M)*US
     1(M)*DNS(M)*DX
      XX3=-(CC8*(NS(M-1)**2)+CC9*NS(M-1)                 -DX*DS(M)*VS(M)*R(M
     1)+DX*R(M)*DS(M)*US(M)*DNS(M))
      NSS1=(-BB1+(BB1**2-4.*AA1*CCI)**0.5)/(2.*AA1)
      NSS2=(-XX2+(XX2**2-4.*XX1*XX3)**0.5)/(2.*XX1)
      NSS3=(NSS2-NSS1)/NSS2
  331 ADC=0.5
  340 NS(M)=ADC*NSS2+(1.-ADC)*NSS1
      IF (NSS3.LT.0.15) GO TO 82
   75 SS1=NS(M)-NS(M-1)
      IF (SS1.GT.0.) GO TO 335
      ADC=ADC+0.011
      GO TO 340
  335 SS2=SS1/NS(M-1)
      ZZ=0.02*M-0.02
      IF (SS2.LT.ZZ  ) GO TO 82
      ADC=ADC-0.007
      GO TO 340
   82 CONTINUE
      INTGF=0.
      DO 58 N=1,49
      CC3(1,N)=0.
      INTGF=DY(N)/2.*((R(M)+NSS2 *Y(N+1)*COS(ZTA(M)))*D(M,N+1)*U(M,N+1)+
     1(R(M)+NSS2 *Y(N)*COS(ZTA(M)))*D(M,N)*U(M,N))+INTGF
      CC3(M,N)=INTGF*NSS2 *DS(M)       *US(M)
      DDD=(CC3(M,N)-CC3(M-1,N))/DX
      K=N+1
      EEE=(R(M)+NSS2 *Y(K)*COS(ZTA(M)))*(1.+NSS2 *Y(K)*CK(M))*DS(M)*VS(M
     1)*D(M,K)
      FFF=-(R(M)+NSS2 *Y(K)*COS(ZTA(M)))*DNS(M)*Y(K)*DS(M)*US(M)*D(M,K)*
     1U(M,K)
      V(M,K)=-(DDD+FFF)/EEE
```

```
   58 CONTINUE
      ANTGF=0.
      DO 351 N=1,49
      ANTGF=DY(N)/2.*((R(M)+NS(M)*Y(N+1)*COS(ZTA(M)))*D(M,N+1)*U(M,N+1)+
     1(R(M)+NS(M)*Y(N)*COS(ZTA(M)))*D(M,N)*U(M,N))+ANTGF
      CC3(M,N)=ANTGF*NS(M)*DS(M)        *US( M)
  351 CONTINUE
  350 P(M,K)=1.
      IF (I111.GT.1) GO TO 60
      DO 62 N1=1,50
      N=51-N1
      P(M,N)=P(M,N+1)-DY(N)*NS(M)*D(M,N)*DS( M )*U(M,N)**2*US(M)**2*CK(M
     1)/(PS(M)*(1.+NS(M)*Y(N)*CK(M)))
   62 CONTINUE
      GO TO 28
   60 DVS(M)=(VS(M)-VS(M-1))/DX
      DVX(51)=(V(M,51)-V(M-1,51))/DX
      G8=1./(1.+NS(M)*CK(M))*(DVS(M)/VS(M)+DVX(51)-DNS(M)*DVY(51)/NS(M))
      G9=VS(M)*DVY(51)/US(M)/NS(M)
      G10=-US(M)*CK(M)/(VS(M)*(1.+NS(M)*CK(M)))
      G7=PS(M)/(DS(M)*US(M)*VS(M)*NS(M))
      AING1=(G8+G9+G10)/G7
   64 DO 68 N1=1,K11
      N=51-N1
      IF (M.EQ.MBP) GO TO 93
      DVX(N)=(V(M+1,N)-V(M-1,N))/DX/2.
      GO TO 94
   93 DVX(N)=(V(MBP,N)-V(MA2,N))/DX
   94 G4=D(M,N)*U(M,N)/(1+NS(M)*Y(N)*CK(M))*(DVS(M)*V(M,N)/VS(M)+DVX(N)-
     1DNS(M)*Y(N)*DVY(N)/NS(M))
      G5=VS(M)*D(M,N)*V(M,N)*DVY(N)/US(M)/NS(M)
      G6=-US(M)*CK(M)*D(M,N)*U(M,N)**2/(1.+NS(M)*Y(N)*CK(M))/VS(M)
      AING2=(G4+G5+G6)/G7
      P(M,N)=P(M,N+1)+DY(N)*(AING1+AING2)/2.
      AING1=AING2
   68 CONTINUE
   28 DO 79 N=1,K11
      PP=P(M,N)*PS(M)
      PP1=PP*DINF*VINF**2
      TT=T(M,N)*TS(M)
      TT1=TT*VINF**2/CPI
  105 PP2=(PP1/1013250.)**AL
      IF (TT1.GT.8500) GO TO 71
      CT3=CT*0.9075
```

```
      CTT=(CT-CT3)*(T-4000)/4500+CT3
      TT2=TT1/CTT
      GO TO 73
   71 TT2=TT1/CT
   73 DD1=0.001292*(PP2/TT2)**(1./AK)
   61 DD=DD1/DINF
      D(M,N)=DD/DS(M)
   79 CONTINUE
      RETURN
      END
```